

JAERI-M

8 0 6 8

EFFECTS OF NEUTRON IRRADIATION ON PHYSICAL
AND MECHANICAL PROPERTIES OF SM1-24 AND
IG-11 GRAPHITES

—Report on JAERI/KFA Jülich Graphite
Irradiation Experiment HFR GG14—

February 1979

Division of Nuclear Fuel Research

日本原子力研究所
Japan Atomic Energy Research Institute

この報告書は、日本原子力研究所が JAERI-M レポートとして、不定期に刊行している研究報告書です。入手、複製などのお問合せは、日本原子力研究所技術情報部（茨城県那珂郡東海村）あて、お申しこしください。

JAERI-M reports, issued irregularly, describe the results of research works carried out in JAERI. Inquiries about the availability of reports and their reproduction should be addressed to Division of Technical Information, Japan Atomic Energy Research Institute, Tokai-mura, Naka-gun, Ibaraki-ken, Japan.

Effects of Neutron Irradiation on Physical and Mechanical Properties of
SM1-24 and IG-11 Graphites

----Report on JAERI/KFA Jülich Graphite Irradiation Experiment HFR GG14----

Division of Nuclear Fuel Research, Tokai Research Establishment, JAERI
(Received January 8, 1979)

Results of the neutron irradiation tests of near-isotropic graphites (SM1-24 and IG-11) for HTGR with HFR in Petten through KFA Jülich are described, together with those of the preirradiation tests which were performed in JAERI and KFA.

Irradiations were made to a maximum of about $2.5 \times 10^{21} \text{n/cm}^2$ (EDN) at temperatures from 1050°C to 1150°C. Measured were dimensional change, Young's modulus, thermal expansion coefficient up to 1000°C, apparent density, electrical resistivity at room temperature, open porosity, thermal conductivity, and electrical resistivity between 100 to about 1000°C, and ring compressive strength (for IG-11).

1) Dimensional change of IG-11 by high temperature irradiation was similar to that of 7477PT graphite irradiated in JMTR under same condition as HFR. Dimensional change of SM1-24 was the same as those obtained in JAERI and other institutes.

2) Increase in the Young's modulus was about 30 %-40 % for both graphites.

3) Thermal expansivity of IG-11 graphite was not much changed by irradiation.

4) The increase in apparent density was about 2 % in IG-11 and about 3 % in SM1-24.

5) The decrease in thermal conductivity by irradiation at 1100°C was not as large as expected, especially in SM1-24.

6) The increases in strength were about 15 % for the large and about 30 % for the small ring specimens.

Keywords: Graphite, Neutron Irradiation, Dimensional change, Young's Modulus, Apparent Density, Thermal Conductivity, Thermal Expansivity, Electrical Resistivity, Ring Compressive Strength, Open Porosity, Radiation Effects

* S. Nomura, J. Shimokawa, Y. Sasaki, T. Oku, H. Imai, H. Matsuo, M. Eto, Y. Fukuda, K. Fujisaki

SM1 - 24 と IG - 11 黒鉛の物理的機械的性質に
及ぼす HFR における中性子照射の影響

日本原子力研究所燃料工学部

(1979年1月8日受理)

この報告は、KFA Jiilich 研究所を通じてオランダペッテンにあるHFRにおいて2種類の黒鉛材料(SM1 - 24 と IG - 11 黒鉛)の照射試験を行った結果を照射前諸試験の結果とともにまとめたものである。

最大照射量は $2.5 \times 10^{21} n/cm^2$ (EDN) であり、照射温度は $1050 \sim 1150^\circ\text{C}$ であった。SM1 - 24 黒鉛と IG - 11 黒鉛について、寸法変化、ヤング率の変化、 1000°C までの熱膨張係数、見かけ密度、室温電気抵抗、開気孔率、 $100 \sim 1000^\circ\text{C}$ の間の電気抵抗と熱伝導率およびリング圧縮強さ (IG - 11 黒鉛のみ) が測定された。

得られたおもな結果は、次のとおりであった。

- 1) IG - 11 黒鉛の寸法変化は HFR と類似の照射条件について得られた 7477 PT 黒鉛の結果と同程度であった。SM1 - 24 黒鉛については、JAERI その他で得られた結果と一致することがわかった。
- 2) ヤング率の増加は両黒鉛について約 30 - 40% であった。
- 3) IG - 11 黒鉛の熱膨張係数は照射によって大きく変化しなかった。
- 4) 見かけ密度は IG - 11 黒鉛では約 2%，SM1 - 24 黒鉛では約 3% 増加した。
- 5) 熱伝導率の減少は SM1 - 24 黒鉛の場合とくに予期されるほど大きくなかった。
- 6) 強度の増加は大きなリングでは 15%，小さなリングでは 30% となった。

Contents

1. Introduction	1
2. Experimental	4
2.1 Materials and Specimen preparation	4
2.2 Irradiation Facility	5
2.3 Irradiation Conditions	6
2.4 Methods of Measurement	8
2.4.1 Determination of Linear Dimensions	8
2.4.2 Determination of Apparent Density	9
2.4.3 Determination of Dynamic Young's Modulus	10
2.4.4 Determination of Thermal Conductivity	12
2.4.5 Determination of Strength	13
3. Preirradiation Characterization	14
4. Results of post-irradiation examinations	15
4.1 Irradiation Induced Changes in Length, Density, Electrical Resistivity (room temp.), Dynamic Young's Modulus, Thermal Expansion and Open Porosity	15
4.2 Irradiation Induced Changes in Thermal Conductivity and Electrical Resistivity (100-1000 °C)	15
4.3 Irradiation Induced Changes in Strength	15
4.3.1 Optimization of the tensile specimens	16
4.3.2 Evaluation of the tensile tests	17
4.3.3 Ring compressive tests	17
4.3.4 Evaluation of the ring compressive tests	17
4.3.5 Measured values	19
4.3.6 Statistically estimated values	19
4.3.7 Comparison of the results from the tensile and ring - compressive tests	19
5. Summary	21

目 次

1. まえがき.....	1
2. 実験.....	4
2.1 材料及び試験片.....	4
2.2 照射装置.....	5
2.3 照射条件.....	6
2.4 測定方法.....	8
2.4.1 寸法.....	8
2.4.2 見掛け密度.....	9
2.4.3 動的ヤング率.....	10
2.4.4 热伝導率.....	12
2.4.5 強度.....	13
3. 照射前特性.....	14
4. 照射後試験結果.....	15
4.1 照射による寸法, 密度, 電気伝導(室温), 動的ヤング率 熱膨張率及び開気孔率の変化.....	15
4.2 照射による熱伝導度及び電気伝導度(100 ~ 1000°C)の変化.....	15
4.3 照射による強度の変化.....	15
4.3.1 最適引張試験片形状.....	16
4.3.2 引張試験の評価.....	17
4.3.3 リング圧縮試験法.....	17
4.3.4 リング圧縮試験の評価.....	17
4.3.5 測定値.....	19
4.3.6 統計的推定値.....	19
4.3.7 引張試験とリング圧縮試験の結果の比較.....	19
5. 総括.....	21

1. Introduction

In the period between the fall of 1977 and the summer of 1978, high-temperature irradiation and post-irradiation examinations of two kinds of nuclear graphites were performed for the Japan Atomic Energy Research Institute (JAERI) under the contract between KFA Jülich and JAERI. The agreement was signed by the representatives of both institutions on 1st of April 1977. This programme was named Graphite Irradiation Experiment HFR-GGI4. In this programme, neutron irradiation was performed in the HFR Petten and pre- and post-irradiation examinations were carried out in KFA Jülich. The purpose of this report is to compile the pre-irradiation report and the final report published by KFA Jülich for the effective use of the obtained data in the JAERI's VHTR* project and to add the specimen preparation details and some pre-irradiation data to be described by JAERI. For this reason, discussion of the results will be limited to the necessary minimum. Detailed discussion of the results of the post-irradiation examinations, including the comparison of the data with those which have been obtained in JAERI, will be presented by the specialists concerned with each item of the post-irradiation measurements.

The purpose of this graphite irradiation was to obtain some fundamental data for the design and safety analysis of the VHTR and to ensure the effective use of the results of graphite irradiations which have been obtained both in Japan and abroad. Another aspect of this experiment was that we were able to exchange information on the graphite researches, and irradiation and post-irradiation techniques in Japan, KFA Jülich, EURATOM Petten and ECN Petten.

The personnel contributed to this experiment and report are as follows.

* The Experimental Very High Temperature Gas-Cooled Reactor

Japan Atomic Energy Research Institute
(Division of Nuclear Fuel Research)

Name	Task	Laboratory
S. Nomura [*]	: Supervision	Division Head
J. Shimokawa	: Supervision	Division Head
Y. Sasaki	: Planning and Evaluation	Chief, Graphite Research Lab.
T. Oku ^{**}	: Planning and Evaluation	Chief, Materials Strength Lab.
H. Imai	: Specimen preparation and Data analysis	Graphite Research Lab.
H. Matsuo	: Specimen preparation and Data analysis	Graphite Research Lab.
M. Eto ^{***}	: Specimen preparation and Data analysis Coordination	Materials Strength Lab.
Y. Fukuda	: Specimen preparation	Graphite Research Lab.
K. Fujisaki ^{***}	: Specimen preparation	Materials Strength Lab.

* Now : Head, Office of Planning.

** Now : Chief, Materials Strength Lab., Division of
High-temperature Engineering.

*** Now : Materials Strength Lab., Division of
High-temperature Engineering.

KFA Jülich

Name	Task	KFA-Department
M.F. O'Connor	: Overall Coordination	HBK
G. Pott F. Putsch	: Coordination with Euratom and Evaluation of the Irradiation Conditions	ZBB
W. Delle	: Coordination of Specimen Examination	IRW
G. Haag	: Measurement of Linear Dimensions, Density, Specific Electrical Resistance (room temp.), Dynamic Young's Modulus, Thermal Coefficient of Expansion and Open Porosity	IRW
L. Binkele	: Measurement of High Temperature Thermal Conductivity and Specific Electrical Resistance	IRW
H. Schiffers	: Measurement of Strength	IRW
D. Mindermann	: Sample Management	HBK

2. Experimental

2.1 Materials and Specimen preparation

The graphites used in the experiment were SM1-24 from AGL Corporation and IG-11 from Toyo Tanso Co. Ltd., both of which have been well-known in the institute. A block of IG-11 graphite $100 \times 600 \times 1000$ mm in size was purified using halogen gas in Nippon Carbon Co. Ltd. The specimens for the irradiation were machined from this purified block. Fig. 1 shows the location of different kinds of specimens cut out from one half of the above block. Cylindrical specimens 20 mm in diameter and 150 mm in length were machined from the portion designated as TEN in Fig. 1. 60 specimens were specified as TEN-T1, TEN-T2, , and TEN-T60, whose locations within the TEN block are shown in Fig. 2. From the portion R in Fig. 1 two kinds of ring compression specimens were cut out. Enlargement of the portion R is shown in Fig. 3. The larger ring specimens ($20/10$) $\text{mm}\phi \times 10 \text{ mm}\ell$ and the smaller ones ($10/5$) $\text{mm}\phi \times 5 \text{ mm}\ell$, were machined in the manner shown in the right-hand side of Fig. 4. From the blocks F and G shown in Fig. 3, 54 larger ring specimens and 108 smaller ring specimens were cut out. In the figure specimen designations were shown for the block E. From the blocks A, B, C, D and E 30 larger rings and 60 smaller rings were cut out. In Fig. 5 specimen designations were shown in the case of block A.

In Figs. 6 and 7, the locations of cut-out specimens are shown for the longitudinal direction. The manner of machining the transverse specimens are shown also in Figs. 8 and 9. In Fig. 10 the locations of SM1-24 graphite specimens in a block are shown, where Types A, B and C specimens are those of $5 \text{ mm}\phi \times 20 \text{ mm}\ell$, $6 \text{ mm}\phi \times 25 \text{ mm}\ell$, $5 \text{ mm}\phi \times 50 \text{ mm}\ell$, respectively. Tables 1 and 2 show the number and designations of the specimens made from SM1-24 and IG-11 graphites, respectively. The specimens made from the TEN blocks in Fig. 2 are listed in Table 3. Fig. 11 shows the dimensions of the specimens made in JAERI for pre-irradiation characterization of IG-11 graphite.

Specimens which were sent to KFA Jülich from JAERI are summarized in Table 4. These specimens were selected using a random number table from those whose Young's modulus and apparent density were within $\pm 2\sigma$ (IG-11) and whose apparent density was within $\pm \sigma$ (SM1-24),

where σ is the standard deviation. All of the specimens 6 mm in diameter and 25 mm in length, and 6 mm ϕ \times 32 mm l are listed in Appendix A1 with the data obtained in JAERI.

2.2 Irradiation Facility

(1) The HFR - Petten

The High Flux reactor (HFR) at the Energy Research Center was used for the irradiation. This reactor is a material testing reactor which contains water as coolant and moderator. The nominal operating power is 45 MW. The core lattice is a 9 \times 9 array containing 31 fuel assemblies, 6 control members, 14 experiment positions and 30 beryllium reflector elements shown in Fig. 12. Adjacent to the reactor pool there are two smaller pools for storage and handling purpose. There is a hot cell for the dismantling of irradiated capsules on the top of one of these two pools.

The normal operating period is 24-26 days followed by a 2-3 days shut down period for changing fuel elements and experiments. Two extended shut down periods at the beginning of the year and during the summer interrupt the reactor operation during each year.

(2) Irradiation Device

(A) Capsule

The experiment will be performed in a TRIO 129 type capsule.

The main characteristics of this capsule are the following:

- Reloadable facility for different reactor positions
- Standard thimble for various irradiations to be used with special sample carriers
- Thimble consisting of 3 different legs, which can be used independently (Fig. 13)
- Incorporated vertical displacement unit, which aligns the experiment with the neutron flux and nuclear heating curves.

(B) Sample Holder

The sample holder is composed of two parts:

- the upper (non active) part to be used as a standard part for several irradiations, including the thermocouples compensation and extension cables, an additional shielding plug and the vertical displacement unit.

- the lower (active) part including the drum, the centering device, the thermocouples and the shielding plug.

This lower part of the sample holder consists of 1 drum of 28 mm ϕ and 400 mm length and is made of niobium (Fig. 14). The standard samples (6 mm ϕ) are located in the upper part of the carrier in 8 vertical holes. Due to the large size of the ring-samples, it was only possible to insert them at the lower end of the sample-carrier, so as to achieve a good centering of the sample-carrier and facilitate the loading procedure. The temperatures of the sample holder are measured and controlled by 6 W/WRe and 6 Ni/CrNi thermocouples all with Nb sheaths. The measuring points are partly near the surface of the carrier and partly near the centre. The temperature regulation will be made by changing a He/Ne gas mixture in the gap between carrier and thimble, and by vertical displacement of the sample carrier according to the variation of the nuclear heating curve.

Loading of specimens in the capsule is shown in Fig. 15, according to specimen number. Characterization programme together with the specimen direction is shown in Fig. 16, where characterization programme number 1, 2 or 3 means:

- 1 : Dimensional change, Dynamic modulus at RT,
Thermal expansion between RT and 1000 °C
Density, Electrical resistivity at RT
- 2 : Dimensional change, Dynamic modulus at RT,
Density, Electrical resistivity at RT
- 3 : Electrical resistivity and thermal conductivity between RT and
1000 °C.

2.3 Irradiation Conditions

(1) Course of the experiment

The irradiation was carried out between November 3, 1977 and March 6, 1978 which corresponds to an irradiation period of 101 full power days, referring to a reactor performance of 45 MW. A survey of the sequence of the irradiation cycles is given in Fig. 17 and details are given in Table 5. No special disruptions were experienced during the irradiation.

After being characterized in the Institute of Reactor Materials

(IRW) of the KFA, the irradiation specimens were sent to Euratom, Petten, where they were included in the irradiation device in accordance with the loading plan. At the end of the experiment the device was disassembled by Euratom and the specimens transported to Jülich. Although all specimens were received, the following three were broken :

Ring specimen no. 10 (10/5 mm ϕ)

Cylindrical specimens nos. 54 and 87 (6 mm ϕ × 25 mm)

(2) Temperatures

Temperatures in the experiment were measured using 1 W/WRe and 11 Ni/CrNi thermocouples. The measuring leads were arranged such that the temperatures in the direct environment of the specimens could be determined. The radial distribution of the thermocouples in the top and bottom parts of the sample holder are shown in Fig. 18 along with the temperature correction values which had to be used for the thermocouple readouts.

Thermocouple no. 1 (W/WRh) was only partly considered in the evaluation since the irradiation-induced drift of the electromotive force leads to incorrect measured values. Thermocouple 3 failed after 23 days. It must also be stated that thermocouple no. 8 registered values which could not be interpreted unambiguously. This thermocouple was also only partly considered during the evaluation. The remaining 9 measuring leads showed relatively constant values. The variations in the thermocouple registrations with time are enclosed in Appendix A II.

The axial temperature distributions for the periphery and central samples were determined from the measured values (see Figs. 19 and 20). It is noticeable here that the temperature at the ends of the sample holder, which was lower than specified, increased (approx. 20 °C) during the course of the experiment and thus became compatible with the specifications. The maximum and minimum irradiation temperatures, which were obtained from the cumulative curves in Figs. 21 and 22, are included in Figs. 19 and 20. The following specifications were applied here :

Minimum temperature - temperature which was not fallen below
for 95 % of the irradiation time

Mean temperature - mean value (50 % value) from the cumulative curve

Maximum temperature - temperature which was not exceeded for 95 % of the irradiation time.

The individual values are compiled in Table 6. The variation in the thermocouple temperatures during the irradiation is shown in Appendix A II.

(3) Dosimetry

Due to the high irradiation temperature, no fluence measuring probe could be included in the capsule. Monitor wires were therefore placed in the filler pieces of the TRIO sample holder (i.e. outside the irradiation capsule) and were evaluated after the irradiation (see Table 7). Using computer programming the fast fluence in the centre of the capsule was determined from the monitor values. The results are shown in Fig. 23. According to Euratom, in order to obtain fluence values for the energy range $E > 0.1$ MeV, the END-values for the irradiation positions E5 and E3 must be multiplied by a factor of 1.54.

2.4 Methods of Measurement

2.4.1 Determination of Linear Dimensions

(1) The vertical length measuring device

The vertical length measuring device from the LEITZ company was used to determine the initial sample lengths (see Fig. 24). After the test specimen is laid on the instrument table, a probe is brought into contact force of 0.6 N. The vertical length is measured electrically, registered digitally and stored in a data system. The movement of the probe is electrically triggered so that no hand heat is transferred to the specimen. As an extra safeguard, the instrument is in a temperature-stabilized environment. The limit of the measurement error for the instrument is $0.5 \mu\text{m}$, so that the accuracy of the dimension measurement is mainly determined by the precision of the mechanical finishing.

(2) The measuring microscope

A schematic diagram of the Universal measuring microscope (UWM III) from the LEITZ company used to determine the inside diameter

of the ring specimens is shown in Fig. 25. The microscope has a measuring table which can be used to determine lengths and angles. For the X- and Y-directions a precision cut glass piece, whose reference lines are projected onto a ground glass plate, is used as reference. A resolution of 1 μm can be achieved here. The measuring ranges is 150 mm in the X-direction and 75 mm in the Y-direction.

The object can be viewed through the binocular measuring tube which incorporates a projection device allowing photographic documentation of the object.

2.4.2 Determination of Apparent Density

The ratio of the mass of a body to its geometrical volume is defined there as the apparent density. However for ring specimens the exact determination of the volume from the linear dimensions is not possible and thus the density is determined using the buoyancy method. According to elementary physics, the density of a body can be calculated by the formula

$$d = \frac{m}{B} W_{\text{liq}}$$

where m is the mass of the sample and B the buoyancy which the sample experiences in a liquid with specific weight W_{liq} . It is equal to the difference between the weight of the sample in air and in the liquid neglecting the buoyancy in air. In the case of samples with measurable porosity however, the liquid penetrates the pores during the measurement and the sample weight in the liquid increases as the volume of the displaced liquid decreases. Thus for the determination of the apparent density the "outer" volume of displacing body must also be known. To this end the sample is previously impregnated with the same liquid (namely xylene) as used to determine the displacement. The samples must first or all be evacuated for two hours at a pressure of 10^{-2} torr before being exposed to the similarly outgassed xylene which then flows into the pores. During the ventilation of the apparatus the liquid is forced still deeper into the pores by the outside pressure. After about an hour as the temperature of the

sample approaches that of the environment, the sample weight in the liquid can be measured. Since xylene evaporates easily at atmosphere pressure and room temperature, the body, which has been freed of surface liquid, is put into a container filled with xylene which has been previously weighed. The container head is opened here for approx. 10s. From numerous previous investigations it is known how much liquid evaporates in this time in the temperature controlled laboratory.

The volume V of the displaced liquid for the outer volume of the sample is used to calculate the buoyancy

$$B = V W_{\text{liq.}}$$

The accuracy of the weight determination is $1 \mu\text{N}$. The temperature of the liquid is measured to within 0.1 degrees so that the specific weight W_{liq} can be read from tables with sufficient accuracy.

2.4.3 Determination of Dynamic Young's Modulus

If a periodically changing force is applied to the axis of a body of small cross-section and appreciable length, the speed of propagation C_1 of the longitudinal wave can be described by the equation

$$C_1 = \sqrt{\frac{E_s}{d}} \quad (1)$$

Where E_s is the elasticity modulus for the strain and d the density of the sample material. For a sample whose thickness is not small compared to its length, the lateral contraction induces an increase in the speed of propagation for the longitudinal waves (1). In the extreme case of a boundless solid body

$$C_1 = K \sqrt{\frac{E_s}{d}}$$

where

$$K^2 = \frac{1-\mu}{(1+\mu)(1-\mu)}$$

For transversal excitation the following applies for the propagation velocity

$$c_t = \sqrt{\frac{G}{d}}$$

independent of the lateral contraction. Here G is the shearing or torsion modulus. The strain modulus and torsion modulus are connected by the poisson's ratio μ :

$$E_s = 2(1+\mu)G \quad (2)$$

Since Poisson's ratio is normally unknown, one normally determines the strain modulus E_s according to equation (1) by measuring the velocity of sound in samples whose diameters are small in relation to their length. The measurements are carried out using an automatically functioning apparatus connected to a data system. (Fig. 26) A synthesizer produces an alternating voltage whose frequency can be continuously varied between 500 Hz and 200 kHz. This alternating voltage triggers a electromechanical oscillator which transmits the oscillations through direct contact with the sample. Longitudinal as well as transverse oscillations are produced in the sample. At the other end of the sample the oscillations are taken up by the pickup VP, again through direct contact, being measured using a digital voltmeter. For a body whose cross-section is small compared to its length l and which is movably fixed at both ends, standing waves are produced when the condition

$$l = n \frac{\lambda}{2} \quad (3)$$

is fulfilled. λ is the wave length in the sample and $n = 1, 2, 3\dots$ the degree of the oscillation. The following relationship applies between the wave length λ , the strain frequency f_s and the propagation velocity c_1 :

$$c_1 = f_s \cdot \lambda \quad (4)$$

From the equations (1), (3) and (4) the equation for the determination

of the elasticity modulus can be deduced

$$E_s = \frac{4l^2 f_s^2 d}{n^2}$$

2.4.4 Determination of Thermal Conductivity

Thermal conductivity measurements were carried out by applying a modified KOHLRAUSCH method.*

Figure 27 is a schematic diagram of the setup used. It shows a water-cooled copper tube with a block coating on the vacuum side. The tube contains the cylindrical graphite specimen held between spring-loaded upper and lower electrodes and centered in position by a multijunction thermocouple with ceramic insulation that protrudes from the lower electrode.

Special design of the thermocouple permitted (after filling the copper tube with helium (~300 torr) measurement of the temperature T_0 at the centre of the specimen (point 0 in figure 27) as well as of the temperature differences ΔT_{01} and ΔT_{02} between the centre of the specimen and points 1 and 2 a fixed distance l away from the centre.

The current flowing through this arrangement and the simultaneous operation of two additional heaters at the electrode tips may generate greatly differing temperature profiles. However, only profiles which are symmetric with respect to the centre of the specimen and with small or disappearing temperature decrease along the test sections 0-1 and 0-2, are of interest for thermal conductivity measurement. For such measurements to be carried out at a given temperature T , the current I flowing through the specimen and the current through the two additional heaters were manually adjusted so as to give

$$T = T_0 ; \Delta T_{01} = \Delta T_{02} = \Delta T \approx 5 \text{ K}$$

Then the current I was reduced and the currents in the additional heaters were simultaneously increased to achieve the state

$$T = T_0 ; \Delta T_{01} = \Delta T_{02} = 0 \quad (5)$$

* L. Binkele : High Temperatures-High Pressures, 1972, vol.4, 401-409

characterized by specimen current I_0 . It is in this state that the resistivity R ($\Omega \text{ cm}$) was determined in the central zone of the specimen by a rapid measurement of potential difference. The results were used to compute the thermal conductivity from the relationship

$$\lambda(T) = \frac{\ell^2 R(I^2 - I_0^2)}{2F \Delta T} (1 + \epsilon), \quad (6)$$

where F is the cross-section area of the specimen, and ϵ is a correction term which in the first approximation can be taken to be equal to zero. To obtain the value of ϵ further measurements according to equation (5) are required at slightly different temperatures. These measurements are used to derive the differential coefficient $d(RI_0^2)/dT$ and then to calculate ϵ from the expression

$$\epsilon \approx \frac{\ell^2 d(RI_0^2)}{12F\lambda' dT} \quad (7)$$

where λ' is the thermal conductivity computed from equation (6) with $\epsilon = 0$.

2.4.5 Determination of Strength

The tensile strength measurements were carried out using testing equipment DIN 51221, class 1, with a transversal pulling rate of 0.1 mm/min. The strain measuring chain consisted of :

- an extensometer, $L_E = 40$ mm, with a double-sided inductive measuring system, class 1 (HBM D32) allowing electrical mean value calculation
- a TF-amplifier class 0.2 (HBM KED/3S-5)

The calibration of the measuring chain was achieved with extensometer calibration equipment.

The tensile force and sample extension were continuously registered to breaking point on a X-Y recorder.

The loading system for the tensile samples consisted of a ball pivot chain with three ball joints above the sample and two below.

3. Preirradiation Characterization

Results of the measurements carried out prior to the irradiation are shown in Tables 8-14. In these tables data are shown on all the cylindrical specimens that were sent to KFA Jülich from JAERI. However for the ring compression specimens, data are summarized only for the specimens for irradiation (Table 11). Strength of unirradiated specimens will be shown in Section 4 together with that of the irradiated. With regard to Table 11 it should be noted that :

- by the determination of the outside diameters with the vertical length measuring instrument, the mean value was formed from two measurements which were carried out at 90 °C to each other.
- by the determination of the inside diameters with the Universal measuring microscope, two measurements were carried out for both the top and bottom of the specimen (perpendicular to each other) and the mean value for all four measured values was calculated.
- by the determination of the lengths with the vertical length instrument, four measurements (again perpendicular to each other) were carried out and a mean value calculated.

4. Results of post-irradiation examinations

4.1 Irradiation Induced Changes in Length, Density, Electrical Resistivity (room temp.), Dynamic Young's Modulus, Thermal Expansion and Open Porosity

The irradiation induced changes in the above-mentioned properties for the graphite grades IG-11 and SMI-24 are documented together with the pre-irradiation property values in Tables 15-22. The changes in length and Young's modulus have additionally been plotted in Figs. 28-31. However no attempt has been made here to define shrinkage or Young's modulus change curves.

4.2 Irradiation Induced Changes in Thermal Conductivity and Electrical Resistivity (100-1000 °C)

Four SMI-24 and six IG-11 thermal conductivity specimens were selected for the irradiation. The dependence of the thermal conductivity and specific electrical resistivity of these specimens with temperature before and after the irradiation was measured and the results are compiled in Tables 23 and 24. The curves for the individual specimens are shown in Figs. 32-37. The fall in thermal conductivity caused by the irradiation, especially in the case of SMI-24 is not as great as expected for 1100 °C. For the presentation in Fig. 38 the thermal conductivity of the IG-11 and SMI-24 specimens at the irradiation temperature was obtained by extrapolation of the curves in Figs. 32-37 and compared with the curves calculated for 1100 °C according to the BINKELE method /1,2/.

4.3 Irradiation Induced Changes in Strength

In this section dealing with the strength results the following symbols are used :

$F_m(N)$ = breaking load

$L_t(mm)$ = total extension or total contraction; see Fig. 40

$S_0(mm^2)$ = initial cross-section of the tensile specimens

$R_m(N/mm^2)$ = tensile strength

/1/ L. Binkele, KFA-report Jü1-1096, August 1974

/2/ L. Binkele, Journal of Non-equilibrium Thermodynamics, 3(4) (1978) in print.

L_E (mm)	= initial measuring length of the extensometer
A_t	= total breaking strain
E_s (N/mm^2)	= Young's modulus (slope of the secant from the curve origin to breaking point for the tensile specimens)
S_R (N/mm^2)	= failure stress for the ring specimens
E_R (N/mm^2)	= Young's modulus for the rings
K_v	= constant
ν	= Poisson's ratio
b	= ring width
D_A	= outside diameter of the ring
D_I	= inside diameter of the ring
K_4	= constant
\bar{x}	= mean value for random sample selection
s	= Standard deviation of a random sample
μ	= mean value for the population
σ	= Standard deviation for the population
0	= index for unirradiated material
+	= index for irradiated material

4.3.1 Optimization of the tensile specimens

Preliminary tests were conducted to optimize the sample shape and connections. Since the number of JAERI raw sample was limited (thirty), these investigations were conducted using the German graphite grade EK 88 which has similar properties to IG-11. The transition radius, the shape of the sample head and connection possibilities were all varied and the final chosen specimen form is shown in Fig. 39. It has an elastic stress concentration factor at the transition radius according to /1/ of approx. 1.01 and a thread head. The direct confirmation for the successful optimization can be seen from the breaking point distribution (see Fig. 39) obtained for the thirty IG-11 samples. The sample breakage points are seemingly uniformly distributed over the test length. With the exception of one sample which broke at the contact point for the extensometer knife edge.

/1/ R.E. Peterson, Stress Concentration Design Factors, John Wiley & Sons, Second Edition (1959)

4.3.2 Evaluation of the tensile tests

The load extension diagrams for the tensile tests were evaluated according to the total extension L_t and maximum load F_m at breaking point. The tensile strength was calculated from the mean initial cross section S_o and F_m . The total breaking strain was determined from the initial measuring length of the extensometer L_E and ΔL_t . Using S_o , F_m and E_t , the Young's modulus (E_s) of the samples was determined for the secant between origin and breaking point.

4.3.3 Ring compressive tests

The ring compressive tests were carried out using the same equipment as for the tensile measurements. The traverse speed was 0.1 mm/min. The rings were pressed between plane lapped steel plates and the compressive strains of the rings were measured as distance changes for the compressive plates between diametrically opposite positions.

Two extensometers, class 0.1 (HBMDDI), and a TF-amplifier (HBM KWS/3 S-5) were used here and the two extensometers were switched in parallel to obtain a mean value. The calibration of the compressive strain measuring chain was achieved with the end measures. The compressive load and compressive strain of the samples were continuously registered on the X-Y recorder of the testing machine until breaking point. Crack formation took place only in one of the two most highly stressed ring regions, either at the top or the bottom. The testing machine was set up so that the sample was immediately unloaded with the same traverse speed after a drop in load.

The irradiated specimens were tested with the middle of the engraving at an angle of less than 45° to the loading direction. No sample breakage occurred at the engraving zone.

4.3.4 Evaluation of the ring compressive tests

The method of diagram evaluation can be explained using the example of the load-compressive strain diagram shown in Fig. 40.

The characteristic initial curvature of the load curve is typical for ring compressive specimens and can also to a certain extent be obtained for aluminium samples. The slope of the initial curvature which is not consistent with the main curvature can be explained by the

superimposed HERTZ compression. One finds, in fact, flattening at the loading positions caused by permanent shape changes for both graphite and aluminium samples even when a sample is loaded to only a fraction of its breaking load. The permanent changes cannot be predicted by the HERTZ equation. There are empirical solutions according to /1/ but they are only applicable for hardened steel with hardness values between 800 and 850 HV. The neglect of the initial curvature, however, seems to be justified when one consideres that the whole equations for bending are strictly only applicable for linear-elastic material behaviour. The Young's modulus E_R was calculated from F_m and ΔL_t using the drawn in auxiliary straight line according to the equation described in /2/:

$$E_R = K_v [1 + f_1(v)] \frac{F_m}{L_t \cdot b}$$

The constant $K_v [1 + f_1(v)]$ in this equation was determined using the details in /1/. Poisson's ratio for graphite was taken as approx. 0.1.* The maximum tensile stress at the breaking point for the pressed rings was determined using the FROCHT equation /3/:

$$S_R = \frac{F_m \cdot K_4}{(D_A - D_I) \cdot b}$$

The constant K_4 was also taken according to Borth and Lund. K_4 for $D_I/D_A = 0.5$ was taken as 6 for the evaluation conducted here.

- /1/ A. Palmgren : "Grundlagen der Wälzlagertechnik", edition 3 (1964)
Publisher Franck, Stuttgart
- /2/ A.J. Durelli, L. Ferrer, Journal of Materials Research and Standards Dec. 1963, p.988-991
- /3/ S.A. Borth, H.H. Lund, Proc. of Fourth Carbon Conference, Pergamon Press (1960) p.531-536
- * Measurements in JAERI showed that the ratio was 0-15 for IG-11 graphite.

4.3.5 Measured values

The results of the strength measurements are detailed in tables 25-29. To allow distinction between the different characteristic quantities the indices 0 and $^+$ has been used here

e.g. E^0 = Young's modulus of unirradiated samples

E^+ = Young's modulus of irradiated samples

4.3.6 Statistically estimated values

The following is assumed for the calculation of the statistically estimated values discussed in section 4.3.7:

- normal distribution of the population
- identity of the direction of maximum tensile stresses relative to the preferred grain orientation for all ring specimens alone and for the ring and tensile specimens together
- negligible influences of the irradiation dose and temperature on the strength results

Table 30 summarizes the data on mechanical properties of IG-11 obtained in JAERI. The specimens which gave us these data were machined in the manner shown in Table 3.

4.3.7 Comparison of the results from the tensile and ring-compressive tests

A clear difference can in principle be expected between the mean values of the randomly selected unirradiated samples R_m^0 and S_R^0 since, besides the different breaking risks dependent on volume, the calculation of bending strengths assumes linear elastic material behaviour up to the breaking point. The ratio of bending strength to maximum tensile strength lies in the region 1.2-1.9 depending on the material, method and sample size.

From the Tables 31 and 32 as well as Fig. 41 it can be seen that $R_m^0 < S_R^0$ and $S_{R_{20}}^0 < S_{R_{10}}^0$. The differences are significant.

In the literature there is no suggestions that different sample sizes lead to different values for S_R^0 . A certain plausibility can however be obtained through examination of the results from the usual bending strength measurements on stretched bending samples made of graphite. The values for the ring strength of irradiated samples also show a slight tendency for $S_{R_{20}}^+ < S_{R_{10}}^+$. However a decision as to its

significance cannot be made because of the superimposing effect of the different irradiation temperatures.

5. Summary

High temperature irradiation of SM1-24 and IG-11 graphites was performed in the HFR, Petten. The maximum fluence was about 2.5×10^{21} n/cm² (EDN) [$\sim 3.9 \times 10^{21}$ n/cm² ($E > 0.1$ MeV)] and the irradiation temperature ranged from 1050 to 1150 °C. Changes in dimensions and Young's modulus, thermal expansivity up to about 1000 °C, apparent density, electrical resistivity at room temperature, and open porosity were measured for 28 specimens of IG-11 graphite. All the properties above except thermal expansivity were measured for 17 specimens* of SM1-24 graphite and 17 specimens* of IG-11 graphite. Thermal conductivity and electrical resistivity between 100 and about 1000 °C were measured for 2 SM1-24 graphite specimens and 4 IG-11 graphite specimens.

Ring compression tests of irradiated ring specimens were carried out for 10 specimens of $(20^\phi - 10^\phi) \times 10$ mm and 18 specimens* of $(10^\phi - 5^\phi) \times 5$ mm.

Relative length changes of IG-11 graphite specimens caused by the high-temperature irradiation were comparable with those of 7477PT graphite which have been measured in JAERI for irradiation temperature and fluence similar to the HFR irradiation. As to SM1-24 graphite the obtained data, as a whole, seemed to coincide with those obtained in JAERI and other institutions.

Increase in the modulus was about 30-40 % for both graphites and no definite effect of specimen direction was observed for the present irradiation conditions.

Thermal expansivity of IG-11 graphite was not pronouncedly changed by the irradiation. Apparent density increased about 2 % for IG-11 graphite and about 3 % for SM1-24 graphite, which corresponds to the fact that the open porosity decreased 8-10 % for IG-11 and 12-14 % for SM1-24. Resistivity increase was pronounced, i.e. about 140 % for IG-11 and 160 % for SM1-24. The decrease in thermal conductivity caused by irradiation especially in the case of SM1-24 is not as great as expected for the irradiation temperature of 1100 °C. Strength increase was about 15 % for the larger ring specimens and about 30 % for the smaller ones. The variance of strength became smaller by the irradiation in the case of the larger rings.

* Two cylindrical specimens, one for SM1-24 and the other for IG-11, and two ring specimens were broken before post-irradiation test.

Further researches are expected in relation to the irradiation experiments. Some of the subjects are:

- (1) thermal expansion of SM1-24 graphite
- (2) tensile test of both graphites using cylindrical specimens
- (3) size effect on strength of IG-11 graphite
- (4) comparison and evaluation of measuring techniques different between JAERI and KFA Jülich.

It is also expected that the operational work on graphite research will develop in the close contact between two institutions within the framework of the projects of both countries.

Table 1 List of the specimens of SM1-24 graphite

Block	Kind of specimen	Specimen size (mm)	Specimen number		Number of specimen
			//	⊥	
No. 1	Thermal * expansion	5 ^Φ × 20	1 - 5	16 - 20	10
	Dimensional change Young's Modulus	6 ^Φ × 25	1 - 15	46 - 60	30
	Thermal * conductivity	5 ^Φ × 50	1 - 5	16 - 20	10
	Thermal * expansion	5 ^Φ × 20	6 - 10	21 - 25	10
No. 2	Dimensional change Young's Modulus	6 ^Φ × 25	16 - 30	61 - 75	30
	Thermal * conductivity	5 ^Φ × 50	6 - 10	21 - 25	10
	Thermal * expansion	5 ^Φ × 20	11 - 15	26 - 30	10
No. 3	Dimensional change Young's Modulus	6 ^Φ × 25	31 - 45	76 - 90	30
	Thermal * conductivity	5 ^Φ × 50	11 - 15	26 - 30	10

* For the use in JAERI.

Table 2 List of the IG-11 specimens machined from the blocks shown in Fig. 1

Block	Kind of specimen	Size (mm)	Specimen designation	Number of specimen	Direction
R	Ring compression (I)	(20-10) $\phi \times 10$	ROT 1 - ROT 84	84	\perp
	Ring compression (II)	(10- 5) $\phi \times 5$	RIT 1 - RIT168	168	\perp
BL	Dimensional change Young's modulus	6 $\phi \times 25$	DE-L1-L64	64	//
	Thermal conductivity	6 $\phi \times 32$	RT-L1-L32	32	//
	Compression	15×15×25 *	COM-L1-L96	96	//
	Bending	15×15×75 *	BEN-L1-L64	64	//
BT	Thermal conductivity	15×15×30 *	CTE-L1-L32	32	//
	Dimensional change Young's modulus	6 $\phi \times 25$	DE-T1-T64	64	\perp
	Thermal conductivity	6 $\phi \times 32$	RT-T1-T32	32	\perp
	Compression	15×15×25 *	COM-T1-T96	96	\perp
	Bending	15×15×75 *	BEN-T1-T64	64	\perp
	Thermal conductivity	15×15×30 *	CTE-T1-T32	32	\perp

* Not shaped into the final form. For the use in JAERI.

Table 3 List of the specimens machined from the block TEN
shown in Fig. 1.

Block number	Diameter (mm)	Length (mm)	Density (g/cm ³)	Young's modulus (N/mm ²)	Machined specimen*	Place **
TEN-T1	20.032	149.95	1.764	9.80	Z	KFA
	20.035	149.95	1.762	9.68	TCB	JAERI
	20.030	149.95	1.761	9.63	-	R
	20.033	149.95	1.763	10.0	-	R
	20.034	149.94	1.764	9.99	Z	KFA
6	20.037	149.95	1.766	9.97	TCB	JAERI
7	20.020	149.95	1.759	9.90	Z	KFA
8	20.037	149.94	1.762	9.95	Z	KFA
9	20.021	149.96	1.763	9.99	Z	KFA
10	20.030	149.95	1.759	9.78	TCB	JAERI
11	20.052	149.95	1.757	9.88	Z	KFA
12	20.044	149.95	1.760	9.89	Z	KFA
13	20.026	149.95	1.758	9.84	Z	KFA
14	20.034	149.96	1.754	9.66	-	R Ex
15	20.022	149.95	1.763	9.88	Z	KFA
16	20.040	149.95	1.757	9.94	Z	KFA
17	20.041	149.95	1.754	9.89	-	R Ex
18	20.029	149.96	1.762	9.91	TCB	JAERI
19	20.036	149.95	1.757	9.80	Z	KFA
20	20.040	149.95	1.756	9.74	TCB	JAERI
21	20.028	149.95	1.765	10.1	Z	KFA
22	20.024	149.95	1.762	9.83	TCB	JAERI
23	20.033	149.93	1.759	9.57	TCB	JAERI
24	20.044	149.94	1.756	9.61	-	R
25	20.036	149.96	1.756	9.55	Z	KFA
26	20.024	149.94	1.760	9.36	TCB	JAERI
27	20.034	149.95	1.763	9.52	-	R
28	20.026	149.94	1.762	9.45	-	R
29	20.032	149.94	1.756	9.21	Z	KFA
TEN-T30	20.020	149.94	1.758	9.28	TCB	JAERI
31	20.034	149.95	1.756	9.30	Z	KFA
32	20.034	149.95	1.764	9.36	Z	KFA
33	20.034	149.95	1.765	9.32	Z	KFA
34	20.053	149.94	1.763	9.54	TCB	JAERI
35	20.008	149.94	1.763	9.26	-	R
36	20.026	149.94	1.761	9.14	-	R
37	20.020	149.95	1.762	9.59	Z	KFA
38	20.034	149.95	1.761	9.36	TCB	JAERI
39	20.015	149.96	1.766	9.59	TCB	JAERI
40	20.040	149.99	1.757	9.33	-	R
41	20.039	149.93	1.758	9.22	-	R
42	20.025	149.94	1.763	9.51	-	R
43	20.026	149.95	1.759	9.53	-	R
44	20.033	149.95	1.764	9.60	Z	KFA
TEN-T45	20.036	149.95	1.763	9.72	TCB	JAERI

Block number	Diameter (mm)	Length (mm)	Density (g/cm ³)	Young's modulus (N/mm ²)	Machined specimen*	Place **
TEN-T46	20.024	149.94	1.763	9.63	Z	KFA
47	20.039	149.95	1.764	9.65	Z	KFA
48	20.031	149.95	1.760	9.76	Z	KFA
49	20.029	149.95	1.764	9.58	Z	KFA
50	20.029	149.95	1.768	9.65	TCB	JAERI
51	20.040	149.95	1.766	9.67	-	R
52	20.011	149.95	1.763	9.44	Z	KFA
53	20.040	149.95	1.765	9.37	Z	KFA
54	20.027	149.93	1.767	9.74	Z	KFA
55	20.029	149.94	1.760	9.27	Z	KFA
56	20.014	149.95	1.763	9.21	Z	KFA
57	20.030	149.94	1.761	9.42	TCB	JAERI
58	20.020	149.95	1.763	9.56	-	R
59	20.018	149.95	1.764	9.65	Z	KFA
TEN-T60	20.018	149.95	1.768	9.79	Z	KFA

* Z : Tensile specimen shown in Fig. 11.

T : Tensile specimen shown in Fig. 11.

C : Compressive specimen shown in Fig. 11.

B : Bending specimen shown in Fig. 11.

** R : Retained in JAERI.

Table 4 List of specimens sent to KFA Jülich from JAERI

Material	Sample size [mm]	Dir.	I.D. Number	Numbers of Samples	Group Number
IG-11	$6^{\phi} \times 25^1$	// \perp	1- 30 31- 60	30 30	(1)
	$6^{\phi} \times 32^1$	// \perp	61- 65 66- 70	5 5	(2)
SMI-24	$6^{\phi} \times 25^1$	// \perp	71- 85 86-100	15 15	(3)
IG-11	$(20-10)^{\phi} \times 10^1$ Large Ring	\perp	101-140	40	(4)
	$(10-5)^{\phi} \times 5^1$ Small Ring	\perp	141-190	50	(5)
	$20^{\phi} \times 150^1$	\perp	191-220	30	(6)
SMI-24	$6^{\phi} \times 32^1$	// \perp	221-222 223-224	2 2	(7)

Table 5 Irradiation Conditions for HFR-GG14

Nr.	Reactor Cycle		Irradiation time fpd		Pos.
	Start	End	Cycle	Total	
77/10	03.11.77	28.11.77	26, 1		E5
77/11	01.12.77	24.12.77	23, 9	50	E5
78/01	13.01.78	06.02.78	24, 9	74, 9	E3
78/02	09.02.78	06.03.78	26, 1	101	E3

Table 6 Sample temperatures corresponding to thermocouple
position Experiment HFR-GG14

thermocouple	Sample temperature °C					
	average		maximum		minimum	
	central	outer	central	outer	central	outer
2	1065	1055	1085	1075	1045	1035
4	1095	1085	1120	1110	1070	1060
5	1100	1090	1125	1115	1070	1060
7	1100	1085	1120	1105	1080	1065
9	1100	1085	1120	1105	1080	1065
10	1100	1085	1120	1105	1085	1070
11	1090	1075	1115	1100	1070	1055
12	1100	1085	1140	1125	1050	1035

Table 7 Thermal and fast flux density and fluence values, measured in the north-east and south-west corner of the aluminium filler of the experiment GG 14.

(The fast fluence and flux density values are equivalent fission neutron values, measured with the reaction $^{58}\text{Ni}(\text{n},\text{p})$. The thermal fluence and flux density values are obtained from the specific reaction rates, using the 2200 m.s^{-1} cross section of $^{59}\text{Co}(\text{n},\gamma)$).

distance from fuel (in mm)	detector code	ϕ in units of $1.0^{18}\text{m}^{-2}.\text{s}^{-1}$			Φ in units of 10^{24}m^{-2}		
		reaction $^{58}\text{Ni}(\text{n},\text{p})$	^{58}Co	reaction $^{59}\text{Co}(\text{n},\gamma)$	^{60}Co	reaction $^{58}\text{Ni}(\text{n},\text{p})$	^{58}Co
north-east position	-305 NiCo 1-1	0.542		1.52		5.38	14.7
	-205 NiCo 1-2	1.54		1.31		15.3	12.8
	-105 NiCo 1-3	2.00		1.70		19.9	16.5
	- 5 NiCo 1-4	2.07		1.75		20.5	17.0
	+ 95 NiCo 1-5	1.76		1.42		17.5	13.8
	+195 NiCo 1-6	1.14		0.891		11.3	8.66
	+295 NiCo 1-7	0.503		0.456		4.99	4.43
south-west position	-305 NiCo 3-1	0.848		1.78		8.41	17.3
	-205 NiCo 3-2	2.36		1.49		23.4	14.5
	-105 NiCo 3-3	3.13		1.95		31.0	19.0
	- 5 NiCo 3-4	3.23		2.03		32.0	19.7
	+ 95 NiCo 3-5	2.66		1.64		26.4	15.9
	+195 NiCo 3-6	1.52		0.957		15.1	9.30
	+295 NiCo 3-7	0.626		0.441		6.11	4.28

Table 8 Properties of Cylindrical Specimens of IG-11 Graphite (Parallel Orientation)
 * Specimens for irradiation

Specimen Number	Length (mm)	Density (g/cm ³)	Electrical Resistivity (Ohm mm ² /m)	Young's Modulus (10 ³ N/mm ²)	Thermal Expansivity (10 ⁻⁶ /K) 20-500°C	Thermal Expansivity (10 ⁻⁶ /K) 20-1000°C	Open Porosity (%)
1 *	24.976	1.75	10.0	9.4	4.0	5.0	16.0
2 *	24.987	1.76	10.1	9.3	4.1	5.1	15.9
3 *	24.990	1.76	10.3	9.1	4.1	5.1	15.9
4 *	25.003	1.75	10.3	9.1	4.1	5.2	15.9
5 *	24.980	1.75	10.1	9.1	4.2	5.3	16.2
6 *	24.982	1.76	10.2	9.1	4.2	5.3	16.0
7 *	24.983	1.76	10.2	9.1	4.2	5.1	16.3
8 *	24.985	1.76	10.3	9.0	4.0	5.0	15.8
9 *	24.992	1.76	10.4	8.9	4.1	5.0	15.9
10 *	24.981	1.76	10.1	9.1	4.5	5.2	16.0
11 *	24.986	1.76	9.6	9.9	3.8	4.7	15.5
12 *	24.989	1.77	9.4	10.1	3.8	4.8	15.2
13 *	24.984	1.76	9.8	9.6	4.0	4.9	15.8
14 *	24.993	1.77	9.5	9.8	3.9	4.9	15.3
15	24.990	1.76	9.8	9.2	4.0	4.8	15.6
16 *	24.987	1.76	9.6	9.6			15.6
17 *	24.986	1.75	10.1	9.1			16.0
18 *	24.994	1.76	10.2	9.0			15.6
19 *	24.991	1.76	9.7	9.7			15.8
20 *	24.998	1.77	9.6	9.6			15.4
21 *	24.986	1.76	10.2	9.2			15.9
22 *	24.987	1.76	10.3	8.8			15.7
23 *	24.990	1.77	9.8	9.5			15.8
24 *	24.991	1.75	9.9	9.4			16.0
25	24.989	1.76	10.0	9.3			15.9
26	24.989	1.77	9.8	9.6			15.3
27	24.991	1.76	10.3	8.8			15.9
28	24.997	1.76	10.2	8.9			15.8
29	24.997	1.77	9.9	9.5			15.5
30	24.981	1.77	10.0	9.3			15.7

Table 9 Properties of Cylindrical Specimens of IG-11 Graphite
(Perpendicular Orientation)

* Specimens for irradiation

Specimen Number	Length (mm)	Density (g/cm ³)	Electrical Resistivity (Ω mm ² /m)	Young's Modulus (10 ³ N/mm ²)	Thermal Expansion (10 ⁻⁶ /K) 20-500°C	Thermal Expansion (10 ⁻⁶ /K) 20-1000°C	Open Porosity (%)
31 *	24.995	1.76	10.1	9.1	3.9	5.0	16.3
32 *	24.983	1.76	10.3	8.8	4.0	5.0	16.2
33 *	24.978	1.75	10.2	9.1	4.0	5.1	16.5
34 *	24.978	1.75	10.1	8.9	3.9	4.9	16.6
35 *	24.994	1.76	9.7	9.6	3.9	5.0	16.2
36 *	24.982	1.76	9.8	9.4	3.9	5.0	16.1
37 *	24.990	1.76	9.8	9.3	3.9	4.9	15.9
38 *	24.978	1.76	9.9	9.2	3.7	4.7	16.0
39 *	24.984	1.76	9.9	9.3	3.8	4.8	16.1
40 *	24.976	1.76	9.9	9.3	3.8	4.8	16.3
41 *	24.979	1.76	9.7	9.5	4.0	5.0	16.3
42 *	24.976	1.77	9.5	9.4	3.9	4.8	15.9
43 *	24.979	1.77	9.8	9.2	3.9	4.9	16.0
44 *	24.995	1.77	10.3	8.7	4.1	5.0	15.8
45	24.980	1.77	9.5	9.5	3.7	4.5	15.8
46 *	24.956	1.77	9.4	9.5			
47 *	24.948	1.76	9.5	9.5			
48 *	24.977	1.76	9.9	8.9			
49 *	24.981	1.76	9.5	9.7			
50 *	24.971	1.77	9.1	10.1			
51 *	24.969	1.77	9.1	10.3			
52 *	24.903	1.77	9.2	10.3			
53 *	24.977	1.77	9.1	10.2			
54 *	24.973	1.76	9.4	9.8			
55	24.966	1.77	9.0	10.3			
56	24.978	1.77	9.3	10.0			
57	24.980	1.76	9.5	9.7			
58	24.981	1.77	9.2	10.0			
59	24.983	1.76	9.3	9.8			
60	24.988	1.77	9.1	10.2			

Table 10 Properties of Cylindrical Specimens of SMI-24 Graphite
 (Numbers 71 - 85 Parallel, Numbers 86 - 100 Perpendicular Orientation)
 * Specimens for irradiation

Specimen Number	Length (mm)	Density (g/cm ³)	Electrical Resistivity (Ωmm ² /m)	Young's Modulus (10 ³ N/mm ²)	Thermal Expansivity (10 ⁻⁶ /K) 20-500°C	Thermal Expansivity (10 ⁻⁶ /K) 20-1000°C	Open Porosity (%)
71 *	24.946	1.74	7.9	8.7	8.7	8.7	14.7
72 *	24.948	1.74	8.0	8.8	8.8	8.8	14.6
73 *	24.949	1.74	7.9	8.8	8.8	8.8	14.4
74 *	24.930	1.74	7.9	8.8	8.8	8.8	14.6
75 *	24.973	1.74	7.9	8.7	8.7	8.7	14.6
76 *	24.927	1.74	7.8	9.0	9.0	9.0	14.1
77 *	24.912	1.74	7.9	8.7	8.7	8.7	14.4
78 *	24.919	1.74	7.7	8.8	8.8	8.8	14.6
79 *	24.929	1.74	7.9	8.7	8.7	8.7	14.3
80	24.914	1.74	8.1	8.6	8.6	8.6	14.4
81	24.924	1.73	8.0	8.7	8.7	8.7	14.6
82	24.933	1.73	8.0	8.9	8.9	8.9	14.6
83	24.925	1.74	8.0	8.8	8.8	8.8	14.5
84	24.927	1.74	8.0	9.0	9.0	9.0	14.7
85	24.929	1.73	8.1	8.8	8.8	8.8	14.9
86 *	24.942	1.74	7.6	9.3	9.3	9.3	14.5
87 *	24.933	1.74	7.6	9.2	9.2	9.2	14.3
88 *	24.932	1.74	7.4	9.4	9.4	9.4	14.3
89 *	24.951	1.74	7.6	9.2	9.2	9.2	14.4
90 *	24.945	1.75	7.4	9.3	9.3	9.3	14.0
91 *	24.930	1.74	7.6	9.1	9.1	9.1	14.3
92 *	24.931	1.76	7.3	9.5	9.5	9.5	14.3
93 *	24.915	1.75	7.4	9.3	9.3	9.3	14.4
94 *	24.919	1.74	7.6	9.1	9.1	9.1	14.4
95	24.956	1.74	7.7	9.2	9.2	9.2	14.3
96	24.934	1.75	7.4	9.5	9.5	9.5	14.5
97	24.971	1.74	7.4	9.5	9.5	9.5	14.4
98	24.929	1.75	7.4	9.5	9.5	9.5	14.5
99	24.953	1.75	7.5	9.5	9.5	9.5	14.5
100	24.929	1.75	7.3	9.8	9.8	9.8	14.5

Table 11 Properties of the Ring Specimens of IG-11 Graphite

Specimen * Number	Outside Diameter (mm)	Inside Diameter (mm)	Length (mm)	Density (g/cm ³)
1 - 131	20,001	10,117	9,962	1,77
2 - 132	19,999	10,124	9,962	1,76
3 - 133	19,993	10,101	9,961	1,76
4 - 134	19,996	10,110	9,961	1,77
5 - 135	19,989	10,098	9,960	1,75
6 - 136	19,990	10,102	9,964	1,76
7 - 137	19,993	10,115	9,963	1,76
8 - 138	19,991	10,108	9,965	1,76
9 - 139	19,994	10,100	9,963	1,75
10 - 140	19,995	10,108	9,966	1,76
<hr/>				
1 - 171	9,984	5,039	4,976	1,76
2 - 172	9,983	5,033	4,978	1,75
3 - 173	9,978	5,041	4,975	1,77
4 - 174	9,982	5,023	4,976	1,76
5 - 175	9,983	5,046	4,980	1,76
6 - 176	9,981	5,039	4,978	1,76
7 - 177	9,986	5,028	4,979	1,75
8 - 178	9,983	5,048	4,980	1,75
9 - 179	9,984	5,051	4,981	1,75
10 - 180	9,983	5,042	4,978	1,76
11 - 181	9,984	5,034	4,973	1,76
12 - 182	9,984	5,041	4,975	1,76
13 - 183	9,981	5,039	4,974	1,76
14 - 184	9,986	5,029	4,970	1,76
15 - 185	9,985	5,034	4,973	1,74
16 - 186	9,988	5,041	4,994	1,75
17 - 187	9,986	5,046	4,990	1,76
18 - 188	9,986	5,042	4,962	1,76
19 - 189	9,982	5,030	4,963	1,77
20 - 190	9,988	5,052	4,975	1,76

* The first part of the specimen number has been engraved on the ring samples ; the second part is the corresponding JAERI code.

Table 12 Mean Values and Standard Deviations of the Property Measurements for the Cylindrical Samples

<u>Cylindrical Specimen</u>				
<u>IG-11</u>	Density	(g/cm ³):	1,762 ± 0,006	
	Electr. Resist.	(Ohm mm ² /m):	9,99 ± 0,28 9,60 ± 0,39	(//) (⊥)
	Young's Modulus	(10 ³ N/mm ²):	9,30 ± 0,33 9,55 ± 0,47	(//) (⊥)
	CTE (20 - 500°C)	(10 ⁻⁶ /K):	4,07 ± 0,18 3,89 ± 0,11	(//) (⊥)
	CTE (20 - 1000°C)	(10 ⁻⁶ /K):	5,03 ± 0,18 4,89 ± 0,15	(//) (⊥)
	Open Porosity	(%):	15,88 ± 0,30	
<u>SM 1-24</u>	Density	(g/cm ³):	1,742 ± 0,006	
	Electr. Resist.	(Ohm mm ² /m):	7,94 ± 0,11 7,48 ± 0,13	(//) (⊥)
	Young's Modulus	(10 ³ N/mm ²):	8,78 ± 0,11 9,36 ± 0,19	(//) (⊥)
	CTE (20 - 500°C)	(10 ⁻⁶ /K):	not measured	
	CTE (20 - 1000°C)	(10 ⁻⁶ /K):	not measured	
	Open Porosity	(%):	14,44 ± 0,20	

Table 13 Compilation of Thermal Conductivity Measurements (W/cmK)
 * Specimens for irradiation

Graphite Grade	SM 1 - 24						1G-11							
	221 11*	222 11	223 1	224 1	61 11	62 11	63 11*	64 11	65 11*	66 11*	67 1	68 1	69 1	70 1*
Specimen Number	221 11*	222 11	223 1	224 1	61 11	62 11	63 11*	64 11	65 11*	66 11*	67 1	68 1	69 1	70 1*
Specimen Temperature (°C)														
100	1,474	1,514	1,478	1,553	1,172	1,204	1,255	1,100	1,122	1,129	1,200	1,255	1,228	1,245
200	1,217	1,240	1,253	1,282	1,071	1,041	1,075	0,992	1,006	1,000	1,042	1,082	1,039	1,074
300	1,041	1,045	1,113	1,131	0,921	0,924	0,977	0,878	0,898	0,889	0,907	0,925	0,929	0,955
399	0,906	0,917	1,001	0,978	0,820	0,831	0,862	0,786	0,801	0,792	0,806	0,823	0,817	0,850
499	0,776	0,790	0,840	0,849	0,726	0,745	0,772	0,701	0,717	0,715	0,729	0,737	0,730	0,768
599	0,707	0,726	0,773	0,784	0,656	0,692	0,709	0,655	0,674	0,656	0,685	0,682	0,679	0,706
699	0,652	0,655	0,696	0,712	0,598	0,624	0,652	0,611	0,609	0,602	0,628	0,625	0,627	0,645
798	0,610	0,627	0,650	0,663	0,552	0,585	0,599	0,567	0,560	0,571	0,582	0,588	0,575	0,612
898	0,570	0,595	0,620	0,617	0,517	0,549	0,576	0,524	0,526	0,533	0,554	0,558	0,544	0,578
998	0,538	0,565	0,589	0,587	0,498	0,530	0,536	-	0,501	0,508	-	0,524	0,514	0,543

Table 14 Compilation of Specific Electrical Resistivity Measurements ($\text{m}\Omega/\text{cm}$)

* Specimens for irradiation

Graphite Grade	SM 1 - 24			IG-11										
	221 II*	222 II	223 I	224 I*	61 II	62 II*	63 II	64 II	65 II*	66 I*	67 I	68 I	69 I	70 I*
Specimen Number →	221 II*	222 II	223 I	224 I*										
Specimen Temperature (°C) ↓														
100	0,707	0,671	0,633	0,659	0,940	0,884	0,843	0,945	0,919	0,939	0,886	0,908	0,903	0,865
200	0,660	0,629	0,594	0,618	0,860	0,813	0,778	0,869	0,845	0,863	0,815	0,837	0,831	0,796
300	0,641	0,610	0,575	0,599	0,819	0,771	0,737	0,823	0,801	0,818	0,771	0,793	0,787	0,754
399	0,633	0,603	0,573	0,592	0,794	0,741	0,715	0,797	0,773	0,792	0,747	0,767	0,763	0,732
499	0,631	0,600	0,570	0,595	0,779	0,730	0,704	0,781	0,759	0,779	0,734	0,755	0,749	0,720
599	0,637	0,610	0,578	0,600	0,777	0,729	0,702	0,775	0,754	0,774	0,730	0,753	0,747	0,717
699	0,651	0,624	0,589	0,616	0,781	0,730	0,706	0,778	0,756	0,778	0,733	0,753	0,749	0,718
798	0,667	0,641	0,603	0,632	0,788	0,739	0,713	0,783	0,764	0,783	0,741	0,759	0,758	0,726
898	0,683	0,657	0,622	0,647	0,800	0,749	0,722	0,796	0,770	0,793	0,752	0,770	0,766	0,737
998	0,704	0,680	0,641	0,671	0,812	0,762	0,738	—	0,786	0,808	—	0,783	0,781	0,745

Table 15 Properties of Cylindrical Specimens of IG-11 Graphite
(Parallel Orientation) before and after Irradiation

Specimen Number	Irrad. Temp. (°C)	fluence (EDN) ($10^{21}/\text{cm}^2$)	Length (mm)	Density (g/cm^3)	Electrical Resistivity ($\Omega\text{m mm}^2/\text{m}$)	Young's Modulus (kN/mm 2)	Thermal Expansivity ($10^{-6}/\text{K}$)	Open Porosity (%)
1	--	--	24,976	1,752	10,0	9,4	4,0	16,0
	1095	1,8	24,887	1,771	22,9	12,6	4,3	5,4
2	--	--	24,987	1,757	10,1	9,3	4,1	5,1
	1085	1,7	24,919	1,774	23,6	12,3	4,4	5,6
3	--	--	24,990	1,756	10,3	9,1	4,1	5,1
	1090	1,9	24,897	1,778	23,8	12,1	4,3	5,3
4	--	--	25,003	1,751	10,3	9,1	4,1	5,2
	1075	1,9	24,930	1,771	24,2	12,2	4,2	5,3
5	--	--	24,980	1,752	10,1	9,1	4,2	5,3
	1075	1,9	24,898	1,769	23,9	12,4	4,2	5,3
6	--	--	24,982	1,758	10,2	9,1	4,2	5,3
	1075	1,9	24,905	1,775	24,0	12,3	4,3	5,4
7	--	--	24,983	1,762	10,2	9,1	4,2	5,1
	1080	2,2	24,887	1,786	24,3	12,2	4,1	5,3
8	--	--	24,985	1,761	10,3	9,0	4,0	5,0
	1095	2,3	24,866	1,788	23,9	12,0	4,3	5,4
9	--	--	24,992	1,759	10,4	8,9	4,1	5,0
	1085	2,3	24,886	1,784	24,6	12,0	4,3	5,4
10	--	--	24,981	1,755	10,1	9,1	4,5	5,2
	1085	2,3	24,866	1,782	23,8	12,3	4,2	5,4

Table 16 Properties of Cylindrical Specimens of IG-II Graphite
(Parallel Orientation) before and after Irradiation

Specimen Number	Irrad. Temp. (°C)	Fluence (EON) ($10^{21}/\text{cm}^2$)	Length (mm)	Density (g/cm³)	Electrical Resistivity (ohm mm²/m)		Young's Modulus (kN/mm²)	Thermal Expansivity ($10^{-6}/\text{K}$) 20-500°C	Thermal Expansivity ($10^{-6}/\text{K}$) 20-1000°C	Open Porosity (%)
					9,6	9,9				
11	--	2,5	24,986	1,763	9,6	9,9	3,8	4,7	15,5	14,3
12	--	2,5	24,826	1,792	22,6	13,0	4,0	5,1	14,3	
13	--	2,5	24,989	1,771	9,4	10,1	3,8	4,8	15,2	13,5
14	--	2,5	24,825	1,800	22,4	13,5	3,8	4,9	14,8	13,7
15	--	2,5	24,984	1,761	9,8	9,6	4,0	4,9	15,8	13,5
16	--	2,5	24,835	1,795	23,0	12,8	3,9	4,8	14,8	
17	--	2,1	24,993	1,771	9,5	9,8	3,9	4,9	15,3	13,5
18	--	2,2	24,845	1,797	22,7	13,3	3,9	4,9	15,6	13,7
19	--	2,3	24,987	1,765	9,6	9,6	4,9	4,9	15,6	
20	--	2,4	24,877	1,787	23,0	13,2				
21	--	2,5	24,986	1,754	10,1	9,1				
	1075		24,889	1,777	23,8	12,6				
	1080		24,899	1,792	23,9	12,4				
	1085		24,991	1,760	9,7	9,7				
	1090		24,829	1,791	22,8	13,4				
	1100		24,998	1,769	9,6	9,6				
			24,847	1,796	22,8	13,2				
			24,986	1,760	10,2	9,2				
			24,828	1,793	23,1	12,6				

Table 17 Properties of Cylindrical Specimens of IG-11 Graphite
(Parallel Orientation) before and after Irradiation

Specimen Number	Irrad. Temp. (°C)	fluence (EDN) ($10^{21}/\text{cm}^2$)	Length (mm)	Density (g/cm^3)	Electrical Resistivity ($\Omega\text{mm}^2/\text{m}$)	Young's Modulus (kN/mm ²)	Thermal Expansivity ($10^{-6}/\text{K}$)	Open porosity (%)
22	--	--	24,987	1,759	10,3	8,8	15,7	
	1100	2,5	24,820	1,795	23,8	12,2		13,6
23	--	--	24,990	1,766	9,8	9,5		15,8
	1085	2,5	24,833	1,801	22,9	13,2		13,4
24	--	--	24,991	1,754	9,9	9,4		16,0
	1085	2,5	24,814	1,785	23,1	13,1		13,9

Table 18 Properties of Cylindrical Specimens of IG-11 Graphite
(Perpendicular Orientation) before and after Irradiation

Specimen Number	Irrad. Temp. (°C)	Fluence (EDN) ($10^{21}/\text{cm}^2$)	Length (mm)	Density (g/cm ³)	Electrical Resistivity ($\Omega \text{m}^2/\text{m}$)	Young's Modulus (kN/mm ²)	Thermal Expansivity ($10^{-6}/\text{K}$) 20-500°C	Thermal Expansivity ($10^{-6}/\text{K}$) 20-1000°C	Open Porosity (%)
31	--	--	24,995	1,756	10,1	9,1	3,9	5,0	16,3
	1080	1,8	24,917	1,766	23,4	12,3	4,1	5,2	15,2
32	--	--	24,983	1,757	10,3	8,8	4,0	5,0	16,2
	1085	1,7	24,913	1,768	23,8	12,0	4,0	5,2	15,0
33	--	--	24,978	1,751	10,2	9,1	4,0	5,1	16,5
	1075	1,9	24,887	1,769	23,8	12,0	4,0	5,0	15,0
34	--	--	24,978	1,751	10,1	8,9	3,9	4,9	16,6
	1075	1,9	24,889	1,765	24,0	12,0	4,1	5,1	15,4
35	--	--	24,994	1,756	9,7	9,6	3,9	5,0	16,2
	1075	1,9	24,896	1,771	23,5	12,6	3,9	5,0	14,7
36	--	--	24,982	1,761	9,8	9,4	3,9	5,0	16,1
	1075	1,9	24,885	1,772	23,2	12,4	4,1	5,1	14,6
37	--	--	24,990	1,762	9,8	9,3	3,9	4,9	15,9
	1080	2,2	24,870	1,780	23,7	12,4	4,1	5,3	14,1
38	--	--	24,978	1,761	9,9	9,2	3,7	4,7	16,0
	1085	2,3	24,863	1,779	23,7	12,2	3,9	5,0	14,2
39	--	--	24,984	1,760	9,9	9,3	3,8	4,8	16,1
	1085	2,3	24,847	1,781	23,8	12,4	4,1	5,2	14,0
40	--	--	24,976	1,761	9,9	9,3	3,8	4,8	16,3
	1085	2,3	24,857	1,778	24,2	12,2	3,8	4,8	14,5

Table 19 Properties of Cylindrical Specimens of IG-11 Graphite
(Perpendicular Orientation) before and after Irradiation

Specimen Number	Irrad. Temp. (°C)	Fluence (EDN) ($10^{21}/\text{cm}^2$)	Length (mm)	Density (g/cm ³)	Electrical Resistivity ($\Omega\text{mm}^2/\text{m}$)	Young's Modulus (kN/mm ²)	Thermal Expansivity ($10^{-6}/\text{K}$)	Open Porosity (%)
41	--	--	24,979	1,758	9,7	9,5	4,0	16,3
	1085	2,5	24,806	1,785	23,1	12,8	3,7	14,0
42	--	--	24,976	1,769	9,5	9,4	3,9	4,8
	1085	2,5	24,800	1,797	22,6	12,9	3,7	4,7
43	--	--	24,979	1,766	9,8	9,2	3,9	15,9
	1085	2,5	24,825	1,792	23,5	12,6	3,8	13,5
44	--	--	24,995	1,766	10,3	8,7	4,1	16,0
	1085	2,5	24,862	1,791	24,6	11,9	4,0	13,6
46	--	--	24,956	1,766	9,4	9,5	4,9	5,0
	1075	2,1	24,836	1,790	22,9	13,1	5,0	5,0
47	--	--	24,948	1,765	9,5	9,5	4,9	13,8
	1075	2,1	24,835	1,786	22,9	13,1	4,9	16,0
48	--	--	24,977	1,757	9,9	8,9	4,9	13,9
	1080	2,2	24,857	1,784	23,8	12,2	4,9	16,3
49	--	--	24,981	1,764	9,5	9,7	5,0	14,0
	1085	2,4	24,795	1,797	22,4	13,4	5,0	15,9
50	--	--	24,971	1,769	9,1	10,1	5,0	13,3
	1085	2,4	24,800	1,799	22,2	13,7	5,0	15,7
51	--	--	24,969	1,765	9,1	10,3	5,0	13,5
	1085	2,5	24,775	1,799	21,5	14,0	5,0	15,9

Table 20 Properties of Cylindrical Specimens of IG-11 Graphite
(Perpendicular Orientation) before and after Irradiation

Specimen Number	Irrad. Temp. (°C)	Fluence ($10^{21}/\text{cm}^2$)	Length (mm)	Density (g/cm^3)	Electrical Resistivity (Ωm)	Young's Modulus (kN/mm^2)	Thermal Expansivity ($10^{-6}/\text{K}$)	Open Porosity (%)
52	--	2,5	24,983	1,771	9,2	10,3	15,4	
	1085		24,777	1,808	21,7	14,0	13,0	
53	--	--	24,977	1,775	9,1	10,2	15,3	
	1085	2,5	24,752	1,812	21,7	14,2	12,7	
54	--	--	24,973	1,758	9,4	9,8		
	1085	2,5			b r o k e n			16,0

Table 21 Properties of Cylindrical Specimens of SMI-24 Graphite
(Parallel Orientation) before and after Irradiation

Specimen Number	Irrad. Temp. (°C)	fluence (EDN) ($10^{21}/\text{cm}^2$)	Length (mm)	Density (g/cm ³)	Electrical Resistivity (Ohm mm ² /m)	Young's Modulus (kN/mm ²)	Thermal Expansivity ($10^{-6}/\text{K}$)	Open porosity (%)
71	--	--	24,946 24,815	1,737 1,770	7,9 19,4	8,7 11,8	14,7 12,9	
72	--	1,7	24,948 24,814	1,736 1,772	8,0 19,5	8,8 11,8	14,6 12,8	
73	--	--	24,949 24,784	1,744 1,787	7,9 20,0	8,8 11,9	14,4 12,4	
74	--	--	24,930 24,743	1,739 1,784	7,9 19,9	8,8 11,9	14,6 12,7	
75	--	2,2	24,973 24,787	1,741 1,789	7,9 20,2	8,7 11,7	14,6 12,5	
76	--	--	24,927 24,707	1,746 1,799	7,8 19,8	9,0 12,0	14,1 12,2	
77	--	--	24,912 24,672	1,738 1,798	7,9 20,1	8,7 11,9	14,4 12,5	
78	--	--	24,919 24,686	1,738 1,791	7,7 20,0	8,8 11,9	14,6 12,6	
79	--	--	24,929 24,697	1,740 1,797	7,9 19,9	8,7 12,2	14,3 12,3	

Table 22 Properties of Cylindrical Specimens of SMI-24 Graphite
(Perpendicular Orientation) before and after Irradiation

Specimen Number	Irrad. Temp. (°C)	Fluence (EDN) ($10^{21}/\text{cm}^2$)	Length (mm)	Density (g/cm^3)	Electrical Resistivity ($\Omega\text{mm mm}^2/\text{m}$)	Young's Modulus (kN/mm^2)	Thermal Expansivity ($10^{-6}/\text{K}$) $20-500^\circ\text{C}$	Thermal Expansivity ($10^{-6}/\text{K}$) $20-1000^\circ\text{C}$	Open Porosity (%)
86	--	--	24,942	1,742	7,6	9,3	14,5		
	1085	1,7	24,795	1,775	18,7	12,4			12,7
87	--	--	24,938	1,741	7,6	9,2			14,3
	1085	1,7	--	--	b r o k e n				
88	--	--	24,932	1,743	7,4	9,4			14,3
	1075	2,1	24,731	1,783	19,3	12,1			12,8
89	--	--	24,951	1,743	7,6	9,2			14,4
	1080	2,2	24,707	1,793	19,5	12,4			12,5
90	--	--	24,945	1,747	7,4	9,3			14,0
	1085	2,3	24,709	1,793	19,3	12,4			12,4
91	--	--	24,930	1,741	7,6	9,1			14,3
	1085	2,4	24,674	1,794	19,8	12,0			12,3
92	--	--	24,931	1,756	7,3	9,5			14,3
	1085	2,5	24,675	1,812	19,1	12,8			11,7
93	--	--	24,915	1,747	7,4	9,3			14,0
	1085	2,5	24,648	1,797	19,5	12,5			12,4
94	--	--	24,919	1,740	7,6	9,1			14,4
	1085	2,5	24,648	1,791	19,9	12,5			12,6

Table 23 Pre- and Post-irradiation Thermal Conductivity Measurements (in W/cm °C)

Graphite grade	AGL/SM 1 - 24				Toyo Tanso / 1G - 11			
Sample number	221 II	221 II	224 I	224 I	63 II	63 II	65 II	66 II
Irradiation temperature (°C)	-	1085	-	1100	-	1075	-	1085
Neutron fluence (10^{21} cm^{-2} EDN)	-	2,38	-	2,38	-	2,10	-	2,48
Temperature of (°C) ↓								
100	1,474	0,709	1,553	0,726	1,255	0,527	1,122	0,492
200	1,217	0,682	1,282	0,717	1,075	0,526	1,006	0,487
299	1,041	0,635	1,131	0,690	0,977	0,514	0,898	0,480
399	0,906	0,586	0,978	0,631	0,862	0,488	0,801	0,455
499	0,776	0,545	0,849	0,574	0,772	0,461	0,717	0,425
598	0,707	0,514	0,784	0,548	0,709	0,442	0,674	0,417
698	0,652	0,477	0,712	0,517	0,652	0,418	0,609	0,386
798	0,610	0,453	0,663	0,491	0,599	0,406	0,560	0,371
898	0,570	0,445	0,617	0,483	0,576	0,394	0,526	0,366
998	0,538	0,426	0,587	0,461	0,536	0,376	0,501	0,352

Table 24 Pre- and Post-irradiation Electrical Resistivity Measurements (in $\text{m}\Omega \text{ cm}$)

Graphite grade	AGL/SM 1 - 24				Toyo Tanso / 1G - 11			
Sample number	221	II	221	II	224	\perp	224	\perp
Irradiation temperature ($^{\circ}\text{C}$)	-	1085	-	1100	-	1075	-	1085
Neutron fluence (10^{21}cm^{-2} EDN)	-	2,38	-	2,38	-	2,10	-	2,48
Temperature of measurement ($^{\circ}\text{C}$) ↓								
100	0,707	1,760	0,659	1,663	0,843	2,052	0,919	2,204
200	0,660	1,550	0,618	1,458	0,778	1,844	0,845	1,976
299	0,641	1,406	0,599	1,321	0,737	1,685	0,801	1,812
399	0,633	1,286	0,592	1,205	0,715	1,541	0,773	1,661
499	0,631	1,191	0,595	1,116	0,704	1,427	0,759	1,537
598	0,637	1,121	0,600	1,051	0,702	1,336	0,754	1,439
698	0,651	1,068	0,616	1,002	0,706	1,262	0,756	1,359
798	0,667	1,026	0,632	0,964	0,713	1,202	0,764	1,292
898	0,683	0,997	0,647	0,939	0,722	1,155	0,770	1,236
998	0,704	0,977	0,671	0,918	0,738	1,117	0,786	1,197

Table 25 Results of the Tensile Measurements on IG-11

Sample Number	R_m^0 (N/mm ²)	A_T^0 (mm/m)	E_S^0 (N/mm ²)
191	22,2	3,92	5,65 x 10 ³
2	21,6	3,51	6,16
3	24,8	4,77	5,19
4	24,3	4,41	5,50
5	23,4	4,54	5,16
6	22,3	4,16	5,38
7	23,9	3,96	6,04
8	23,6	4,21	5,61
9	23,7	4,34	5,46
200	22,7	4,07	5,58
1	24,1	4,50	5,37
2	23,8	4,52	5,27
3	21,3	3,88	5,49
4	21,4	4,11	5,21
5	22,8	4,68	4,86
6	20,8	4,08	5,09
7	21,3	4,11	5,19
8	21,9	3,99	5,48
9	22,2	4,52	4,90
210	22,4	4,22	5,32
1	22,5	4,28	5,25
2	21,9	3,99	5,48
3	23,9	4,70	5,09
4	22,9	4,34	5,27
5	22,8	4,42	5,15
6	24,3	4,72	5,16
7	21,8	4,27	5,09
8	22,3	4,41	5,06
9	22,8	4,44	5,13
220	24,8	4,93	5,02

Table 26. Results of the Ring Compressive Measurements on the Rings $20\phi \times 10\phi \times 10$ of Unirradiated IG-11

Sample Number	F_m^0 (N)	ΔL_t^0 (mm)	S_R^0 (N/mm 2)	E_R^0 (N/mm 2)
101	532,0	0,1216	32,5	$4,39 \times 10^3$
102	495,2	0,1096	30,2	4,53
103	544,0	0,1216	33,1	4,50
104	572,0	0,1291	34,9	4,45
105	570,0	0,1242	34,7	4,61
106	537,6	0,1164	32,8	4,64
107	362,0	0,0804	22,1	4,52
108	509,2	0,1140	31,1	4,49
109	512,0	0,1120	31,2	4,59
110	468,0	0,1016	28,5	4,63
111	444,0	0,08864	27,1	5,03
112	528,0	0,1152	32,2	4,61
113	540,8	0,1180	32,9	4,60
114	544,0	0,12064	33,2	4,53
115	540,0	0,1192	32,9	4,55
116	524,0	0,1037	31,9	5,07
117	554,4	0,1224	33,8	4,55
118	458,0	0,1012	27,9	4,54
119	458,0	0,1039	27,9	4,42
120	516,0	0,1196	31,5	4,33
121	556,0	0,1232	33,9	4,53
122	486,0	0,1080	29,6	4,51
123	448,8	0,0944	27,3	4,77
124	486,0	0,1056	29,5	4,62
125	488,0	0,1068	29,7	4,59
126	505,2	0,1072	30,8	4,73
127	430,0	0,0904	26,1	4,77
128	456,0	0,0944	27,7	4,85
129	511,2	0,1156	31,1	4,44

Table 27 Results of the Ring Compressive Measurements on the Rings $10\phi \times 5\phi \times 5$ of Unirradiated IG-11

Sample Number	E_m^0 (N)	ΔL_t^0 (mm)	S_R^0 (N/mm 2)	E_R^0 (N/mm 2)
141	156,0	0,07176	38,1	$4,37 \times 10^3$
142	153,4	0,07136	37,4	4,32
143	157,2	0,07264	38,3	4,35
144	128,0	0,05744	31,2	4,48
145	130,0	0,0592	31,7	4,43
146	163,0	0,0768	39,9	4,28
147	150,8	0,06976	36,9	4,36
148	160,4	0,0732	39,3	4,42
149	137,2	0,0656	33,5	4,21
150	162,6	0,07784	39,7	4,20
151	133,6	0,06184	32,5	4,34
152	128,0	0,05952	31,0	4,31
153	148,6	0,06936	36,1	4,31
154	140,0	0,066	34,0	4,26
155	130,0	0,0616	31,5	4,24
156	142,4	0,656	34,8	4,37
157	163,6	0,0768	39,9	4,29
158	156,4	0,0724	38,1	4,35
159	156,6	0,07344	38,2	4,29
160	146,0	0,06936	35,5	4,23
161	145,0	0,06704	35,3	4,35
162	149,0	0,0672	36,3	4,46
163	168,4	0,0764	41,0	4,43
164	151,0	0,0664	36,7	4,57
165	160,2	0,0728	38,9	4,42
166	135,2	0,0624	33,0	4,35
167	147,6	0,07024	36,0	4,22
168	142,8	0,0656	34,7	4,38
170	157,6	0,076	38,4	4,17

Table 28 Results of Ring Compressive Tests for the Rings
 $20\phi \times 10\phi \times 10$ from Irradiated IG-11

Sample Number	F_m^+ (N)	L_t^+ (mm)	S_R^+ (N/mm 2)	E_R^+ (N/mm 2)	Fluence (EDN) 10 21 /cm 2
1 - 131	635,2	0,084	39,7	$7,66 \cdot 10^3$	2,4
2 - 132	596,0	0,08208	37,1	7,34	2,4
3 - 133	584,0	0,0784	39,9	7,52	2,4
4 - 134	628,0	0,0864	38,0	7,33	2,3
5 - 135	657,2	0,0892	40,8	7,44	2,3
6 - 136	604,0	0,08416	37,5	7,26	2,2
7 - 137	607,2	0,0824	37,6	7,43	2,1
8 - 138	654,0	0,086	40,5	7,66	2,1
9 - 139	680,0	0,0904	42,1	7,58	2,0
10- 140	628,0	0,0848	38,7	7,47	1,9

Table 29 Results of Ring Compressive Tests for the Rings
10φ × 5φ × 10 from Irradiated IG-11

Sample Number	F_m^+ (N)	L_t^+ (mm)	S_R^+ (N/mm ²)	E_R^+ (N/mm ²)	Fluence (EDN) $10^{21}/\text{cm}^2$
1 - 171	180,8	0,0548	45,1	$6,71 \cdot 10^3$	2,4
2 - 172	170,4	0,0524	42,4	6,61	2,4
3 - 173	175	0,054	43,7	6,58	2,4
4 - 174	147	0,04509	36,5	6,48	2,4
5 - 175	158	0,0488	39,5	6,57	2,4
6 - 176	146	0,0456	36,5	6,51	2,4
7 - 177	180,4	0,05728	45,5	6,40	2,3
8 - 178	163	0,05	40,9	6,62	2,3
9 - 179	157	0,0504	39,2	6,32	2,3
10 - 180	-----	broken	-----	-----	-----
11 - 181	-----	broken	-----	-----	-----
12 - 182	153,4	0,048	38,3	6,48	2,2
13 - 183	140	0,04184	34,9	6,79	2,1
14 - 184	162,4	0,0496	40,4	6,65	2,1
15 - 185	156,4	0,04744	38,9	6,69	2,1
16 - 186	160,4	0,04744	39,7	6,84	2,0
17 - 187	170	0,05136	42,2	6,70	2,0
18 - 188	178	0,05376	44,5	6,73	2,0
19 - 189	166	0,0476	41,3	7,09	1,9
20 - 190	170	0,04904	42,3	7,02	1,9

Table 30 Mechanical properties of IG-11 graphite measured in
JAERI

No.	Block number	Density * (g/cm ³)	Young's modulus (10 ³ N/mm ²)	Tensile strength (N/mm ²)	Compressive strength (N/mm ²)	Bending strength (N/mm ²)
1	TEN- 2	1.753	9.52	26.5	70.0	31.6
2	6	1.765	10.0	21.9	70.0	36.2
3	10	1.756	9.84	22.5	67.2	31.2
4	18	1.757	9.82	25.3	71.2	29.0
5	20	1.743	9.29	23.8	66.8	31.2
6	22	1.758	9.70	23.8	69.4	31.6
7	23	1.754	9.36	22.0	63.6	32.5
8	26	1.756	9.66	20.8	66.6	32.7
9	30	1.756	9.07	21.7	65.7	30.7
10	34	1.758	9.63	22.7	64.6	34.5
11	38	1.759	9.43	21.7	68.3	36.3
12	39	1.753	9.22	23.4	68.1	34.3
13	45	1.756	9.16	22.0	63.9	35.4
14	50	1.758	9.80	23.8	66.3	33.3
15	TEN-57	1.757	9.25	23.0	64.9	32.7
Mean value		1.756 ± 0.005	9.52 ± 0.29	23.0 ± 1.5	67.1 ± 2.4	32.9 ± 2.1

* Measured using the bending specimens.

Table 31 Statistically Estimated Values for the Results of the Tensile Samples

Property	\bar{x}	s _*	v	n	95 % VB für μ
		(%)			(%)
R _m ⁰ (N/mm ²)	22,8216	1,1086	4,86	30	22,4 - 23,2
A _t ⁰ (mm/m)	4,301	0,312	7,26	30	4,18 - 4,42
E _S ⁰ (N/mm ²)	$5,3217 \times 10^3$	$0,2939 \times 10^3$	5,52	30	$5,21 \times 10^3 - 5,43 \times 10^3$

Table 32 Statistically Estimated Values for the Results of the Ring Samples

Ring Type	Property	\bar{x}	s	v	n	95 % VB für μ
				(%)		(%)
unirrad. rings	S _R ⁰ (N/mm ²)	30,6322	29,226	9,54	29	29,5 - 31,7
20 Ø x 10 Ø x 10	E _R ⁰ (N/mm ²)	$4,600 \times 10^3$	$0,170 \times 10^3$	3,69	29	$4,53 \times 10^3 - 4,66 \times 10^3$
rings	S _R ⁰ (N/mm ²)	36,1436	2,9107	8,05	29	35,0 - 37,2
10 Ø x 5 Ø x 5	E _R ⁰ (N/mm ²)	$4,337 \times 10^3$	$0,092 \times 10^3$	2,12	29	$4,30 \times 10^3 - 4,37 \times 10^3$
irrad. rings	S _{R+} ⁺ (N/mm ²)	39,2907	1,6138	4,11	10	38,1 - 40,4
20 Ø x 10 Ø x 10	E _{R+} ⁺ (N/mm ²)	$7,468 \times 10^3$	$0,138 \times 10^3$	1,85	10	$7,37 \times 10^3 - 7,57 \times 10^3$
rings	S _{R+} ⁺ (N/mm ²)	40,6532	3,0213	7,43	18	39,1 - 42,2
10 Ø x 5 Ø x 5	E _{R+} ⁺ (N/mm ²)	$6,656 \times 10^3$	$0,197 \times 10^3$	2,96	18	$6,56 \times 10^3 - 6,75 \times 10^3$

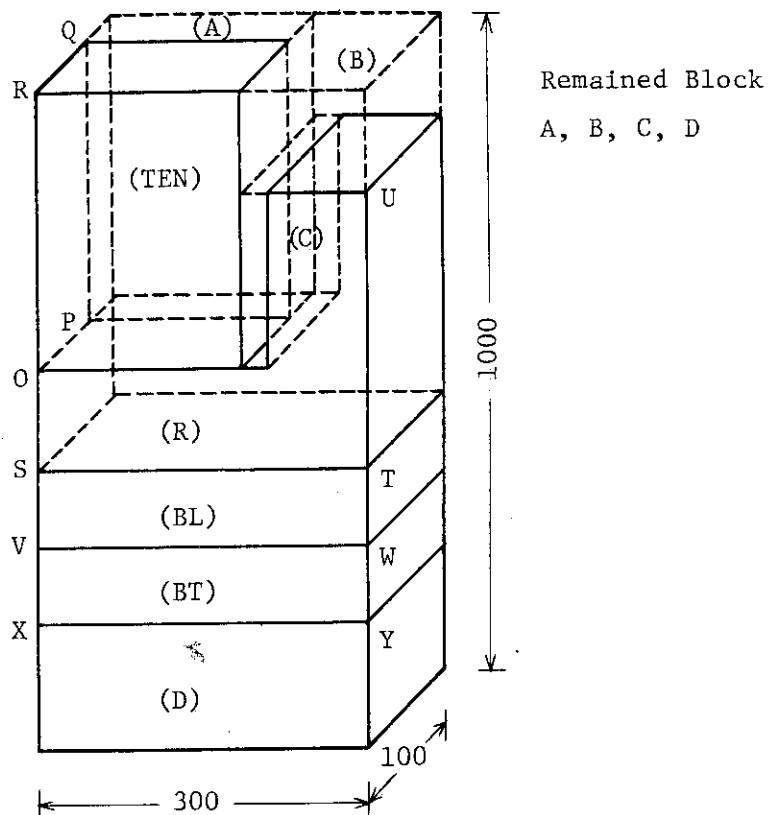


Fig. 1 IG-11 Sample map

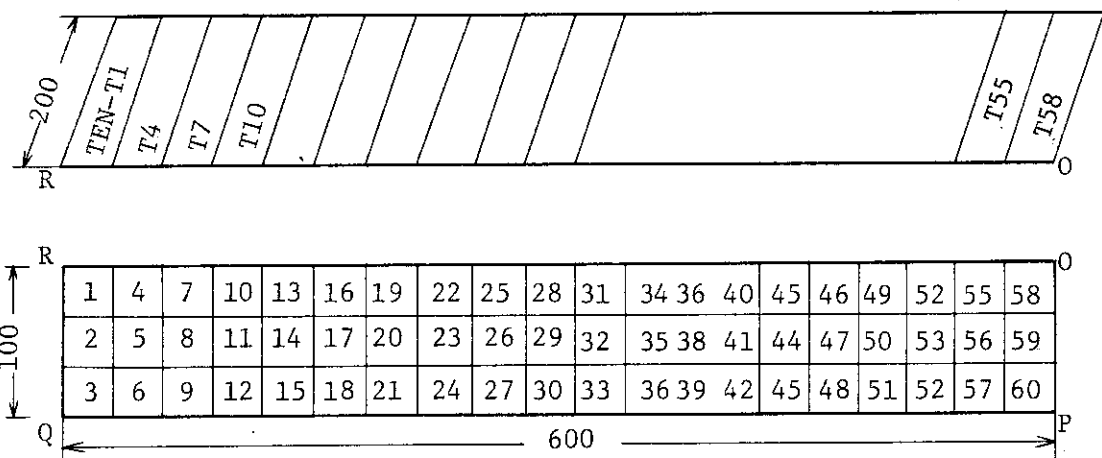


Fig. 2 IG-11 Sample map

(TEN Block)

Block size 100×200×600

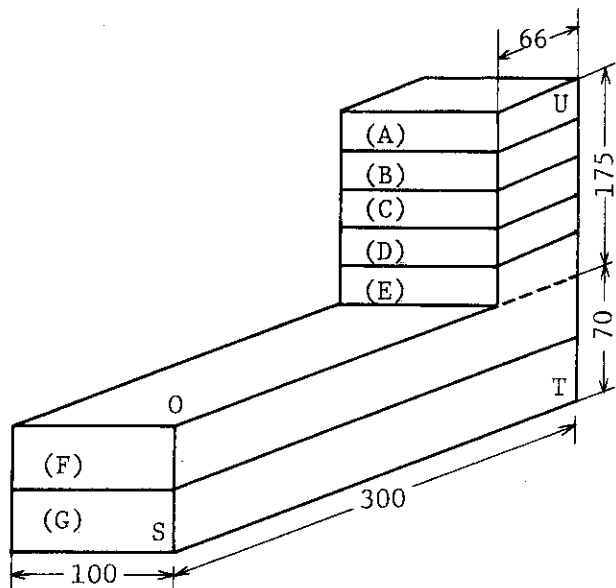


Fig. 3 IG-11 Sample map
(R Block)

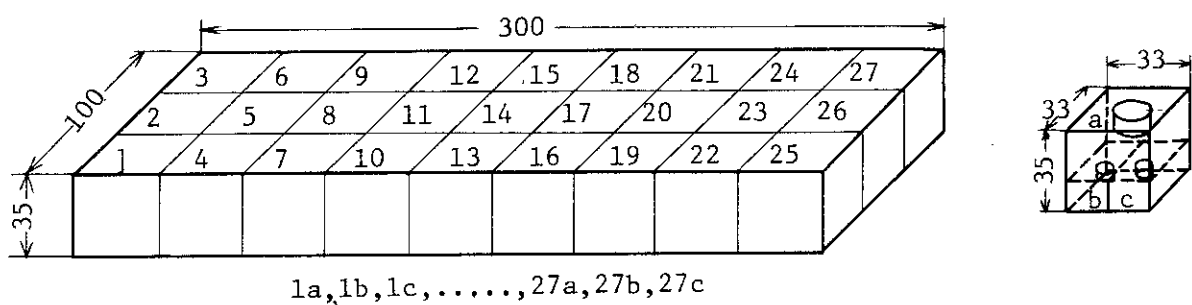


Fig. 4 IG-11 Sample map
(R Block)
Block size 70×100×300
Section F and G $\begin{pmatrix} \text{RO-T1} & \text{Ro-T54} \\ \text{RI-T1} \sim \text{RI-T108} \end{pmatrix}$

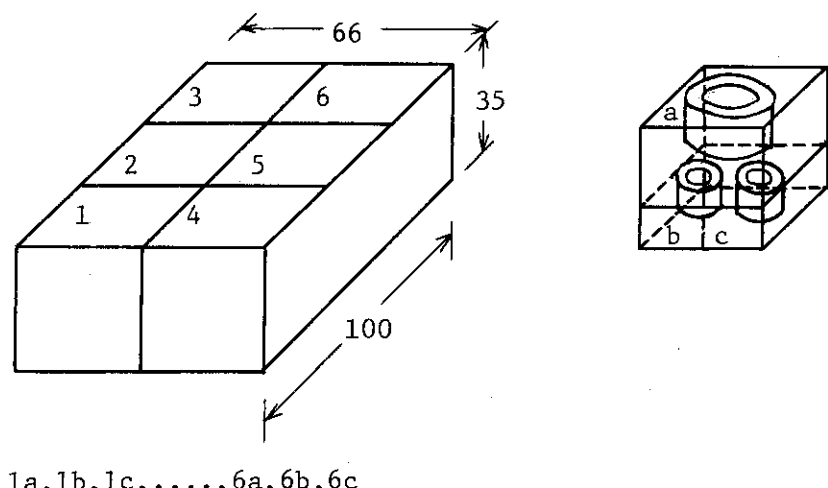
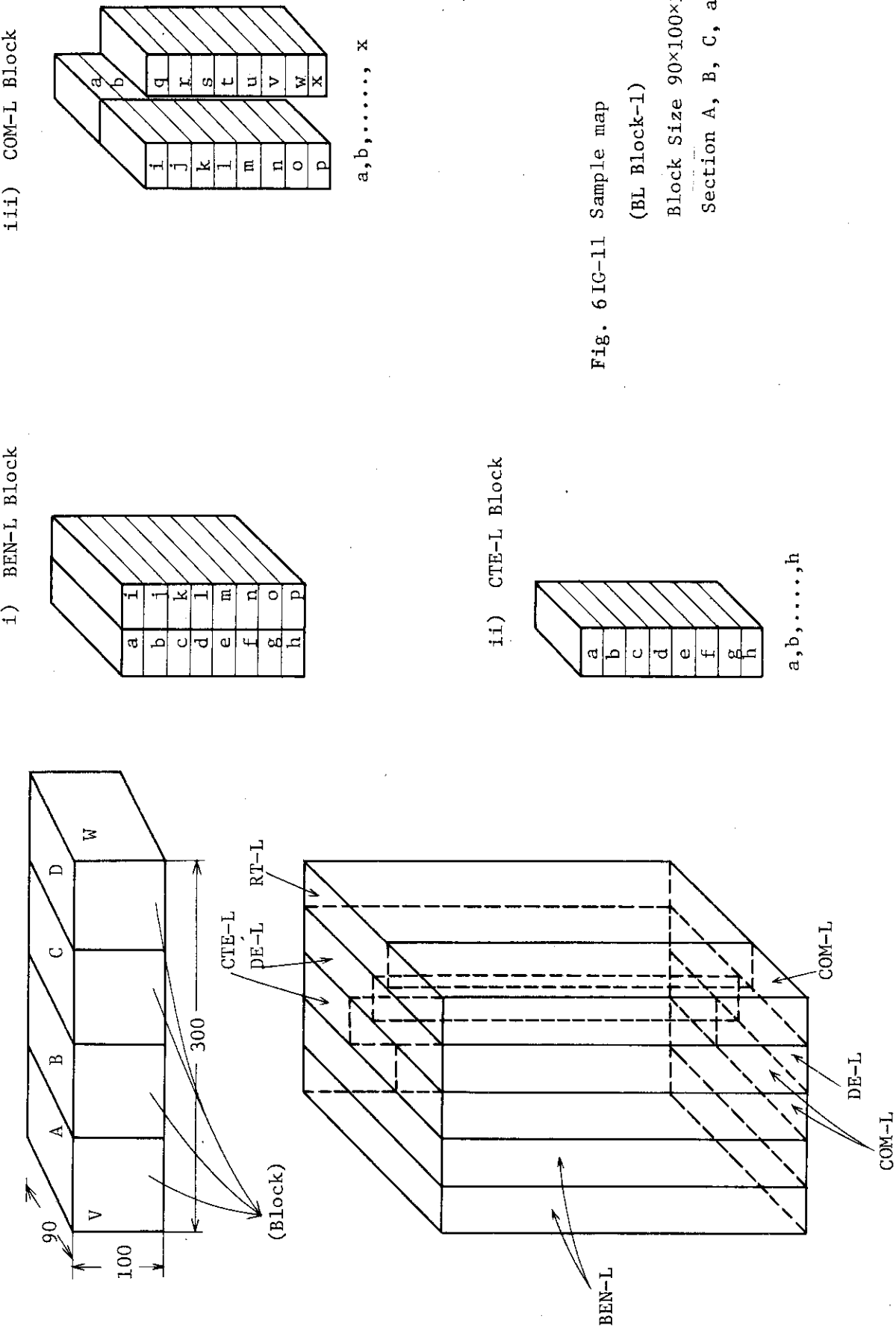
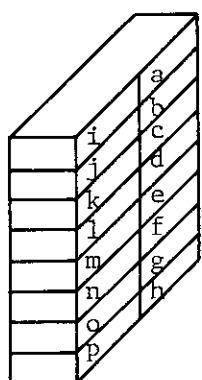


Fig. 5 IG-11 Sample map
(R Block)
Block size $35 \times 66 \times 100$
Section A, B, C, D and E $\left(\begin{array}{l} \text{ROT55} \sim \text{ROT84} \\ \text{RIT109} \sim \text{RIT168} \end{array} \right)$

Fig. 6 IG-11 Sample map
(BL Block-1)

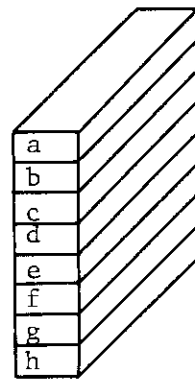
Block Size 90x100x300
Section A, B, C, and D

iv) DE-L Block



a, b, . . . , p

v) R-L Block

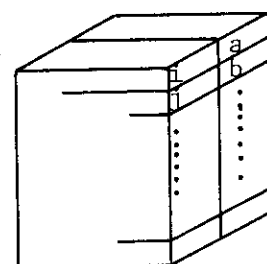
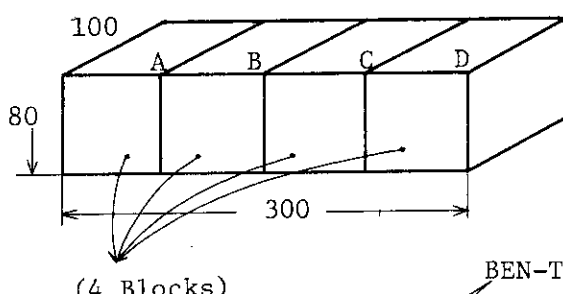


a, b, . . . , h

Fig. 7 IG-11 Sample map

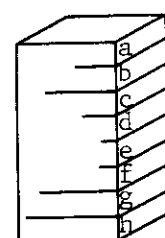
(BT Block-2)

i) BEN-T Block



a, b, . . . , p

ii) CTE-T Block



a, b, . . . , h

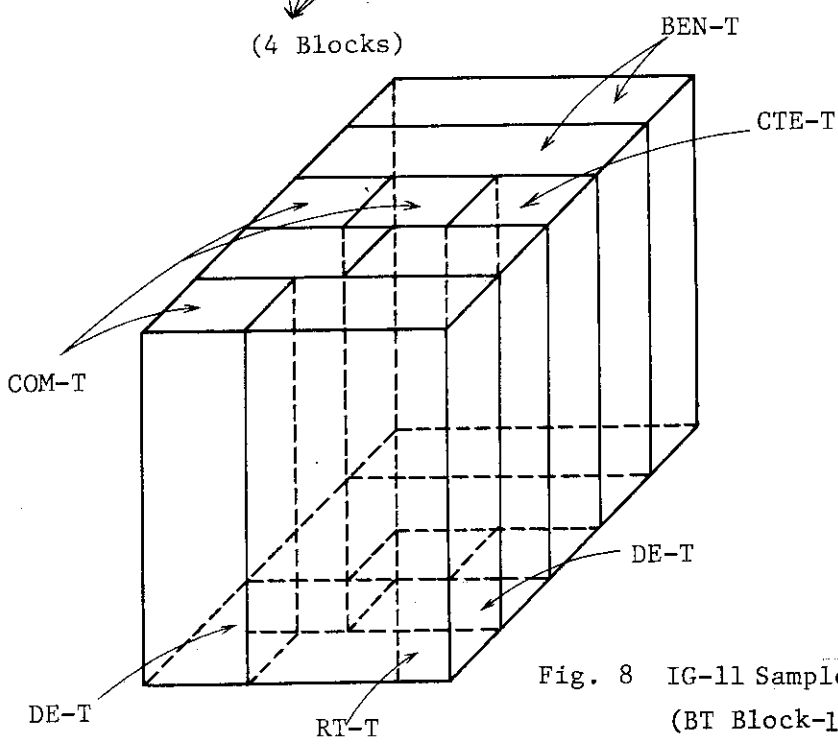


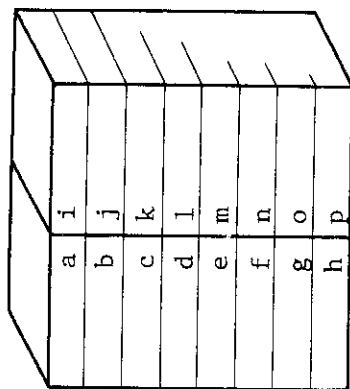
Fig. 8 IG-11 Sample map

(BT Block-1)

Block size 80×100×300

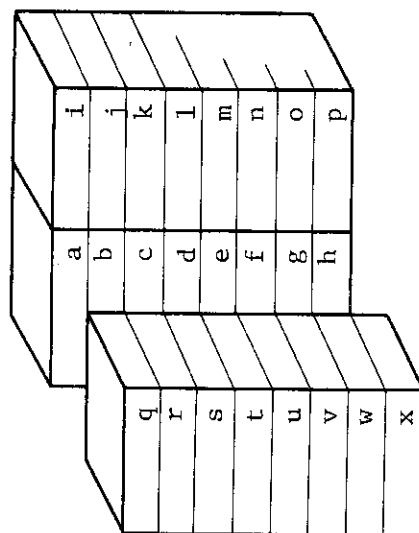
Section A, B, C, and D

iv) DE-T Block



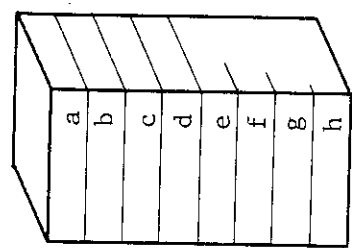
a, b, ..., p,

iii) COM-T Block



a, b, ..., x

v) R-T Block



a, b, ..., h

Fig. 9 Sample map (BT Block-2)

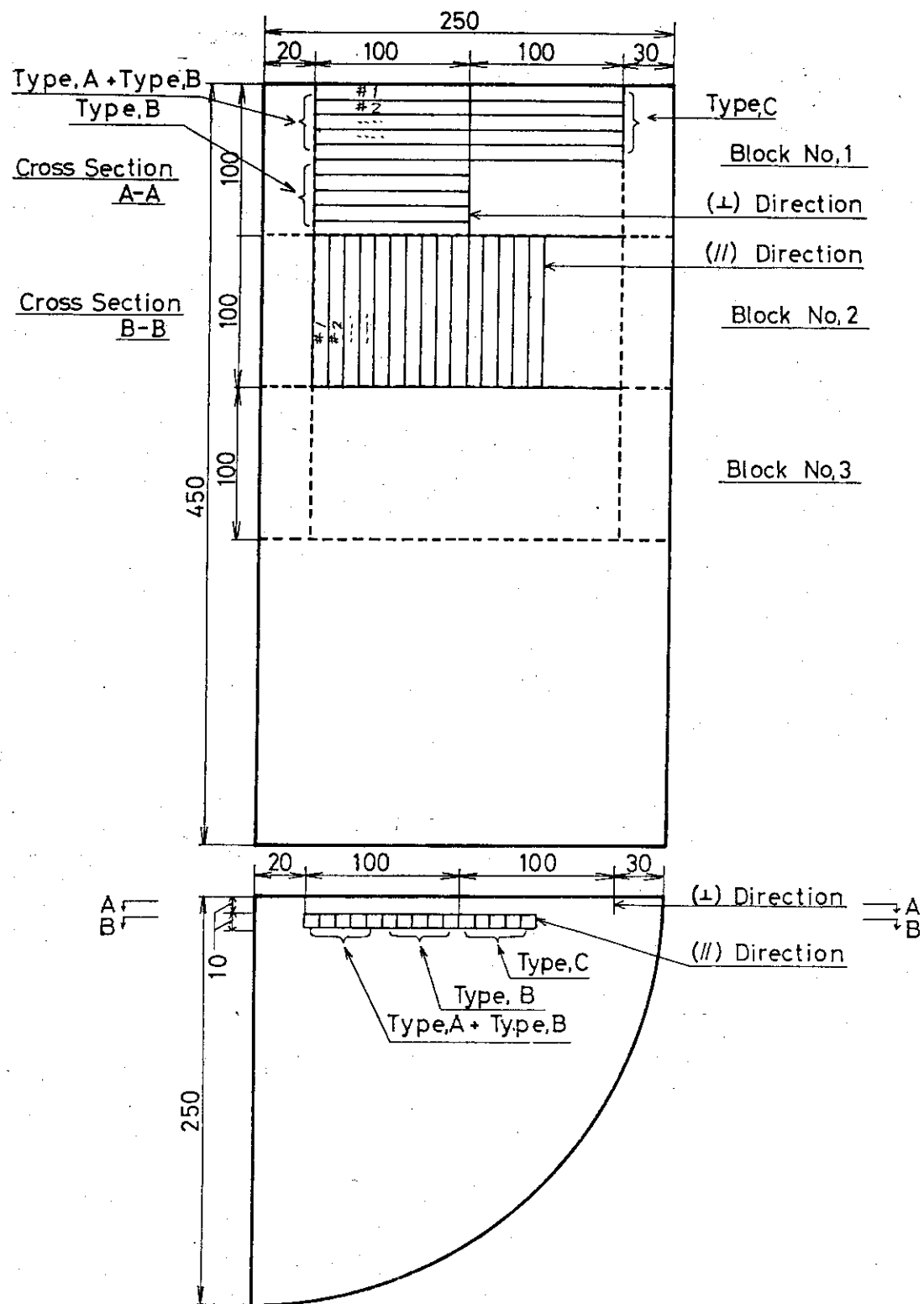
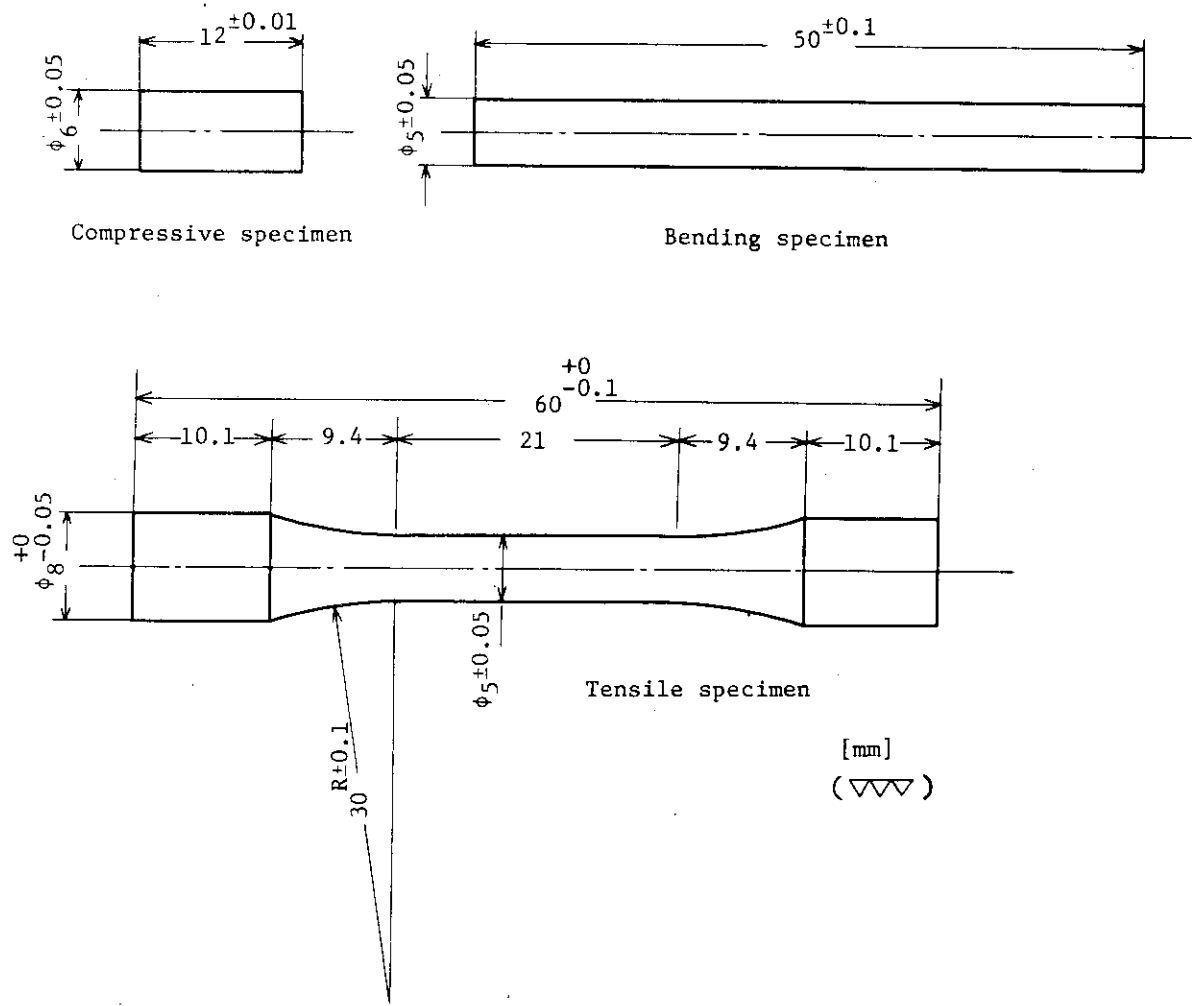


Fig. 10 The Locations of SM1-24 Graphite Specimens in a Block



Specimen							
Graphite Block		Tensile		Compressive		Bend	
No.	Size	Number of specimen	No.	Number of specimen	No.	Number of specimen	No.
TEN-T2	20 150mm	1	T-1	1	C-1	1	B-1
TEN-T6	"	1	T-2	1	C-2	1	B-2
TEN-T10	"	1	T-3	1	C-3	1	B-3
TEN-T18	"	1	T-4	1	C-4	1	B-4
TEN-T20	"	1	T-5	1	C-5	1	B-5
TEN-T22	"	1	T-6	1	C-6	1	B-6
TEN-T26	"	1	T-7	1	C-7	1	B-7
TEN-T30	"	1	T-8	1	C-8	1	B-8
TEN-T23	"	1	T-9	1	C-9	1	B-9
TEN-T34	"	1	T-10	1	C-10	1	B-10
TEN-T38	"	1	T-11	1	C-11	1	B-11
TEN-T39	"	1	T-12	1	C-12	1	B-12
TEN-T45	"	1	T-13	1	C-13	1	B-13
TEN-T50	"	1	T-14	1	C-14	1	B-14
TEN-T57	"	1	T-15	1	C-15	1	B-15

Fig. 11 The dimensions of the specimens

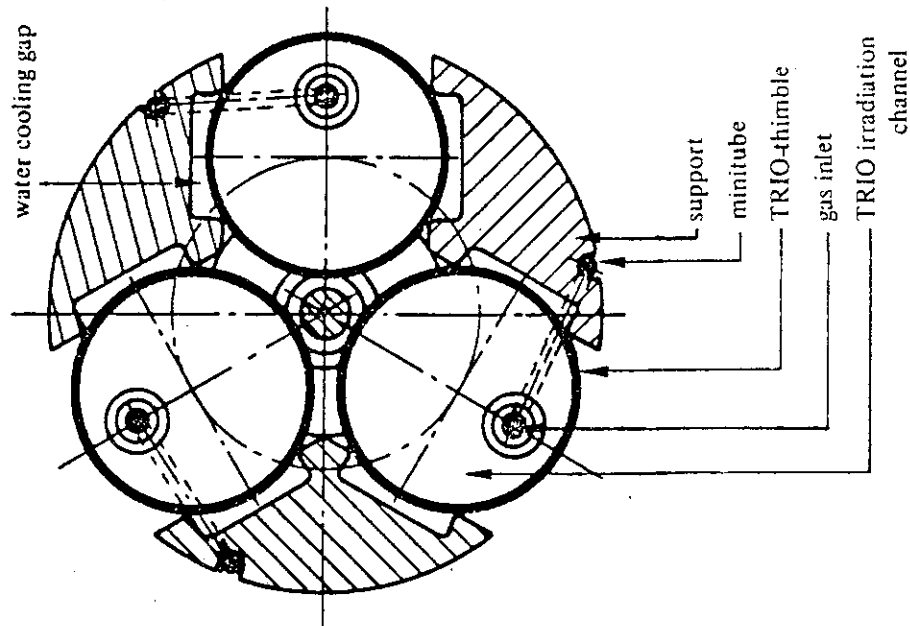


Fig. 13 Horizontal Cross Sections of the TRIO-Capsule without Sample Carriers

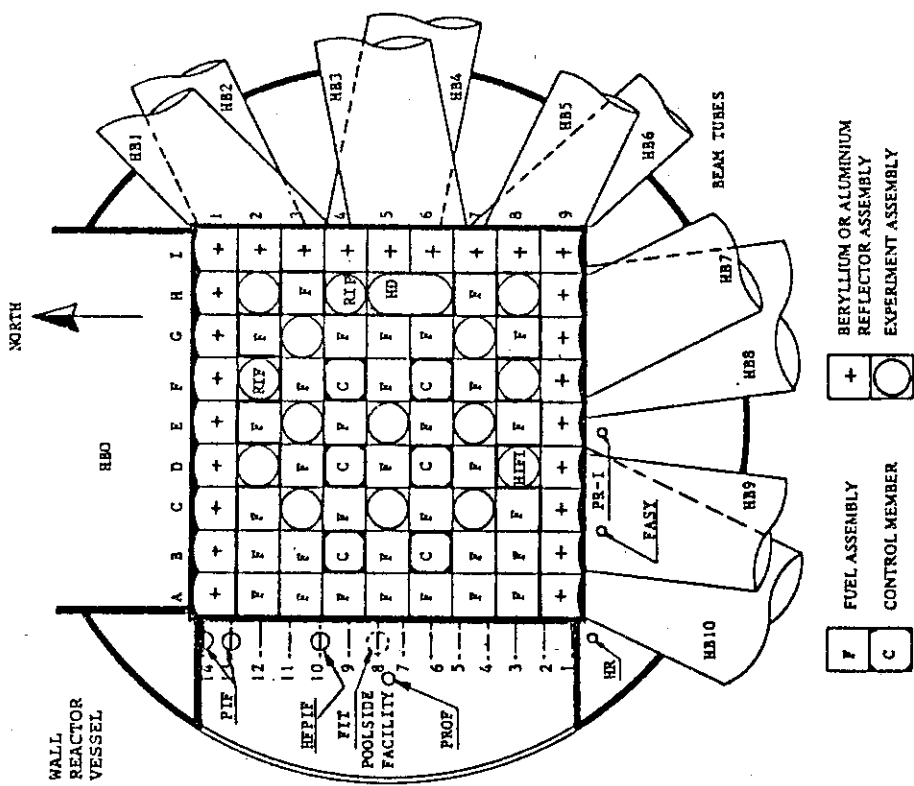


Fig. 12 HFR Core Configuration

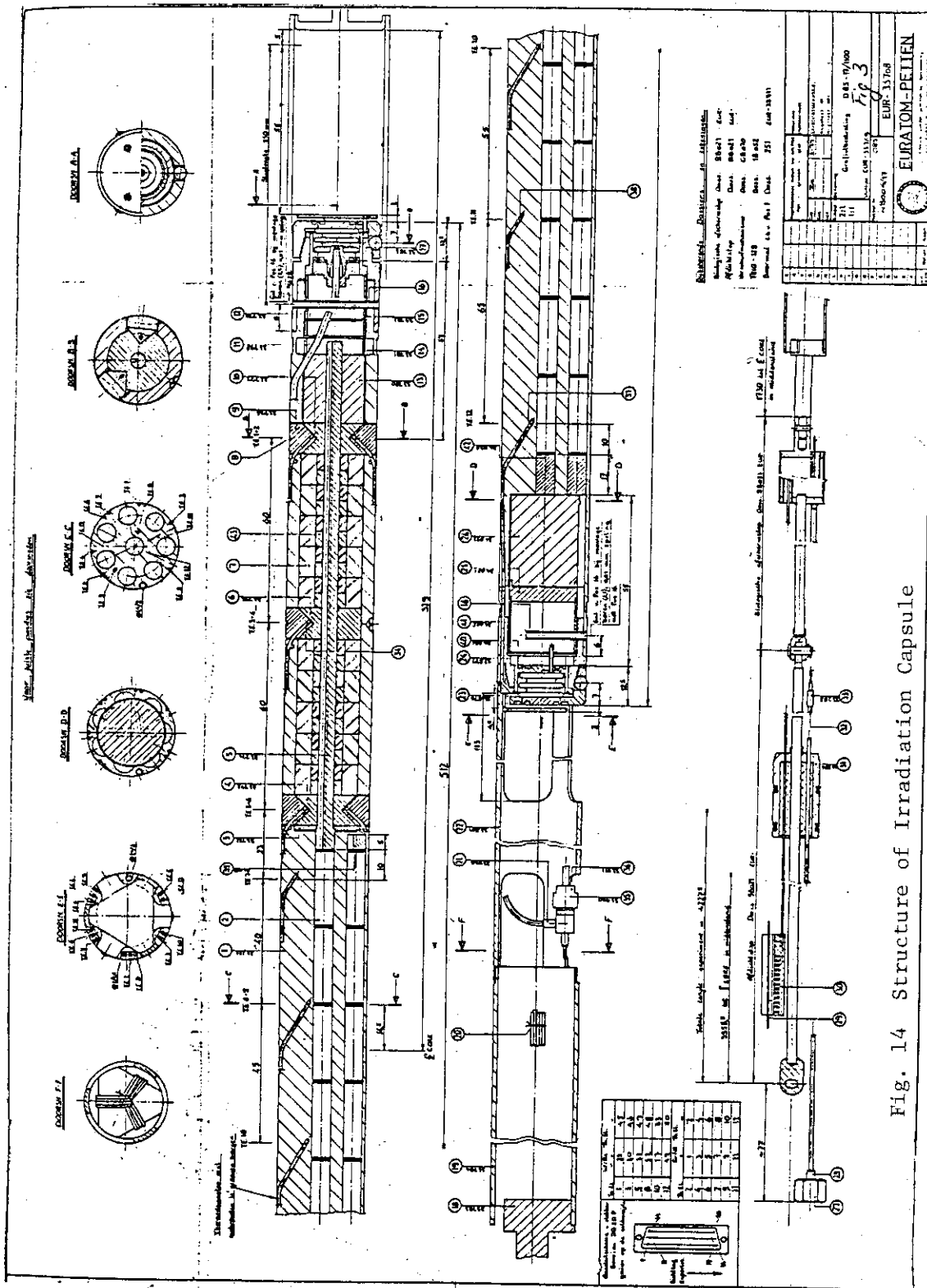
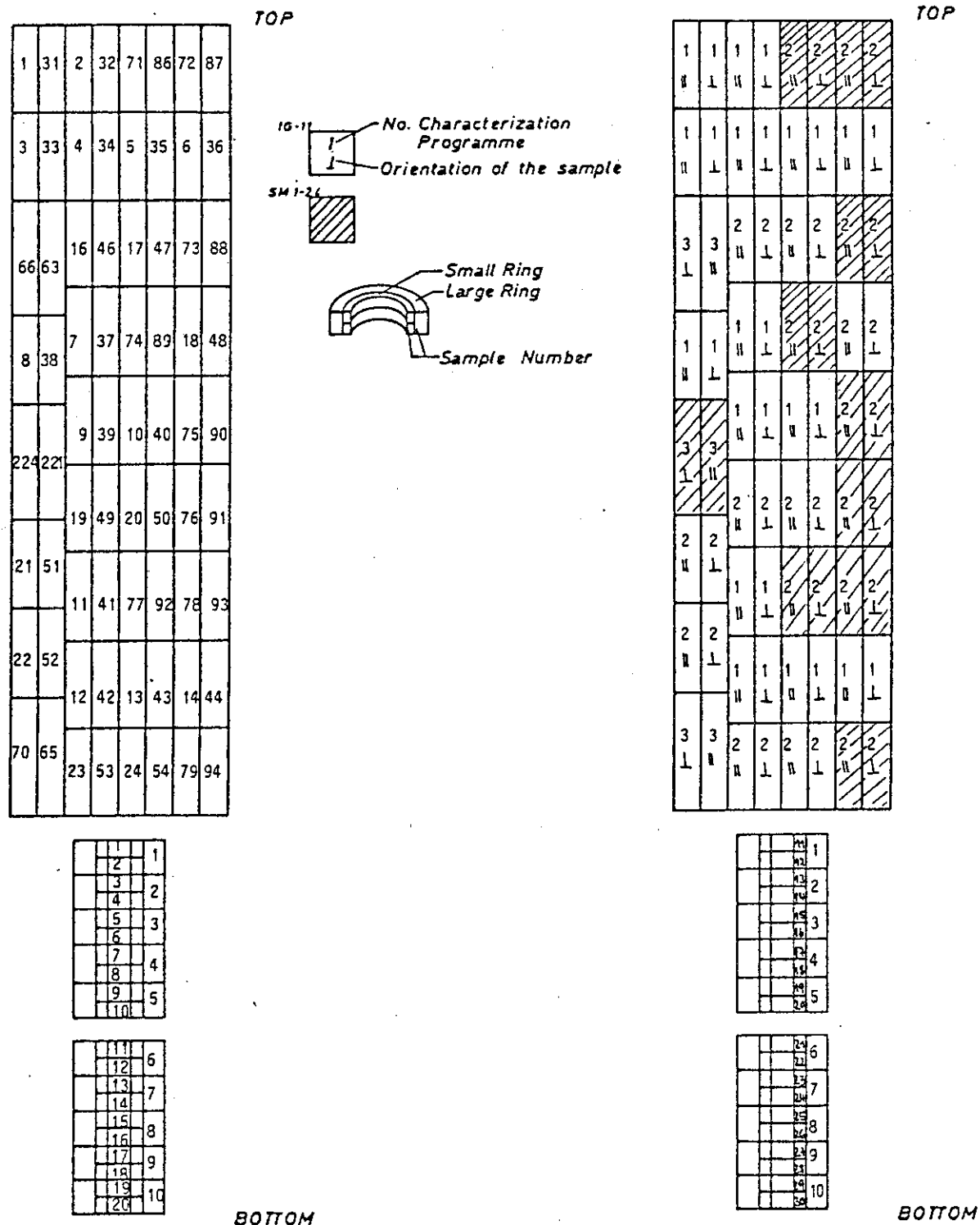


Fig. 14 Structure of Irradiation Capsule



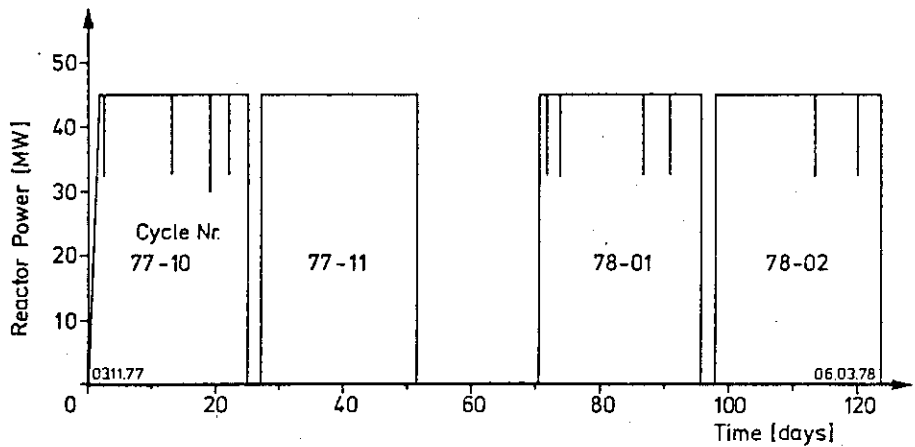
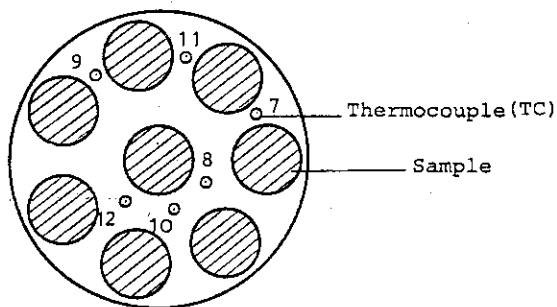
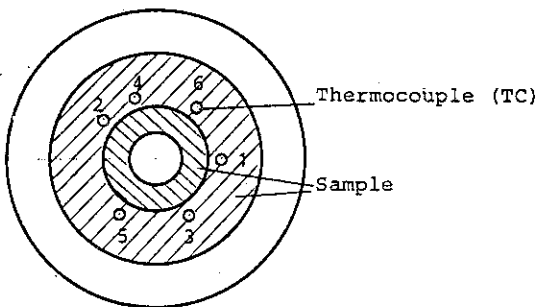


Fig. 17 Irradiation History for Experiment GG 14

Sample temperature for central samples = TC 7,9,11 + 20 °C
= TC 8,10,12 + 5 °C
for outer samples = TC 7,9,11 + 5 °C
= TC 8,10,12 - 10 °C



Upper Part of Sample Carrier



Lower Part of Sample Carrier

Sample temperature for central samples = TC + 5 °C
for outer samples = TC - 5 °C

Fig. 18 Radial Position of Thermocouples in Experiment HFR GG 14

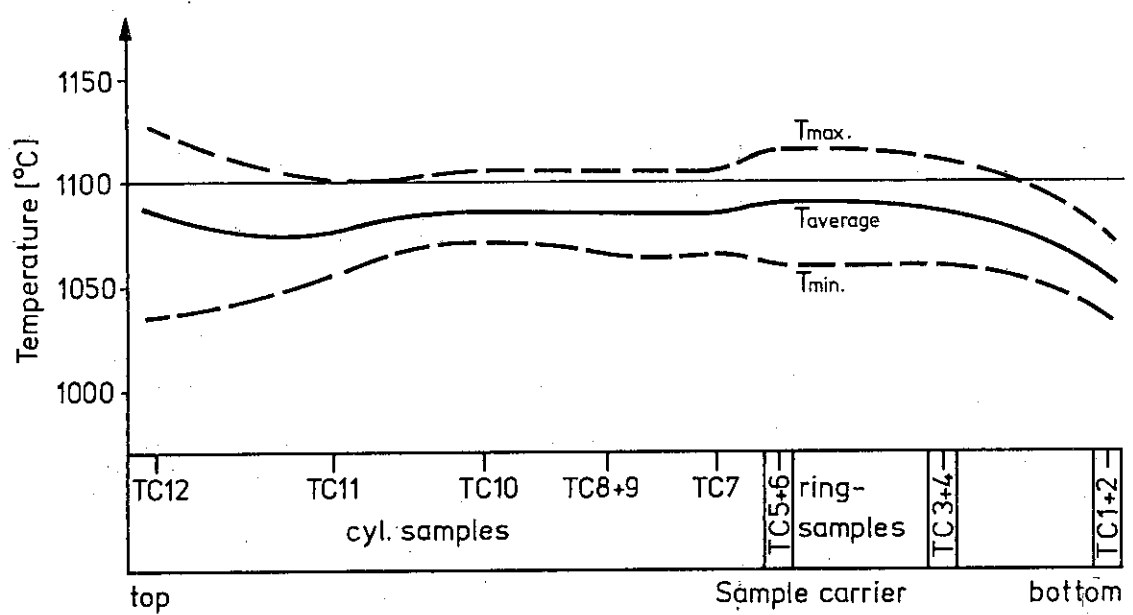


Fig. 19 Axial Temperature Distribution in Experiment

GG 14 - Periphery Samples

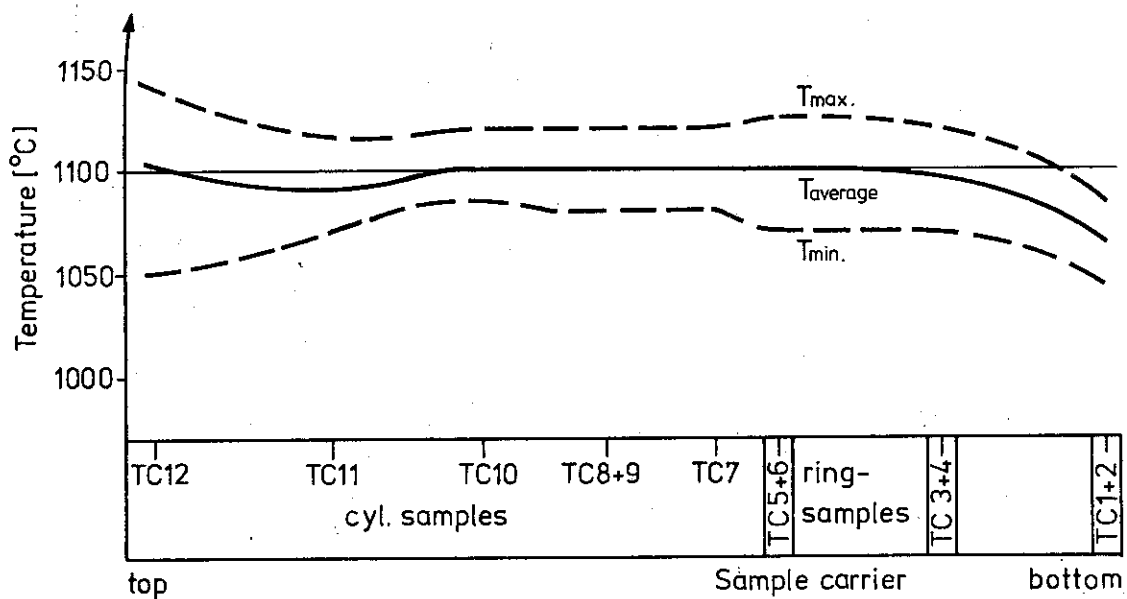


Fig. 20 Axial Temperature Distribution in Experiment

GG 14 - Central Samples

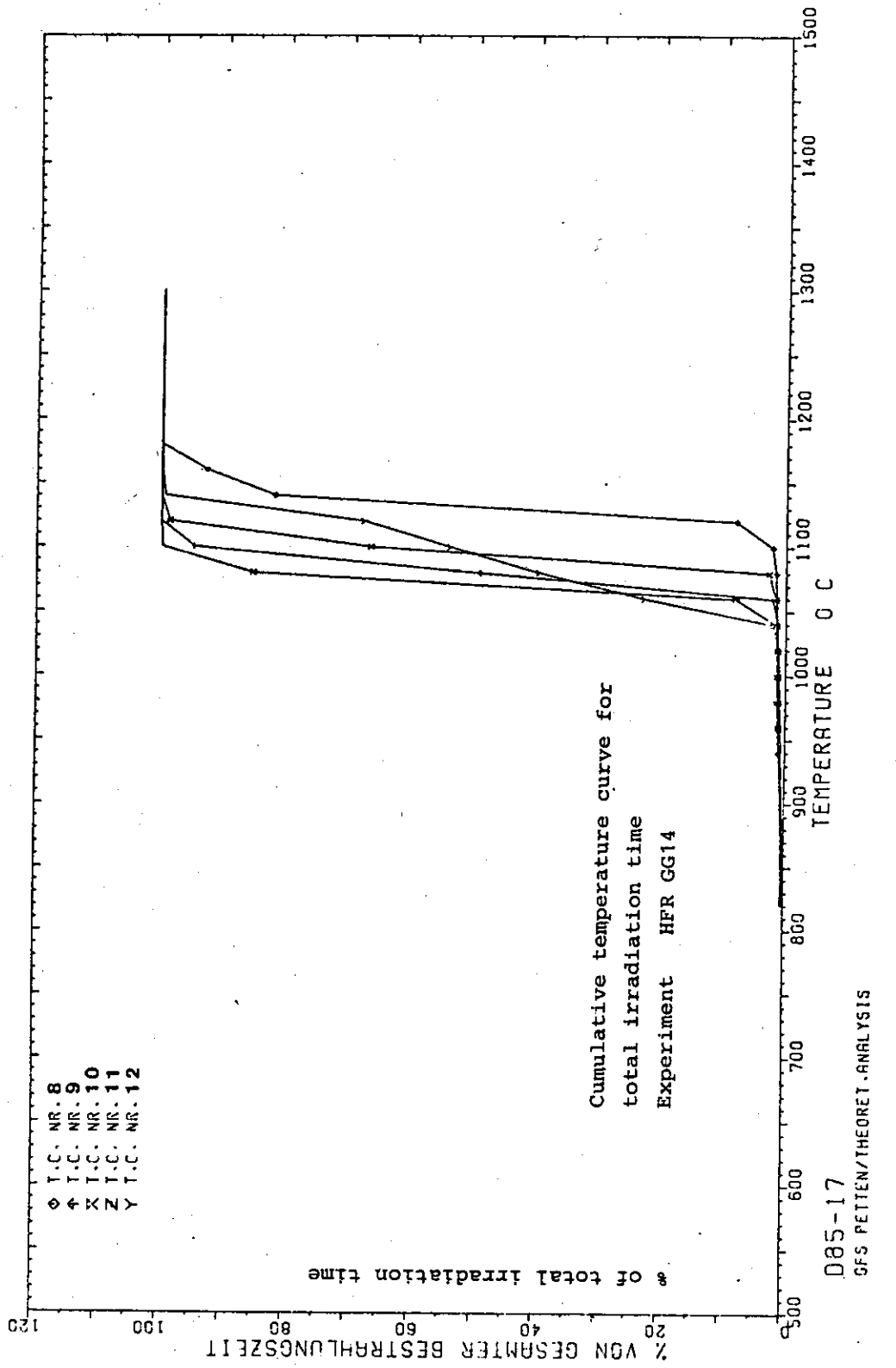


Fig. 21 Cumulative Temperature Curve for Total Irradiation Time
Experiment HFR GG 14

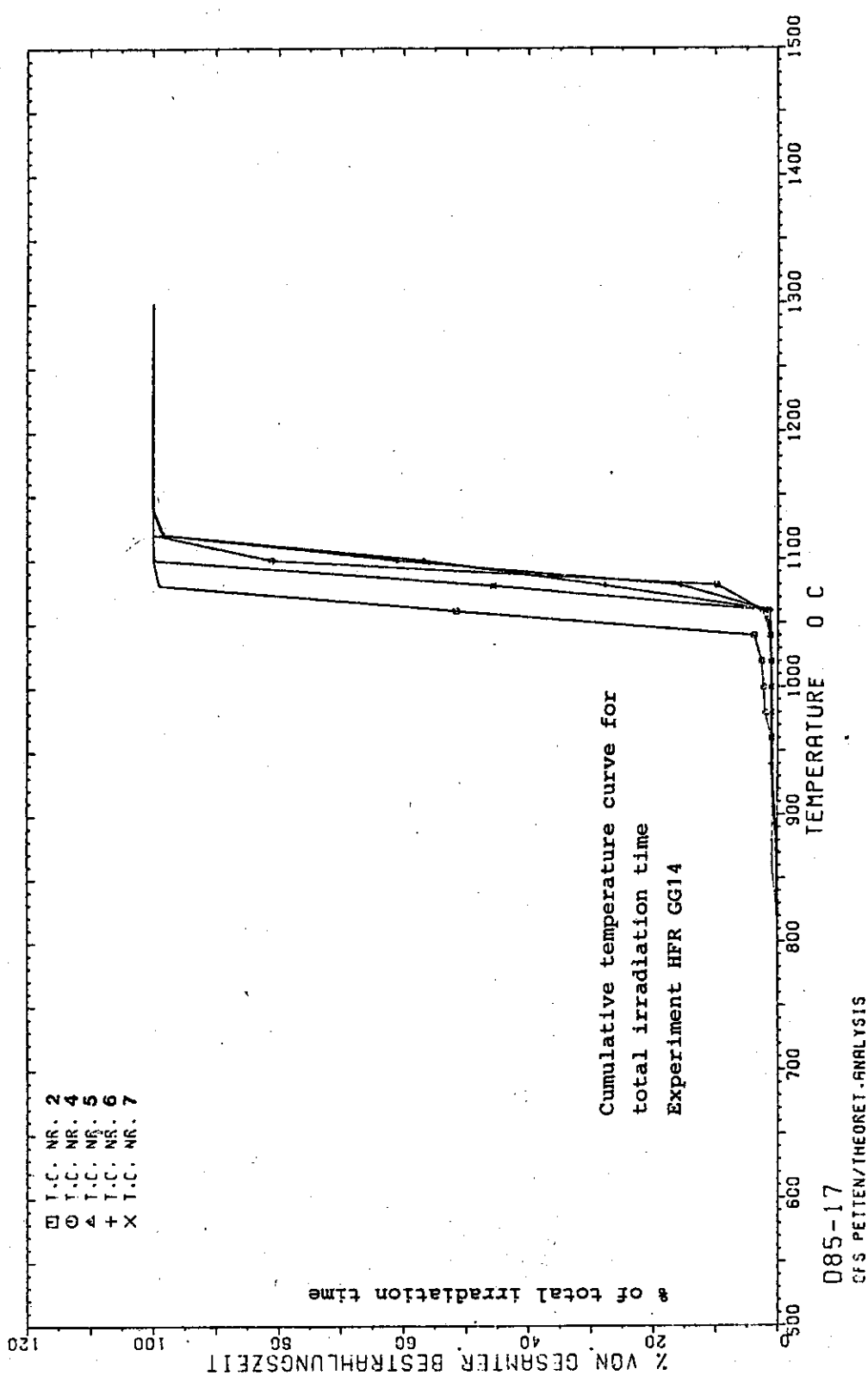


Fig. 22 Cumulative Temperature Curve for Total Irradiation Time
Experiment HFR GG 14

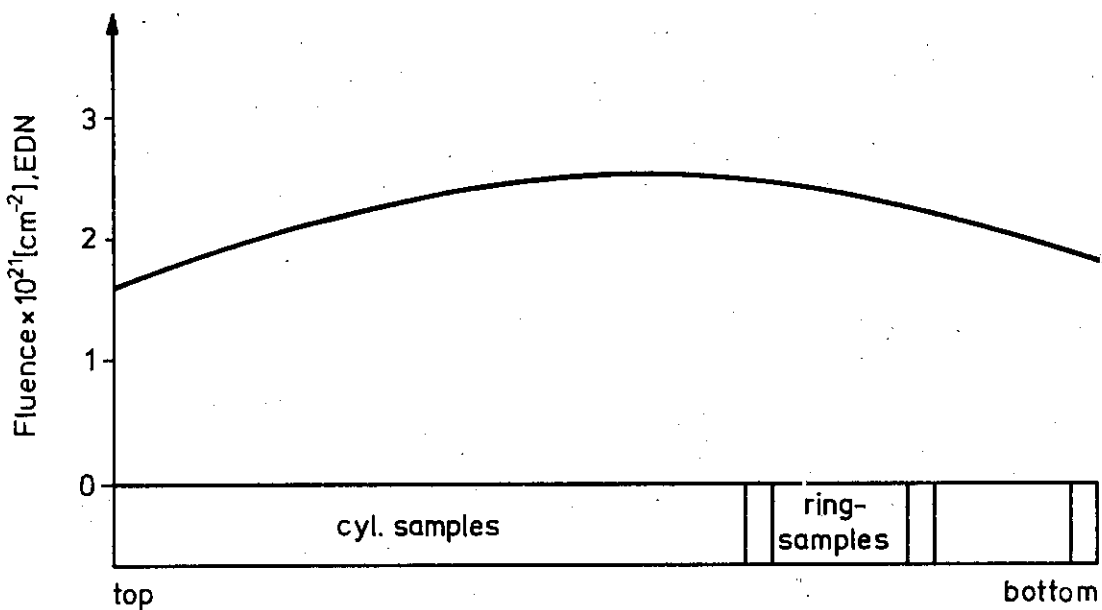


Fig. 23 Axial Fluence Distribution in Experiment GG 14

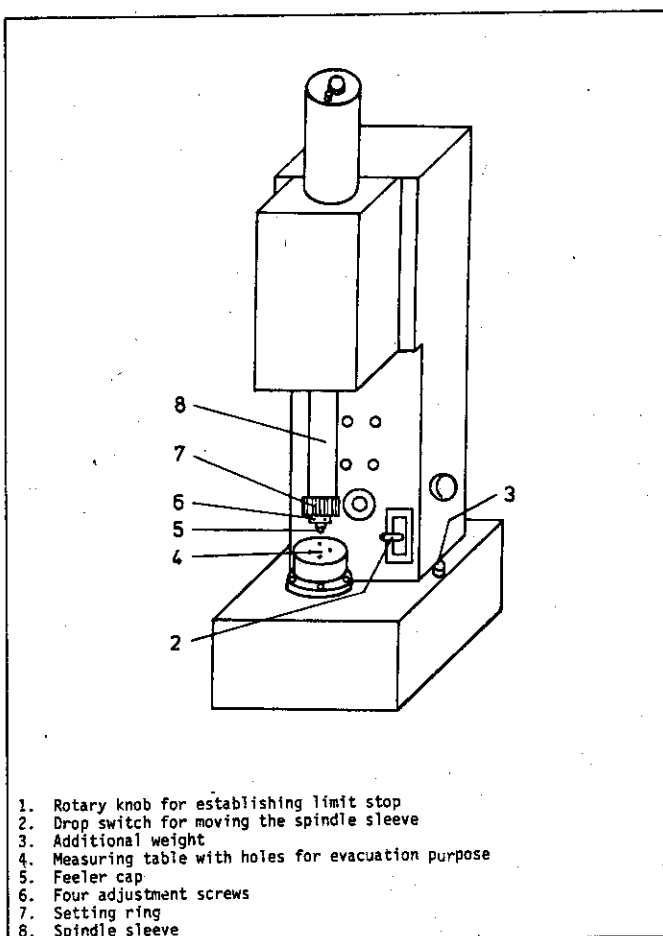


Fig. 24 Vertical Length Measuring Device

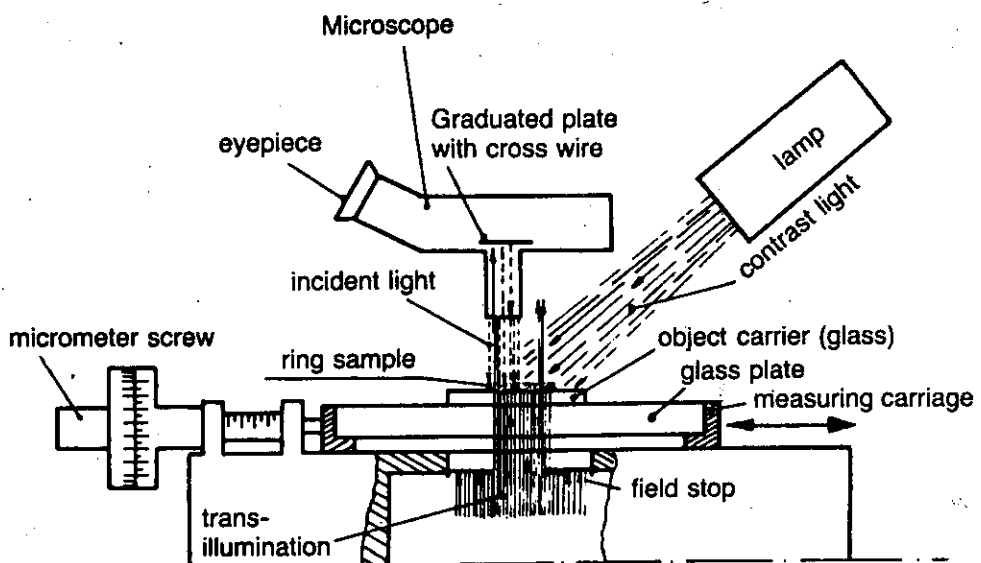


Fig. 25 Universal Measuring Microscope

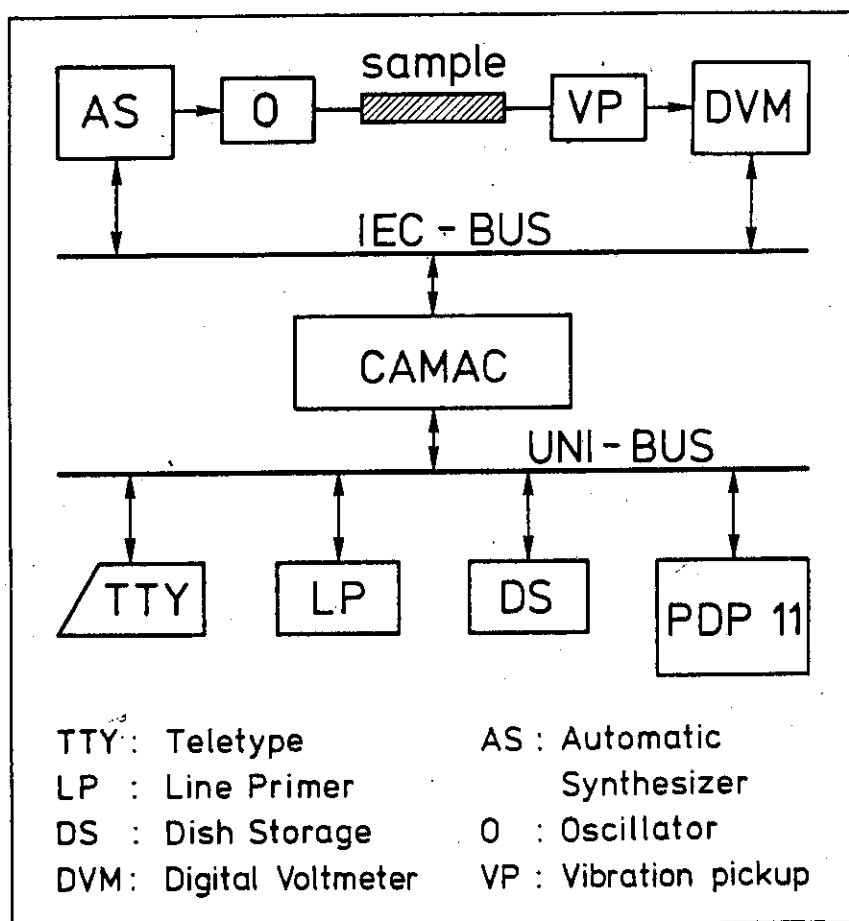


Fig. 26 Schematic Diagram for Young's Modulus Apparatus

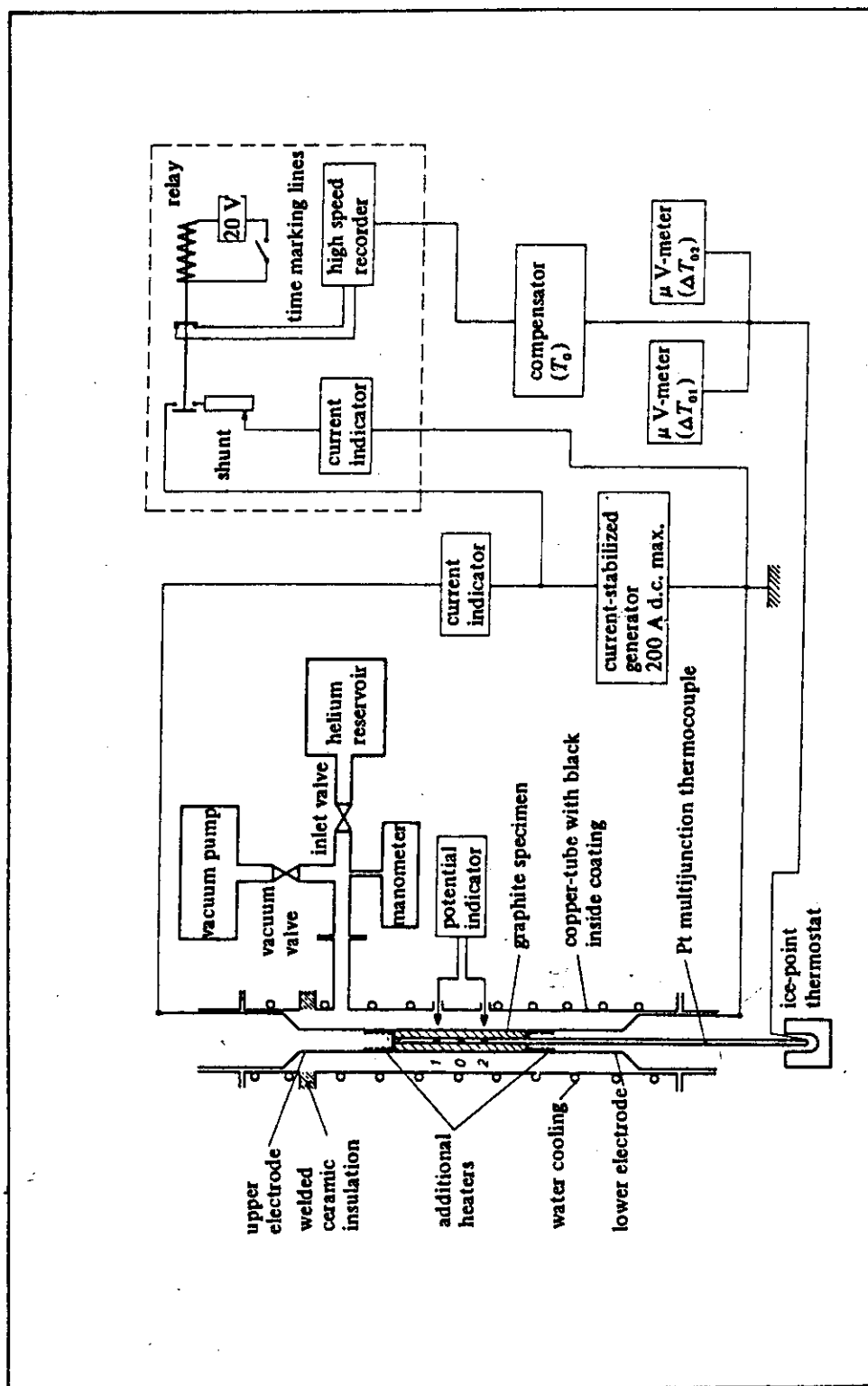


Fig. 27 Schematic Diagram of Thermal Conductivity Equipment

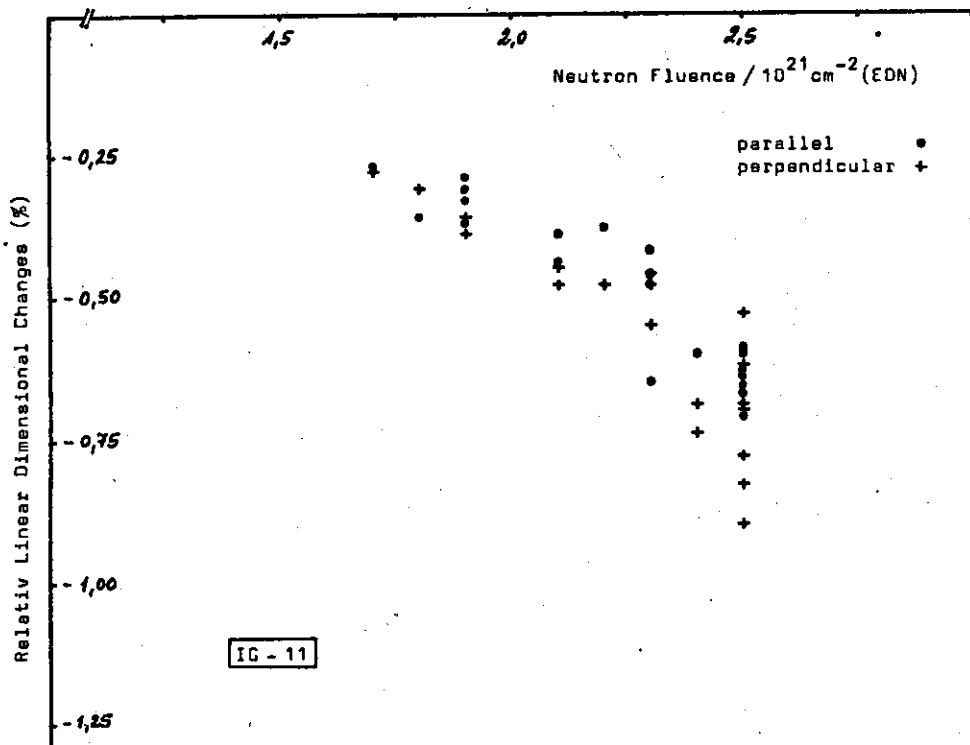


Fig. 28 Irradiation Induced Dimensional Changes for Graphite Grade IG-11

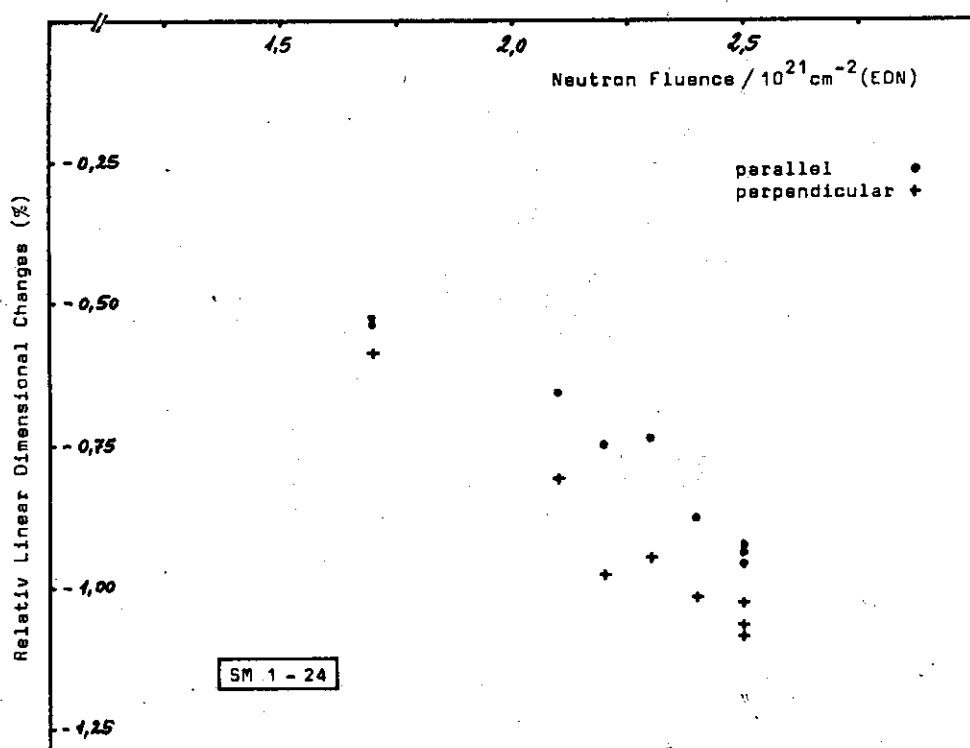


Fig. 29 Irradiation Induced Dimensional Changes for Graphite Grade SMI-24

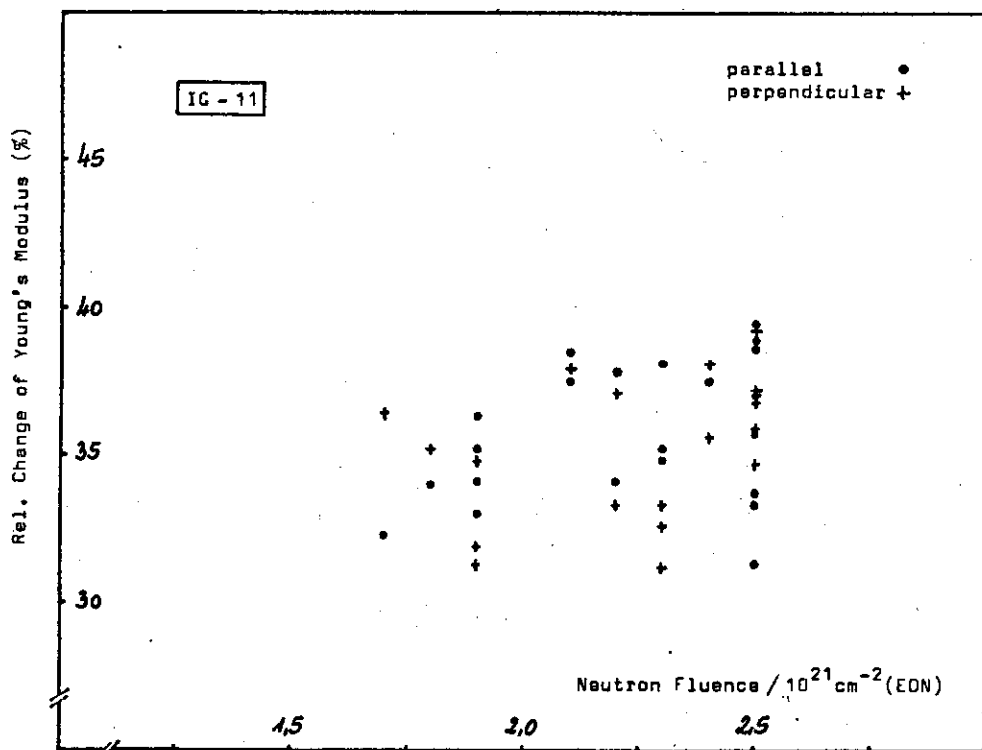


Fig. 30 Irradiation Induced Changes in Dynamic Young's Modulus for Graphite Grade IG-11

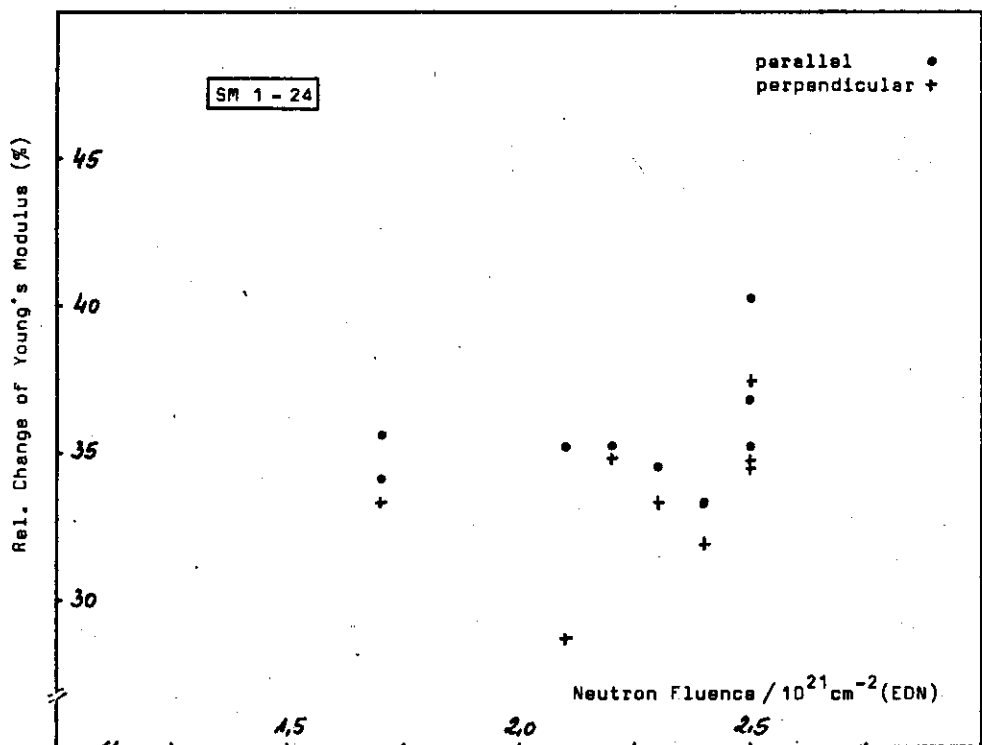


Fig. 31 Irradiation Induced Changes in Dynamic Young's Modulus for Graphite Grade SM1-24

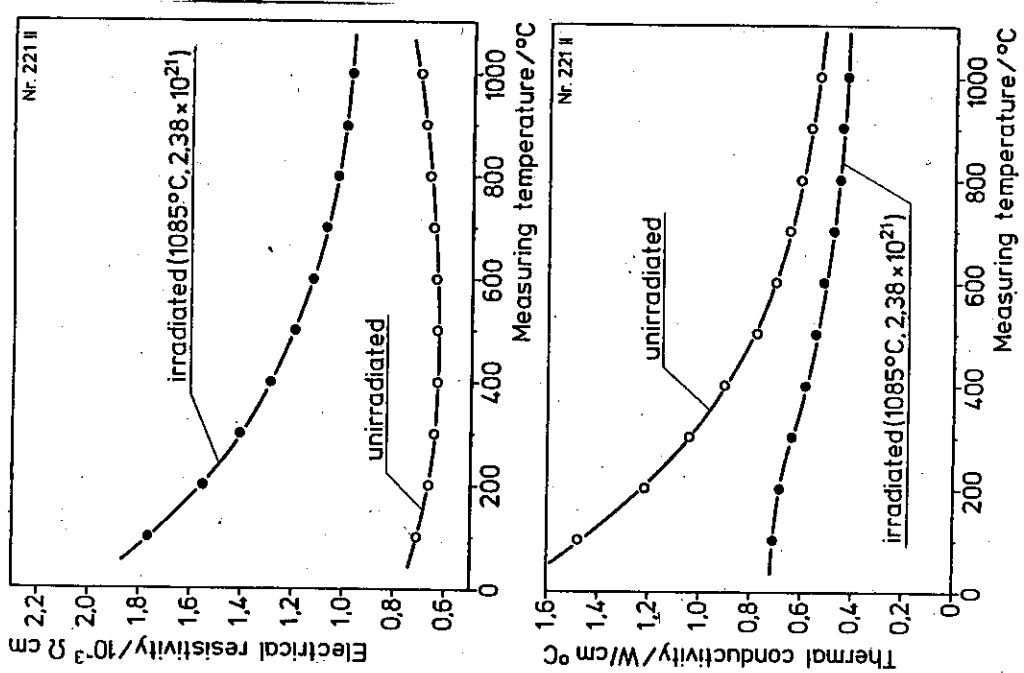


Fig. 32 Curves for Specimen No. 221 (SM1-24)

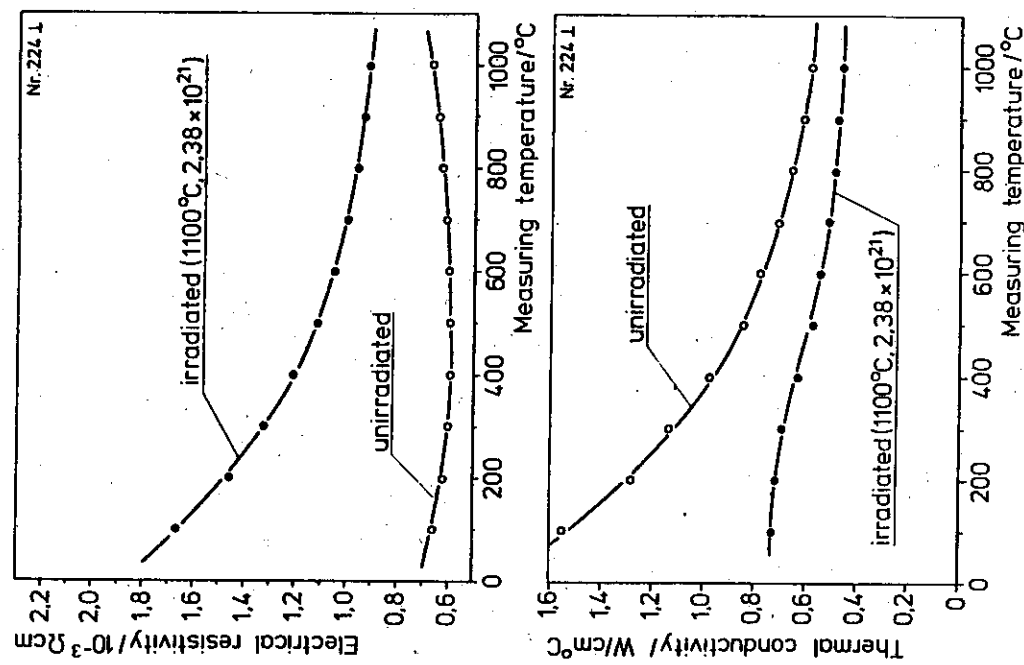


Fig. 33 Curves for Specimen No. 224 (SM1-24)

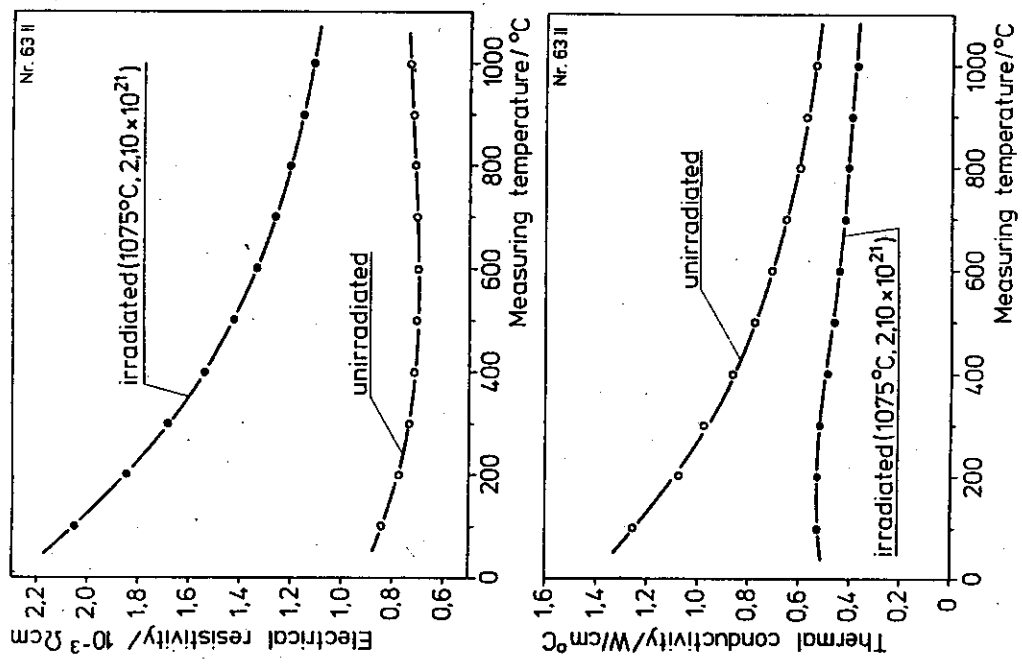


Fig. 34 Curves for Specimen No. 63 (IG-11)

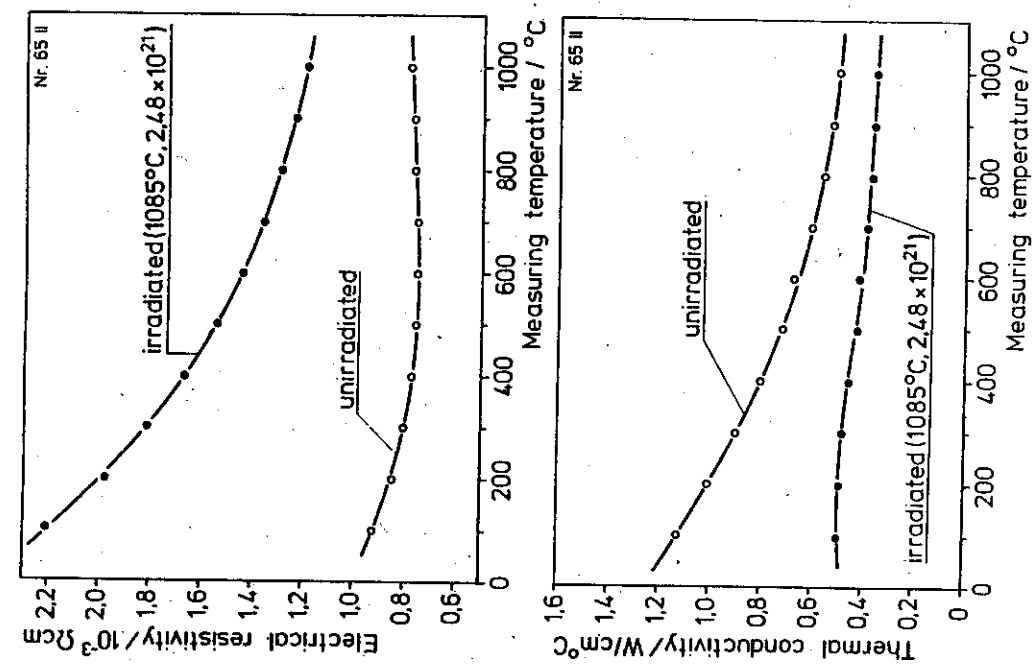


Fig. 35 Curves for Specimen No. 65 (IG-11)

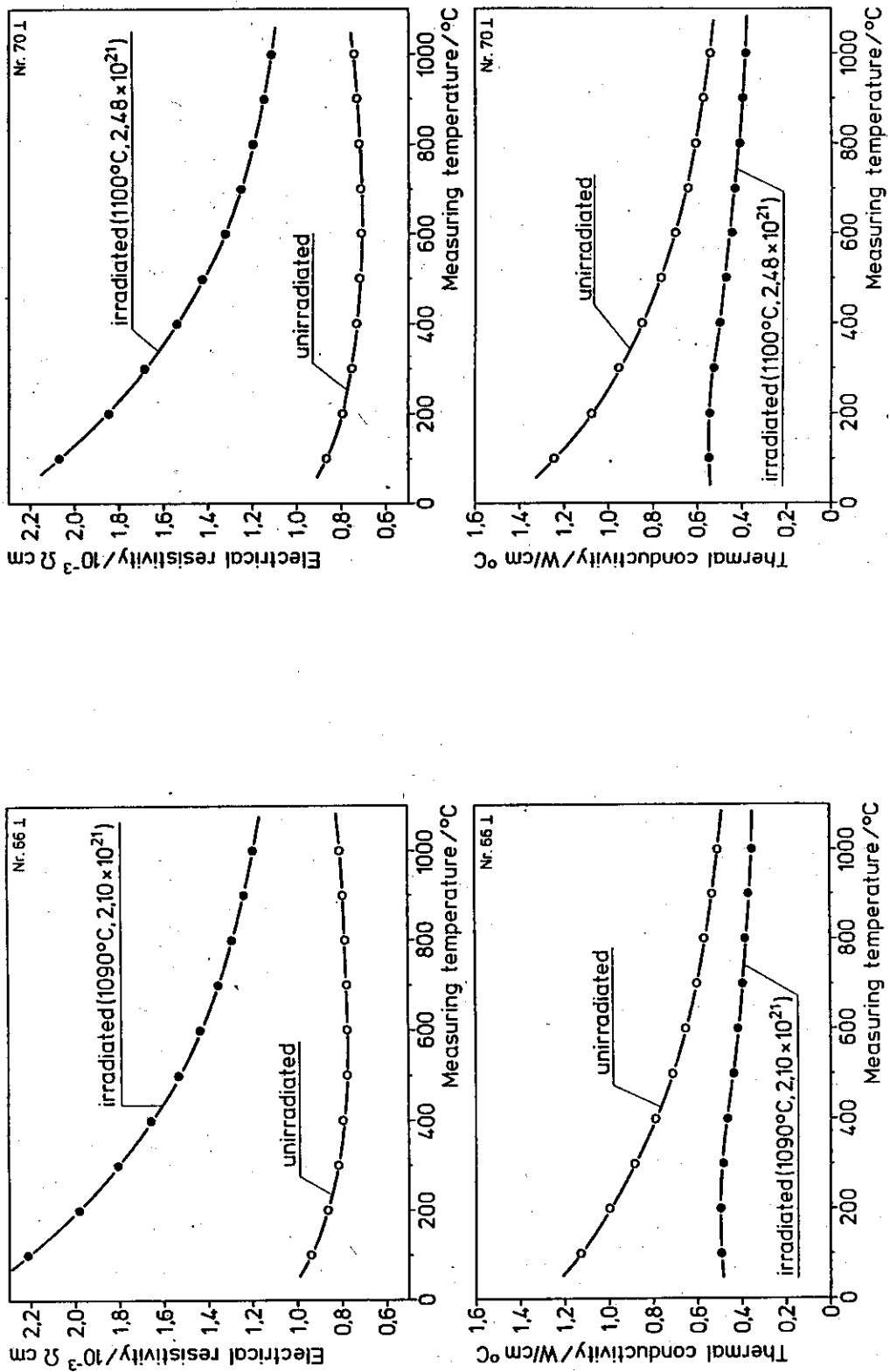


Fig. 36 Curves for Specimen No. 66 (IG-11)

Fig. 37 Curves for Specimen No. 70 (IG-11)

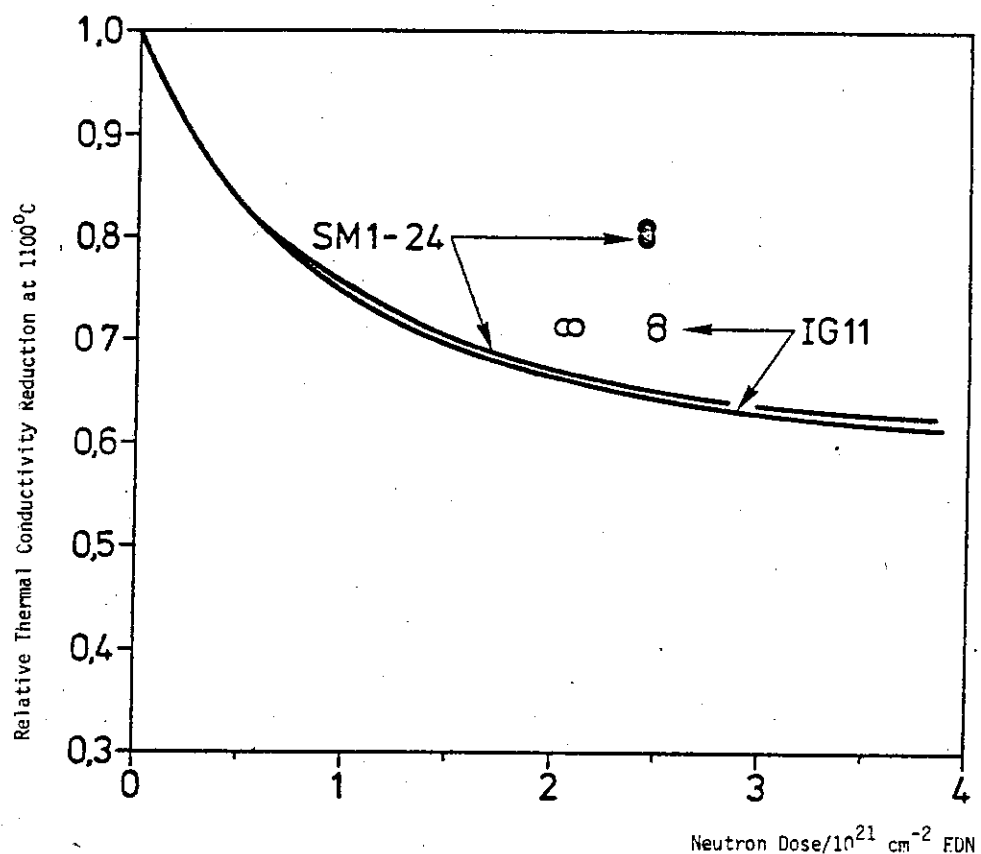


Fig. 38 Comparison of Calculated and Measured Reduction in Thermal Conductivity at an Irradiation Temperature of 1100 °C

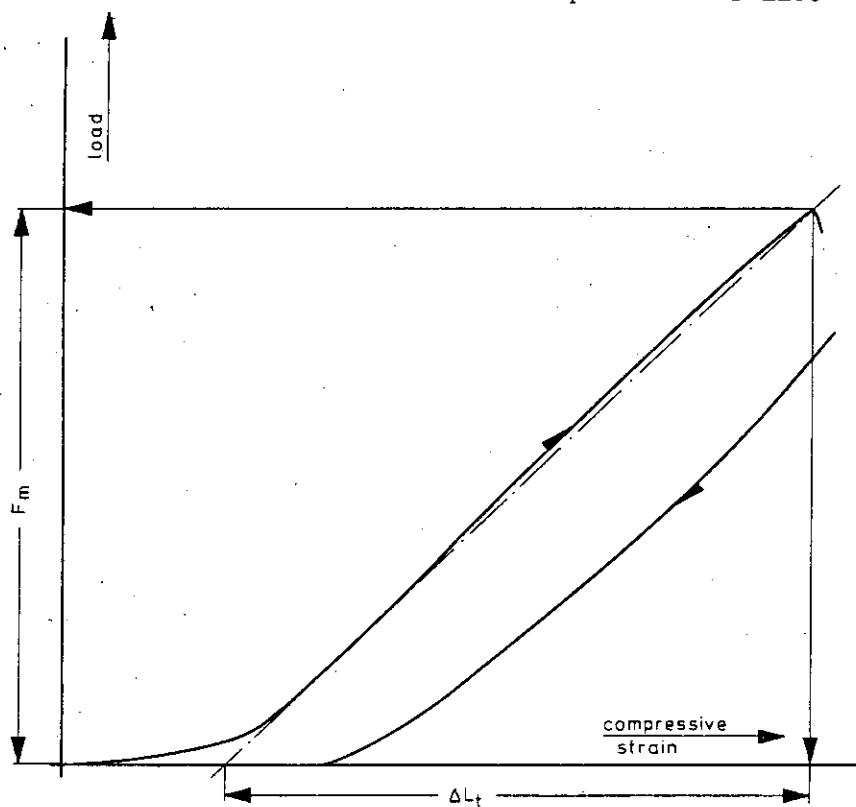
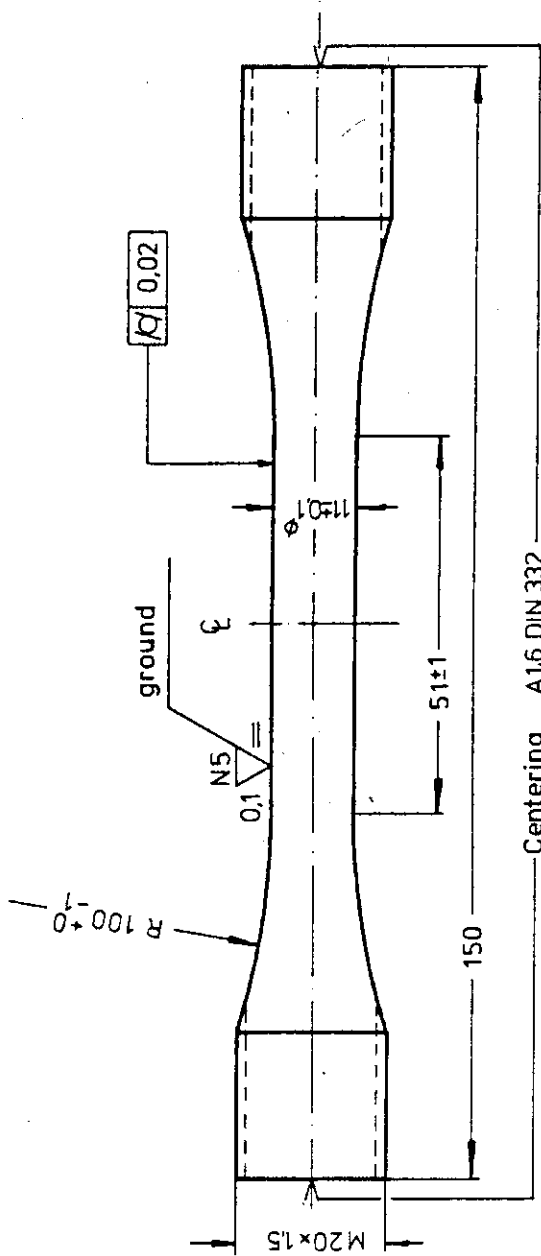


Fig. 40 Load/Compressive Strain Diagram for a Ring Specimen



Optimized Tensile Specimen

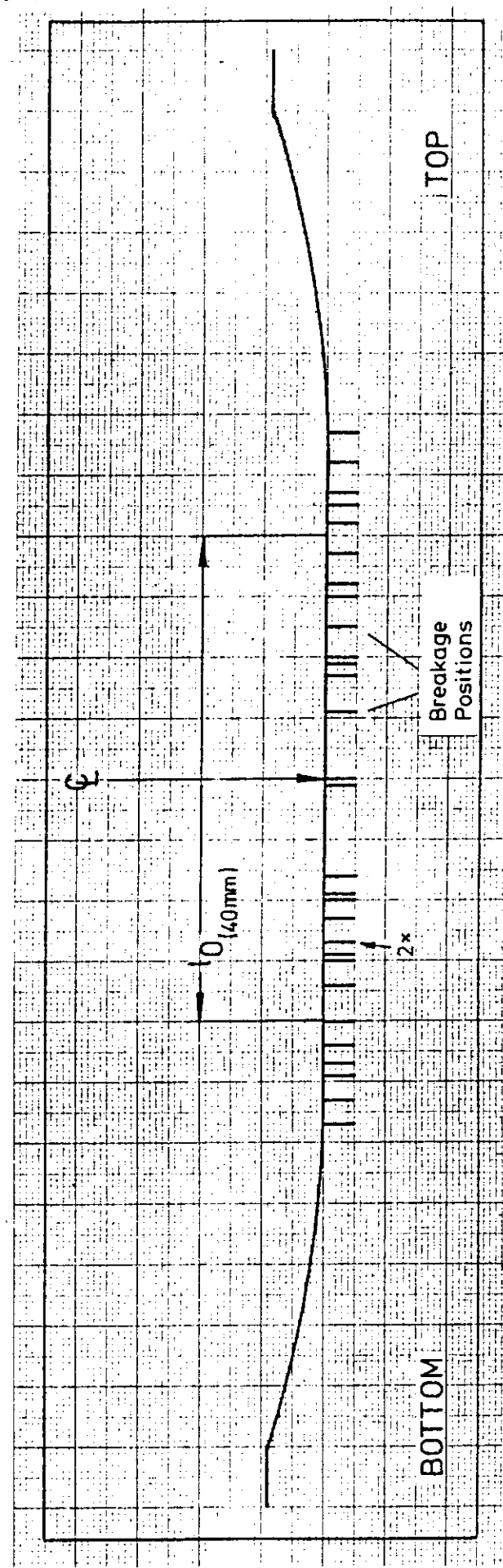


Fig. 39 Optimized Tensile Specimen Breaking Point Distribution for 30 Tensile Specimens of IG-11

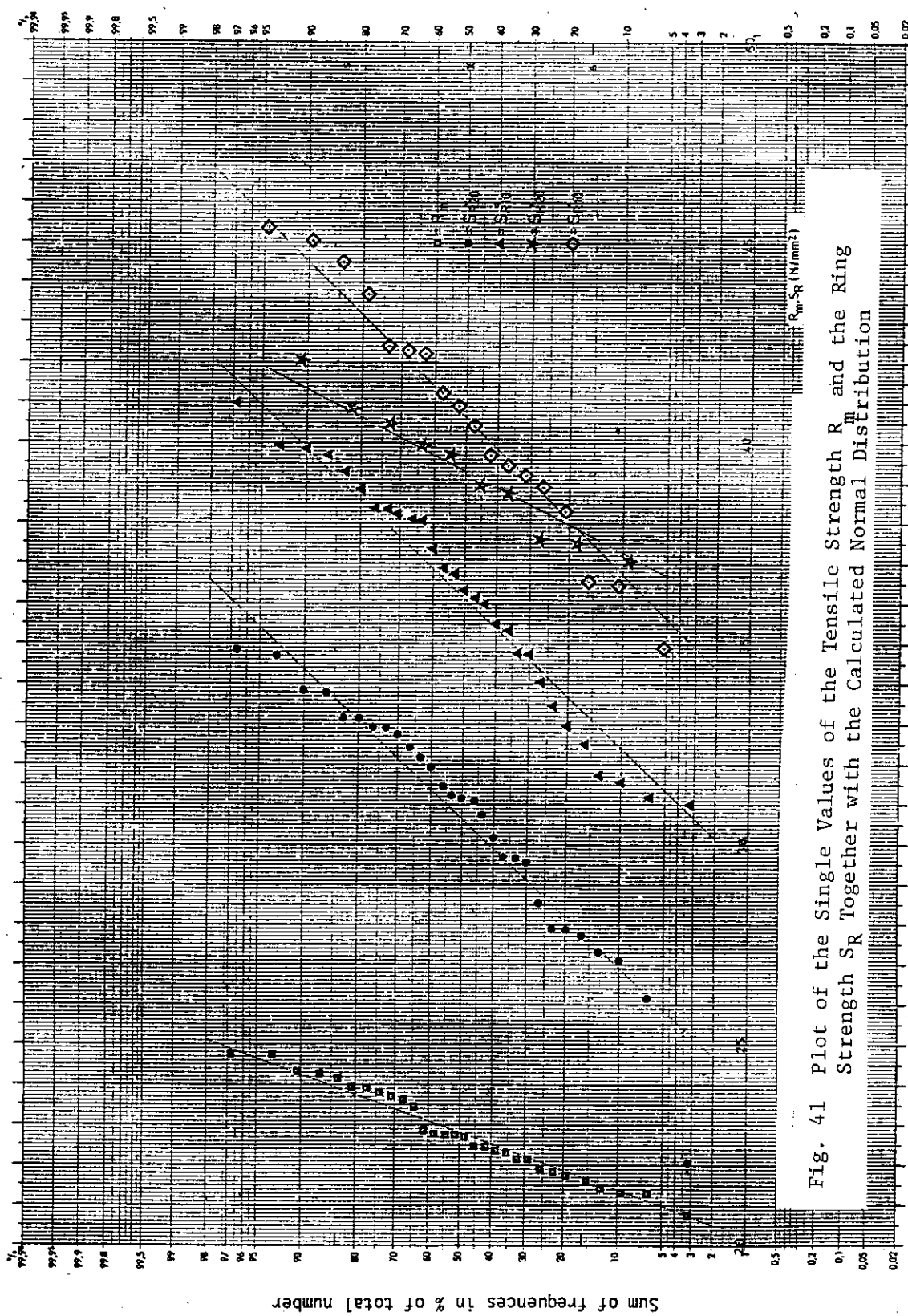


Fig. 41 Plot of the Single Values of the Tensile Strength R_n and the Ring Strength S_r Together with the Calculated Normal Distribution

Appendices

A I. List of specimens made in JAERI and sent to KFA Jülich

Table A1 Pre-irradiation characterization of SM1-24 graphite specimens carried out in JAERI

No.	Specimen No.	direc-tion	Length (mm)	Diameter (mm)	Weight (g)	Apparent density (g/cm ³)	Electrical Resistivity (Ω cm)	Young's Modulus (kg/cm ²)
1	71		24.949	5.995	1.2309	1.748	8.09×10^{-4}	7.83×10^4
2	72		24.948	6.008	1.2321	1.742	8.32	7.80
3	73		24.962	6.000	1.2361	1.752	8.01	7.86
4	74		24.932	6.019	1.2350	1.741	8.09	7.92
5	75		24.985	6.005	1.2373	1.748	7.86	7.72
6	76		24.931	5.997	1.2354	1.755	7.85	7.99
7	77		24.915	6.010	1.2328	1.744	8.05	7.93
8	78		24.926	6.008	1.2324	1.744	8.00	7.67
9	79		24.932	5.992	1.2295	1.748	7.89	8.11
10	80		24.920	6.006	1.2334	1.747	8.06	7.81
11	81		24.928	6.007	1.2305	1.742	8.06	7.92
12	82		24.943	6.015	1.2355	1.743	8.02	7.94
13	83		24.938	6.012	1.2319	1.740	7.97	7.79
14	84		24.927	6.012	1.2362	1.747	8.10	7.95
15	85		24.932	6.010	1.2320	1.742	8.43	8.06
16	86		24.948	5.992	1.2311	1.750	7.72	8.40
17	87		24.936	5.993	1.2302	1.749	7.62	8.53
18	88		24.939	5.994	1.2325	1.751	7.70	8.39
19	89		24.949	5.991	1.2311	1.751	7.77	8.40
20	90		24.951	5.992	1.2353	1.756	7.50	8.57
21	91		24.937	6.000	1.2305	1.745	7.70	8.36
22	92		24.938	5.998	1.2414	1.762	7.41	8.75
23	93		24.921	6.004	1.2366	1.753	7.55	8.54
24	94		24.930	6.000	1.2311	1.747	7.66	8.37
25	95		24.969	6.011	1.2378	1.747	7.83	8.54
26	96		24.947	5.999	1.2386	1.756	7.57	8.72
27	97		24.978	6.007	1.2385	1.750	7.56	8.56
28	98		24.945	6.004	1.2393	1.753	7.59	8.71
29	99		24.965	5.992	1.2369	1.757	7.56	8.59
30	100		24.976	6.001	1.2395	1.755	7.63	8.44
31	221		32.040	6.008	1.5948	1.756	7.86	8.06
32	222		32.078	6.001	1.5926	1.756	7.60	8.18
33	223		32.068	6.007	1.5992	1.760	7.48	8.77
34	224		32.022	6.007	1.5971	1.760	7.47	9.00

Table A 2 List of specimens for thermal conductivity measurement (1)
Parallel to the longitudinal axis (IG-11)

Specimen designation	Specimen number for irrad.	Diameter (mm)		Length (mm)	Density (g/cm ³)	Young's modulus (N/mm ²)
RT - L 1	-	6.007	6.001	31.993	1.759	9.90
	-	6.007	6.001	31.996	1.759	9.14
	-	6.009	6.008	31.995	1.759	9.27
	-	6.009	6.004	31.991	1.764	8.86
	-	6.003	6.002	31.993	1.768	9.03
6	-	6.009	6.004	31.997	1.763	8.85
7	61	6.006	6.002	31.999	1.763	8.76
8	-	6.009	6.009	31.988	1.765	8.92
9	-	6.009	6.003	31.988	1.769	9.24
10	-	6.008	6.005	31.991	1.766	9.59
11	-	6.005	6.005	31.985	1.765	9.59
12	62	6.002	6.000	31.991	1.774	9.09
13	63	6.005	6.003	31.992	1.780	9.29
14	-	6.007	6.003	31.992	1.777	9.43
15	-	6.003	6.000	31.992	1.777	9.72
16	64	6.009	6.006	31.985	1.768	9.49
17	-	6.002	6.000	31.994	1.773	9.02
18	-	6.006	6.006	31.991	1.768	9.06
19	-	5.999	5.994	31.994	1.767	8.59
20	-	6.001	6.001	31.997	1.765	8.77
21	-	6.004	5.998	31.986	1.774	8.98
22	-	6.009	6.005	31.991	1.773	9.20
23	-	6.005	6.003	31.989	1.768	9.12
24	-	6.007	6.005	31.989	1.775	9.12
25	-	6.009	6.004	31.992	1.769	8.97
26	-	6.004	6.003	31.997	1.762	8.75
27	-	6.005	6.000	31.993	1.765	8.71
28	-	6.007	6.003	31.991	1.765	8.70
29	65	6.008	6.006	31.990	1.765	9.10
30	-	6.007	6.001	31.991	1.771	9.31
31	-	6.000	5.999	31.993	1.769	9.30
32	-	6.009	6.005	31.989	1.780	10.1

Table A 3 List of specimens for thermal conductivity measurement (2)
Perpendicular to the longitudinal axis (IG-11)

Specimen designation	Specimen number for irrad.	Diameter (mm)		Length (mm)	Density (g/cm ³)	Young's modulus (N/mm ²)
RT - T 1	-	6.003	6.000	31.998	1.762	9.37
	2	6.010	6.005	31.982	1.762	9.32
	3	6.010	6.007	31.980	1.767	9.15
	4	6.010	6.003	31.980	1.765	9.21
	5	6.009	6.004	31.986	1.764	8.86
6	-	6.008	6.003	31.985	1.765	8.70
7	66	6.009	6.003	31.981	1.760	8.83
8	-	6.009	6.006	31.978	1.762	8.48
9	-	6.006	6.002	31.975	1.765	9.54
10	-	6.010	6.004	31.978	1.764	9.13
11	-	6.005	6.000	31.981	1.769	9.25
12	-	6.005	6.000	31.977	1.774	9.18
13	67	6.010	6.003	31.981	1.771	9.04
14	-	6.007	6.002	31.976	1.768	8.96
15	-	6.009	6.006	31.974	1.768	8.97
16	68	6.009	6.003	31.976	1.773	9.09
17	-	6.010	6.007	31.978	1.771	9.74
18	-	6.008	6.006	31.995	1.762	9.60
19	-	6.009	6.007	31.995	1.760	8.54
20	-	6.010	6.006	31.995	1.761	8.66
21	69	6.003	6.001	31.997	1.760	8.41
22	-	6.009	6.004	31.998	1.765	8.50
23	-	6.008	6.005	31.996	1.770	9.98
24	-	6.008	6.006	31.994	1.762	9.95
25	-	6.005	6.003	31.995	1.770	9.31
26	-	6.007	6.004	31.991	1.761	9.74
27	-	6.007	6.003	31.997	1.758	9.80
28	-	6.004	6.005	31.997	1.758	9.47
29	70	6.007	6.005	31.993	1.762	9.46
30	-	6.009	6.005	31.991	1.761	9.50
31	-	6.009	6.004	31.991	1.764	9.60
T32	-	6.004	6.001	31.990	1.768	10.0

Table A 4 List of specimens for dimensional change measurement (1)
Parallel to the longitudinal axis (IG-11)

Specimen designation	Specimen number for irrad.	Diameter (mm)		Length (mm)	Density (g/cm ³)	Young's modulus (N/mm ²)
DE - L 1	1	6.021	6.012	24.973	1.756	8.95
	2	6.019	6.010	24.982	1.756	8.61
	3	6.017	6.011	24.981	1.758	8.71
	4	6.015	6.007	24.981	1.762	8.60
	5	6.022	6.013	24.978	1.761	8.52
6	-	6.020	6.010	24.984	1.762	8.46
7	3	6.016	6.007	24.986	1.763	8.22
8	4	6.013	6.003	24.999	1.757	8.30
9	5	6.037	6.027	24.975	1.756	8.42
10	-	6.024	6.020	24.978	1.757	8.25
11	-	6.022	6.012	24.973	1.759	8.26
12	6	6.025	6.018	24.976	1.763	8.29
13	7	6.026	6.016	24.977	1.766	8.11
14	8	6.028	6.016	24.980	1.764	7.77
15	9	6.023	6.014	24.978	1.763	7.81
16	10	6.034	6.024	24.975	1.759	8.01
17	-	6.030	6.023	24.977	1.766	8.91
18	-	6.025	6.018	24.980	1.761	9.21
19	11	6.025	6.020	24.983	1.765	8.93
20	-	6.024	6.019	24.981	1.772	9.27
21	12	6.030	6.020	24.976	1.774	9.10
22	-	6.044	6.033	24.976	1.774	8.93
23	-	6.040	6.031	24.974	1.771	8.59
24	-	6.033	6.026	24.974	1.768	8.82
25	13	6.021	6.011	24.983	1.769	8.99
26	-	6.022	6.013	24.983	1.765	9.10
27	-	6.020	6.019	24.982	1.768	8.73
28	-	6.018	6.008	24.981	1.777	9.00
29	14	6.020	6.010	24.982	1.775	8.72
30	-	6.019	6.011	24.983	1.773	8.83
31	-	6.041	6.035	24.983	1.770	8.60
32	15	6.028	6.019	24.979	1.771	8.87
33	16	6.031	6.020	24.979	1.770	8.45
34	--	6.030	6.020	24.983	1.756	8.50
35	--	6.031	6.021	24.980	1.767	8.43
36	-	6.033	6.025	24.973	1.759	8.36
37	17	6.028	6.021	24.980	1.764	8.58
38	-	6.030	6.028	24.979	1.773	8.86
39	-	6.026	6.018	24.979	1.774	9.14
DE - L40	-	6.031	6.017	24.983	1.774	9.23

Table A 4 Continued

Specimen designation	Specimen number for irrad.	Diameter (mm)		Length (mm)	Density (g/cm ³)	Young's modulus (N/mm ²)
DE - L41	-	6.034	6.020	24.975	1.778	8.87
	42	6.040	6.022	24.968	1.771	8.56
	43	6.035	6.023	24.978	1.766	8.22
	44	18	6.037	6.023	24.987	1.769
	45	-	6.039	6.023	24.971	1.772
46	-	6.038	6.019	24.977	1.767	8.75
47	19	6.034	6.021	24.979	1.765	8.88
48	20	6.026	6.018	24.982	1.775	8.81
49	21	6.029	6.017	24.975	1.764	8.80
50	-	6.033	6.018	24.983	1.764	9.03
51	-	6.039	6.030	24.974	1.771	8.52
52	22	6.034	6.027	24.975	1.763	8.58
53	23	6.029	6.022	24.981	1.771	8.81
54	24	6.031	6.025	24.978	1.759	8.74
55	25	6.027	6.019	24.976	1.764	8.31
56	26	6.029	6.020	24.975	1.777	8.83
57	-	6.032	6.021	24.973	1.777	8.16
58	-	6.030	6.022	24.975	1.768	8.16
59	27	6.031	6.025	24.982	1.763	8.21
60	28	6.041	6.031	24.982	1.765	8.40
61	-	6.032	6.026	24.973	1.774	8.44
62	29	6.037	6.031	24.981	1.775	8.61
63	30	6.037	6.028	24.972	1.772	9.06
DE - L64	-	6.038	6.026	24.975	1.778	9.06

Table A 5 List of specimens for dimensional change measurement (2)
Perpendicular to the longitudinal axis (IG-11)

Specimen designation	Specimen number for irrad.	Diameter (mm)		Length (mm)	Density (g/cm ³)	Young's modulus (N/mm ²)
DE - T 1	31	6.032	6.032	24.985	1.758	9.89
	2	6.035	6.025	24.982	1.761	9.49
	3	6.035	6.032	24.975	1.760	9.51
	4	6.040	6.034	24.978	1.757	9.13
	5	6.035	6.032	24.981	1.764	9.45
6	-	6.040	6.032	24.969	1.761	9.58
7	33	6.023	6.015	24.976	1.756	9.40
8	34	6.018	6.010	24.978	1.755	9.21
9	35	6.022	6.015	24.988	1.761	9.51
10	-	6.020	6.015	24.986	1.759	9.24
11	-	6.020	6.012	24.977	1.763	9.69
12	36	6.022	6.015	24.979	1.767	9.53
13	37	6.022	6.012	24.984	1.766	9.64
14	38	6.020	6.013	24.979	1.764	9.83
15	39	6.012	6.005	24.983	1.762	9.44
16	40	6.027	6.019	24.979	1.759	9.23
17	-	6.021	6.014	24.979	1.761	9.36
18	-	6.022	6.016	24.983	1.759	9.56
19	41	6.017	6.011	24.981	1.758	9.44
20	-	6.020	6.013	24.985	1.765	10.0
21	42	6.021	6.011	24.980	1.770	10.0
22	-	6.020	6.012	24.975	1.763	9.94
23	-	6.018	6.015	24.978	1.761	9.91
24	-	6.017	6.011	24.978	1.764	10.3
25	43	6.021	6.011	24.981	1.767	9.96
26	-	6.017	6.007	24.988	1.771	9.65
27	-	6.020	6.010	24.979	1.769	9.65
28	-	6.024	6.013	24.980	1.772	9.56
29	44	6.019	6.011	24.986	1.772	9.27
30	-	6.025	6.015	24.985	1.773	9.40
31	45	6.029	6.022	24.974	1.769	9.54
32	46	6.038	6.032	24.958	1.768	9.47
33	47	6.031	6.028	24.949	1.766	9.74
34	-	6.021	6.015	24.959	1.761	9.81
35	-	6.022	6.014	24.978	1.761	9.21
36	-	6.024	6.014	24.979	1.765	9.23
37	48	6.026	6.016	24.975	1.763	9.42
38	-	6.023	6.011	24.974	1.763	9.84
39	-	6.022	6.013	24.986	1.763	9.61
DE - T40	-	6.022	6.014	24.982	1.764	9.88

Table A 5 Continued

Specimen designation	Specimen number for irrad.	Diameter (mm)		Length (mm)	Density (g/cm ³)	Young's modulus (N/mm ²)
DE - T41	-	6.022	6.018	24.984	1.768	9.81
	-	6.035	6.039	24.980	1.761	9.52
	-	6.039	6.035	24.967	1.756	9.68
	Broken	-	-	-	-	-
	-	6.033	6.031	24.983	1.763	9.64
46	-	6.030	6.028	24.974	1.767	9.87
	49	6.031	6.030	24.972	1.768	10.3
	50	6.029	6.025	24.971	1.773	10.1
	51	6.029	6.024	24.967	1.768	9.99
	-	6.032	6.027	24.972	1.771	10.4
51	-	6.030	6.021	24.979	1.771	10.7
	52	6.023	6.015	24.983	1.777	10.5
	53	6.026	6.022	24.975	1.777	10.3
	54	6.041	6.034	24.972	1.762	10.1
	55	6.037	6.031	24.966	1.772	10.2
56	56	6.037	6.032	24.970	1.768	10.1
	-	6.034	6.029	24.971	1.766	10.3
	-	6.036	6.028	24.971	1.773	10.3
	57	6.038	6.032	24.978	1.766	10.2
	58	6.029	6.025	24.981	1.778	10.2
61	-	6.028	6.023	24.978	1.773	10.3
	59	6.024	6.021	24.981	1.763	10.1
	60	6.027	6.025	24.983	1.770	10.3
DE - T64	-	6.025	6.020	24.976	1.773	10.2

Table A 6 List of the larger ring compression specimens (IG-11)

Specimen designation	Specimen number for irrad.	Outer diameter (mm)	Inner diameter (mm)		Density (g/cm ³)	Young's modulus (N/mm ²)
RO - T 1	101	19.984	10.155	9.967	1.761	10.3
	2	19.985	10.152	9.964	1.766	9.65
	3	19.987	10.152	9.964	1.765	9.60
	4	19.981	10.152	9.966	1.761	10.1
	5	19.982	10.155	9.962	1.766	10.3
6	-	19.995	10.152	9.963	1.769	9.71
7	103	19.998	10.130	9.925	1.767	9.86
8	104	19.994	10.140	9.945	1.768	10.1
9	105	19.998	10.140	9.948	1.771	9.88
10	-	19.993	10.145	9.943	1.766	10.7
11	-	19.985	10.143	9.942	1.775	10.9
12	106	19.985	10.138	9.940	1.777	9.62
13	107	19.984	10.130	9.940	1.766	11.3
14	108	19.993	10.142	9.942	1.773	9.60
15	109	19.993	10.135	9.940	1.772	10.7
16	110	19.991	10.135	9.940	1.766	10.3
17	111	19.986	10.138	9.942	1.772	10.0
18	-	19.987	10.135	9.935	1.772	10.2
19	112	19.989	10.132	9.942	1.770	9.72
20	-	19.987	10.138	9.955	1.772	10.8
21	113	19.942	10.132	9.942	1.774	9.67
22	-	19.945	10.133	9.945	1.763	10.7
23	-	19.945	10.138	9.945	1.768	10.3
24	-	19.943	10.135	9.943	1.774	9.26
25	114	19.942	10.130	9.942	1.764	10.6
26	-	19.945	10.140	9.945	1.761	10.1
27	-	19.945	10.132	9.945	1.764	9.75
28	-	19.948	10.150	9.948	1.758	9.53
29	115	19.945	10.142	9.945	1.768	9.54
30	-	19.943	10.140	9.943	1.773	10.3
31	-	19.989	10.143	9.958	1.764	9.82
32	116	19.983	10.143	9.958	1.776	10.4
33	117	19.989	10.135	9.960	1.768	10.1
34	-	19.987	10.143	9.962	1.766	9.70
35	-	19.987	10.143	9.960	1.780	11.0
36	-	19.990	10.142	9.962	1.777	10.8
37	118	19.985	10.145	9.962	1.771	11.1
38	-	19.987	10.143	9.960	1.775	10.3
39	-	19.985	10.148	9.962	1.775	12.3
RO - T 40	-	19.988	10.150	9.965	1.766	11.1

Table A 6 Continued

Specimen designation	Specimen number for irrad.	Outer diameter (mm)	Inner diameter (mm)		Density (g/cm ³)	Young's modulus (N/mm ²)
RO - T41	-	19.993	10.152	9.932	1.772	10.6
	42	19.993	10.155	9.965	1.778	10.2
	43	19.991	10.158	9.970	1.761	10.8
	44	19.991	10.145	9.965	1.762	9.50
	45	19.991	10.145	9.968	1.773	11.1
46	-	19.992	10.160	9.965	1.765	11.1
	47	19.986	10.152	9.960	1.764	10.6
	48	19.989	10.155	9.962	1.783	12.6
	49	19.989	10.155	9.958	1.769	11.9
	50	19.988	10.155	9.962	1.763	10.8
51	-	19.987	10.130	9.962	1.772	10.7
	52	19.994	10.132	9.960	1.772	10.0
	53	19.993	10.135	9.961	1.763	10.2
	54	19.996	10.132	9.963	1.778	10.8
	55	19.993	10.131	9.960	1.766	9.38
56	127	19.991	10.127	9.957	1.764	9.72
	57	19.984	10.130	9.957	1.767	9.93
	58	19.990	10.137	9.955	1.764	11.0
	59	19.987	10.122	9.962	1.764	10.4
	60	19.987	10.132	9.959	1.761	9.80
61	-	19.987	10.132	9.962	1.759	9.61
	62	19.998	10.135	9.958	1.763	9.76
	63	19.989	10.132	9.958	1.770	9.80
	64	19.994	10.128	9.960	1.757	10.1
	65	19.996	10.128	9.959	1.767	9.52
66	-	19.993	10.138	9.955	1.771	10.6
	67	19.993	10.133	9.955	1.765	10.3
	68	19.989	10.115	9.960	1.773	10.6
	69	19.987	10.135	9.955	1.774	10.3
	70	19.995	10.140	9.955	1.765	10.0
71	133	19.991	10.132	9.955	1.764	9.67
	72	19.994	10.135	9.955	1.770	11.0
	73	19.982	10.133	9.952	1.761	9.65
	74	19.985	10.125	9.960	1.757	9.60
	75	19.983	10.135	9.960	1.765	10.7
76	-	19.987	10.148	9.958	1.761	10.5
	77	19.986	10.145	9.955	1.764	9.54
	78	19.987	10.142	9.955	1.773	10.9
	79	19.989	10.148	9.960	1.760	10.5
	80	19.985	10.141	9.957	1.766	9.59
81	-	19.989	10.159	9.958	1.771	11.1
	82	19.990	10.157	9.961	1.765	10.4
	83	19.989	10.158	9.958	1.760	9.52
RO - T84	139	19.990	10.155	9.960	1.766	9.78
	140	19.990	10.155	9.960	1.766	9.78

Table A 7 List of the smaller ring compression specimens (IG-11)

Specimen designation	Specimen number for irrad.	Outer diameter (mm)	Inner diameter (mm)		Density (g/cm ³)
RI - T 1	-	9.980	5.032	4.970	1.758
	-	9.975	5.040	4.972	1.757
	-	9.985	5.035	4.968	1.761
	141	9.982	5.043	4.967	1.772
	-	9.982	5.042	4.967	1.762
6	142	9.982	5.033	4.969	1.766
7	-	9.980	5.035	4.965	1.763
8	-	9.982	5.032	4.966	1.769
9	143	9.978	5.042	4.965	1.766
10	144	9.980	5.031	4.965	1.771
11	-	9.982	5.030	4.964	1.764
12	145	9.983	5.037	4.959	1.770
13	-	9.982	5.035	4.959	1.767
14	-	9.982	5.037	4.959	1.766
15	-	9.983	5.037	4.961	1.770
16	-	9.981	5.036	4.963	1.766
17	-	9.977	5.038	4.961	1.773
18	-	9.982	5.040	4.957	1.770
19	-	9.983	5.040	4.959	1.766
20	146	9.982	5.045	4.961	1.764
21	147	9.980	5.048	4.963	1.772
22	-	9.980	5.030	4.959	1.769
23	148	9.982	5.045	4.961	1.781
24	-	9.982	5.035	4.961	1.773
25	-	9.980	5.040	4.960	1.769
26	149	9.983	5.030	4.964	1.763
27	-	9.982	5.039	4.954	1.771
28	-	9.982	5.035	4.959	1.770
29	-	9.980	5.032	4.960	1.770
30	-	9.983	5.030	4.961	1.766
31	150	9.980	5.037	4.969	1.765
32	-	9.975	5.020	4.972	1.770
33	-	9.975	5.045	4.974	1.771
34	-	9.975	5.040	4.973	1.776
35	-	9.975	5.040	4.974	1.757
36	151	9.980	5.035	4.975	1.768
37	-	9.973	5.042	4.971	1.767
38	-	9.975	5.048	4.978	1.771
39	-	9.973	5.039	4.976	1.768
40	-	9.972	5.043	4.973	1.774
41	152	9.981	5.035	4.969	1.769
RI - T42	-	9.981	5.030	4.960	1.770

Table A 7 Continued

Specimen designation	Specimen number for irrad.	Outer diameter (mm)	Inner diameter (mm)		Density (g/cm ³)
RI - T43	-	9.985	5.037	4.972	1.771
44	153	9.985	5.040	4.966	1.773
45	154	9.985	5.042	4.972	1.776
46	155	9.985	5.022	4.971	1.779
47	-	9.982	5.030	4.969	1.762
48	-	9.983	5.032	4.965	1.770
49	-	9.983	5.023	4.968	1.760
50	-	9.983	5.025	4.971	1.767
51	-	9.981	5.038	4.958	1.778
52	-	9.975	5.035	4.956	1.776
53	-	9.981	5.035	4.957	1.766
54	-	9.979	5.028	4.962	1.771
55	-	9.978	5.038	4.958	1.750
56	156	9.980	5.035	4.960	1.753
57	-	9.978	5.026	4.958	1.762
58	157	9.978	5.030	4.961	1.758
59	-	9.978	5.032	4.955	1.758
60	-	9.980	5.030	4.956	1.761
61	-	9.972	5.037	4.960	1.760
62	-	9.980	5.037	4.960	1.760
63	-	9.978	5.033	4.962	1.759
64	-	9.975	5.038	4.963	1.786
65	158	9.975	5.035	4.960	1.768
66	159	9.978	5.038	4.959	1.766
67	-	9.978	5.032	4.965	1.761
68	160	9.978	5.025	4.966	1.765
69	161	9.980	5.032	4.966	1.776
70	162	9.979	5.040	4.966	1.778
71	-	9.975	5.045	4.970	1.763
72	163	9.980	5.035	4.973	1.779
73	-	9.985	5.035	4.969	1.766
74	-	9.990	5.031	4.967	1.774
75	-	9.989	5.035	4.968	1.771
76	164	9.985	5.035	4.970	1.772
77	-	9.982	5.035	4.974	1.778
78	-	9.982	5.043	4.970	1.774
79	-	9.973	5.025	4.976	1.770
80	-	9.978	5.040	4.971	1.774
81	-	9.975	5.033	4.963	1.763
82	-	9.973	5.031	4.967	1.769
83	-	9.973	5.039	4.971	1.774
84	-	9.978	5.038	4.978	1.776
RI - T85	-	9.980	5.031	4.971	1.770

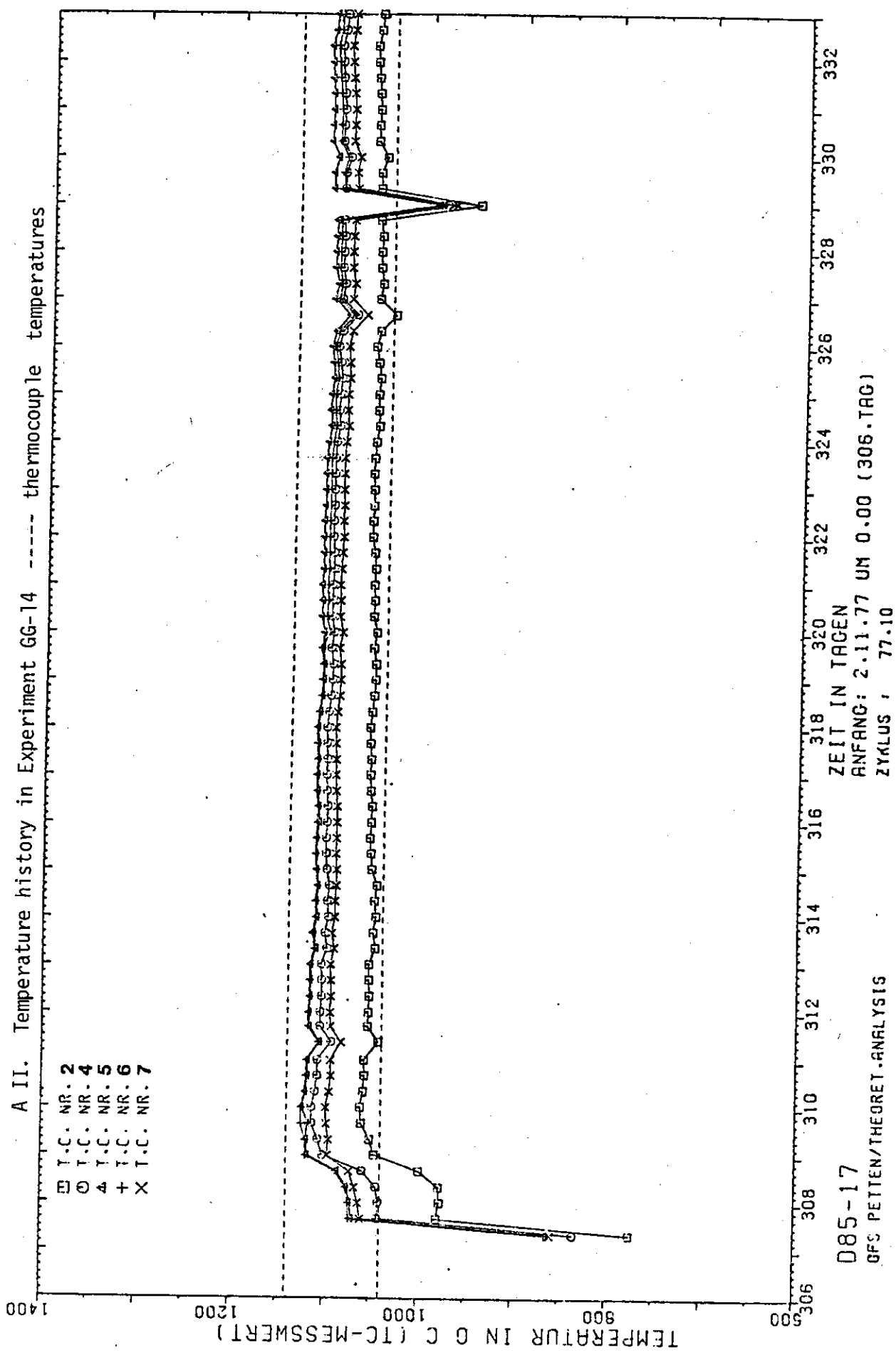
Table A 7 Continued

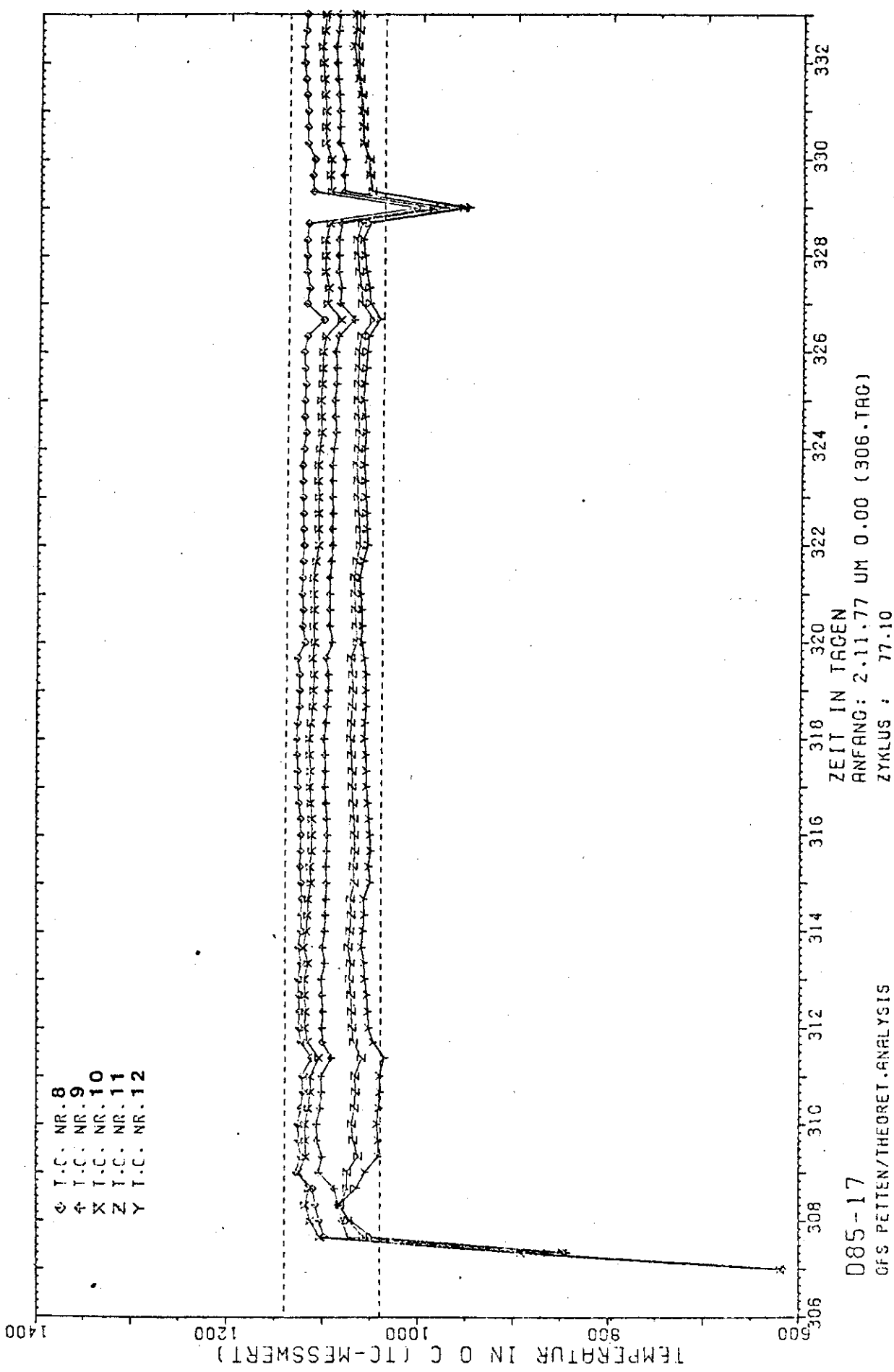
Specimen designation	Specimen number for irrad.	Outer diameter (mm)	Inner diameter (mm)		Density (g/cm ³)
RI - T86	-	9.975	5.041	4.969	1.765
87	165	9.978	5.027	4.967	1.769
88	-	9.975	5.037	4.971	1.761
89	-	9.975	5.036	4.973	1.766
90	166	9.973	5.045	4.972	1.768
91	167	9.975	5.045	4.977	1.766
92	168	9.977	5.022	4.968	1.769
93	-	9.972	5.033	4.970	1.769
94	169	9.975	5.035	4.969	1.767
95	-	9.975	5.037	4.969	1.769
96	-	9.977	5.032	4.969	1.776
97	-	9.975	5.040	4.976	1.766
98	-	9.971	5.022	4.971	1.773
99	-	9.973	5.036	4.967	1.764
100	170	9.975	5.035	4.971	1.763
101	-	9.973	5.046	4.975	1.773
102	-	9.973	5.028	4.971	1.785
103	-	9.975	5.035	4.975	1.765
104	171	9.973	5.041	4.971	1.770
105	172	9.972	5.040	4.969	1.764
106	-	9.973	5.032	4.973	1.761
107	-	9.973	5.035	4.974	1.771
108	-	9.972	5.032	4.975	1.774
109	173	9.972	5.043	4.971	1.772
110	-	9.977	5.035	4.972	1.763
111	174	9.975	5.030	4.974	1.767
112	-	9.975	5.041	4.975	1.767
113	-	9.973	5.035	4.978	1.760
114	-	9.978	5.035	4.969	1.765
115	-	9.973	5.035	4.973	1.764
116	175	9.970	5.040	4.971	1.770
117	-	9.975	5.043	4.974	1.766
118	-	9.973	5.038	4.974	1.762
119	176	9.973	5.030	4.973	1.765
120	-	9.972	5.040	4.973	1.771
121	Broken	-	-	-	-
122	Broken	-	-	-	-
123	-	9.973	5.072	4.974	1.760
124	-	9.980	5.032	4.973	1.749
125	-	9.969	5.048	4.973	1.764
126	-	9.975	5.037	4.975	1.757
127	177	9.977	5.022	4.973	1.757
RI - T128	-	9.973	5.038	4.973	1.760

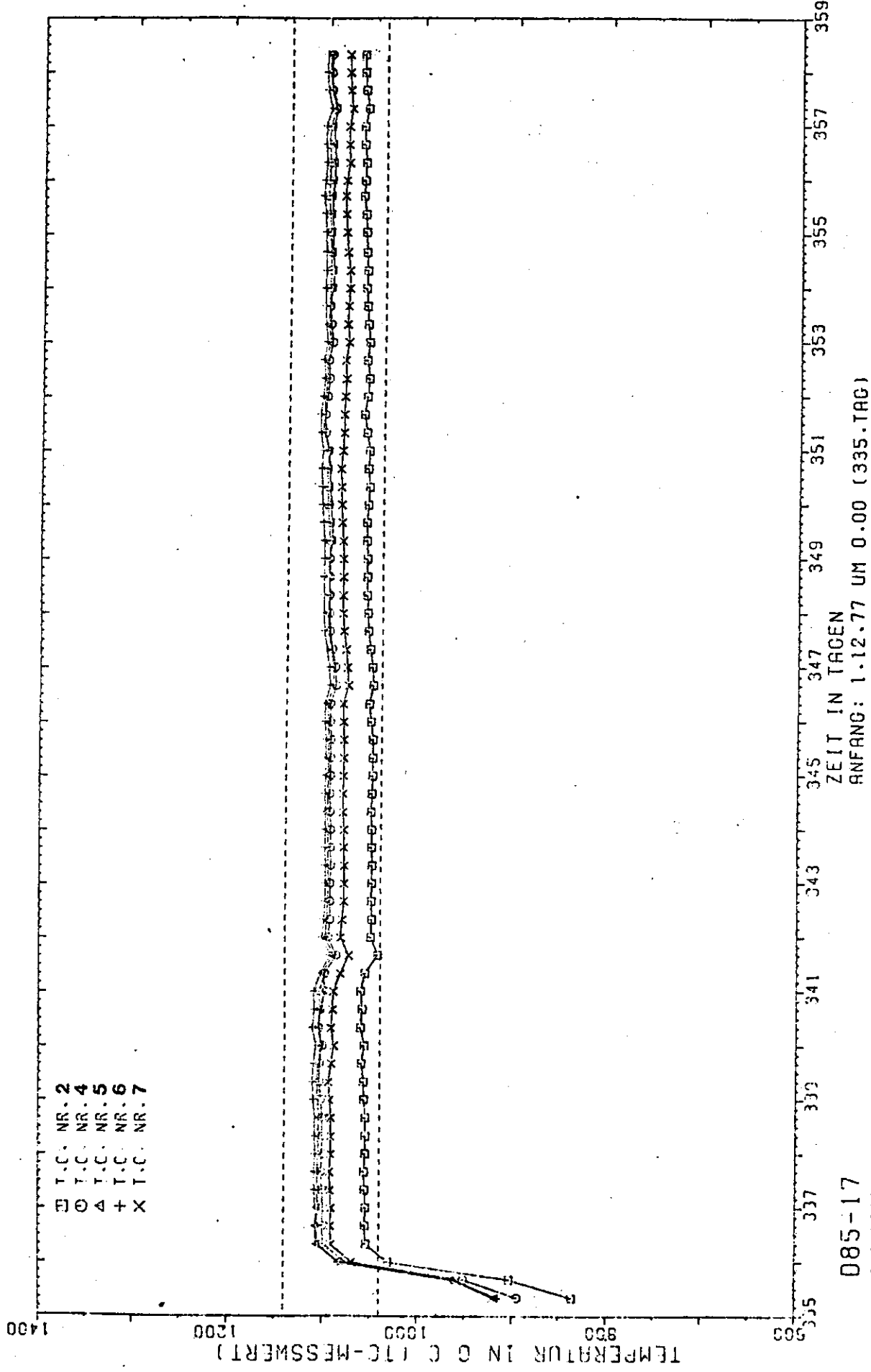
Table A 7 Continued

Specimen designation	Specimen number for irrad.	Outer diameter (mm)	Inner diameter (mm)		Density (g/cm ³)
RI - T129	-	9.973	5.029	4.975	1.753
130	-	9.975	5.032	4.973	1.742
131	178	9.975	5.040	4.973	1.756
132	-	9.968	5.030	4.974	1.759
133	-	9.974	5.035	4.968	1.759
134	179	9.975	5.035	4.973	1.757
135	-	9.975	5.032	4.972	1.763
136	-	9.975	5.031	4.973	1.755
137	-	9.972	5.037	4.971	1.771
138	180	9.977	5.032	4.970	1.766
139	-	9.975	5.040	4.967	1.759
140	181	9.978	5.031	4.971	1.758
141	-	9.975	5.040	4.968	1.762
142	182	9.978	5.035	4.969	1.761
143	-	9.979	5.035	4.964	1.761
144	-	9.978	5.033	4.971	1.759
145	183	9.973	5.035	4.969	1.768
146	184	9.975	5.031	4.964	1.763
147	185	9.977	5.037	4.972	1.754
148	-	9.978	5.032	4.984	1.753
149	-	9.980	5.035	4.985	1.757
150	186	9.980	5.035	4.981	1.759
151	-	9.980	5.039	4.988	1.763
152	182	9.980	5.035	4.955	1.763
153	-	9.981	5.028	4.954	1.758
154	-	9.977	5.035	4.959	1.764
155	183	9.979	5.030	4.957	1.770
156	184	9.979	5.030	4.960	1.768
157	185	9.978	5.035	4.954	1.765
158	-	9.983	5.035	4.973	1.761
159	-	9.983	5.045	4.973	1.760
160	186	9.980	5.043	4.969	1.760
161	187	9.982	5.043	4.967	1.762
162	-	9.982	5.047	4.968	1.769
163	-	9.982	5.046	4.972	1.760
164	188	9.980	5.040	4.973	1.761
165	189	9.978	5.049	4.971	1.753
166	-	9.977	5.035	4.974	1.749
167	-	9.980	5.045	4.967	1.771
RI - T168	-	9.980	5.040	4.970	1.769

1.766
± 0.007







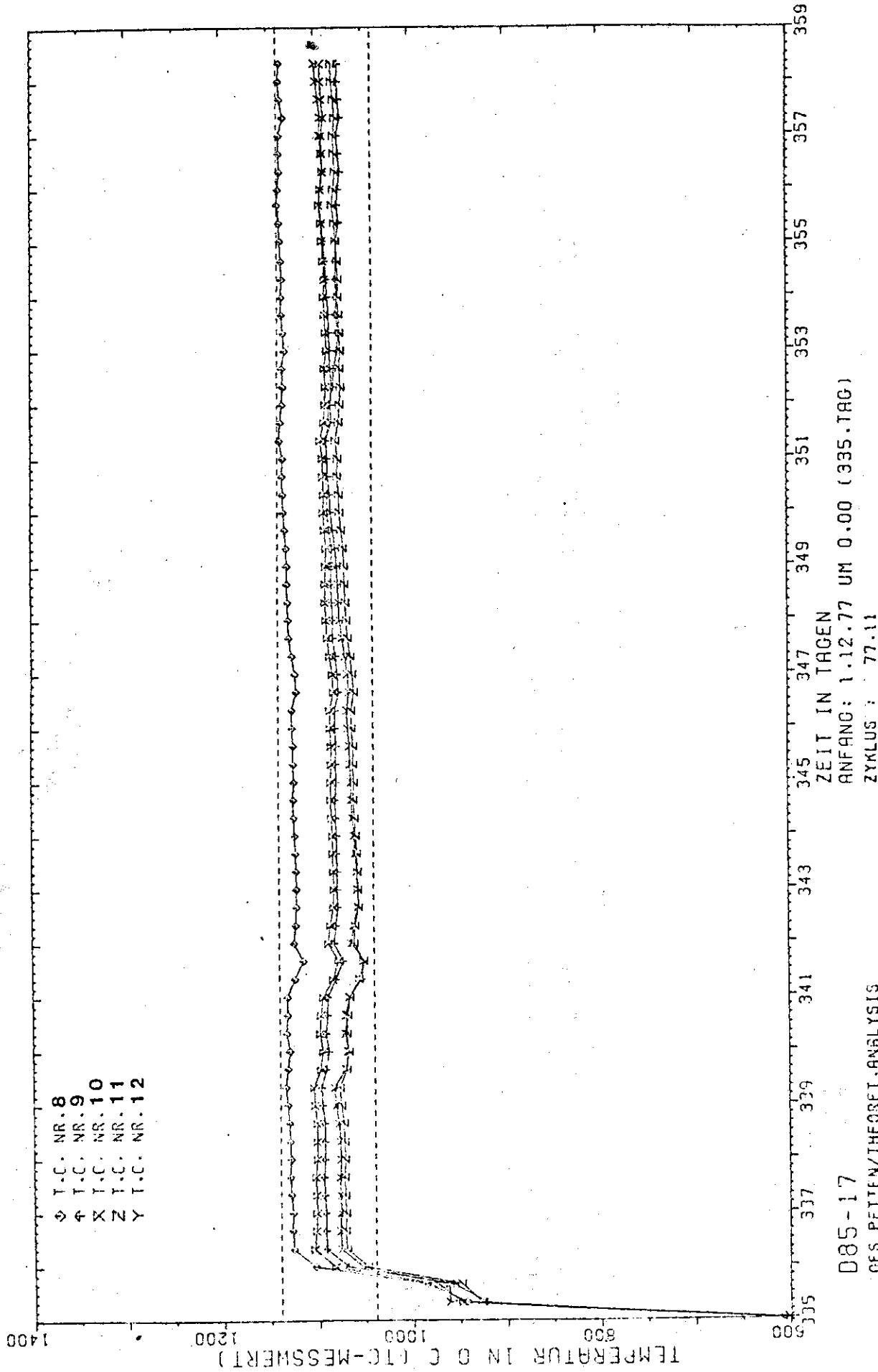
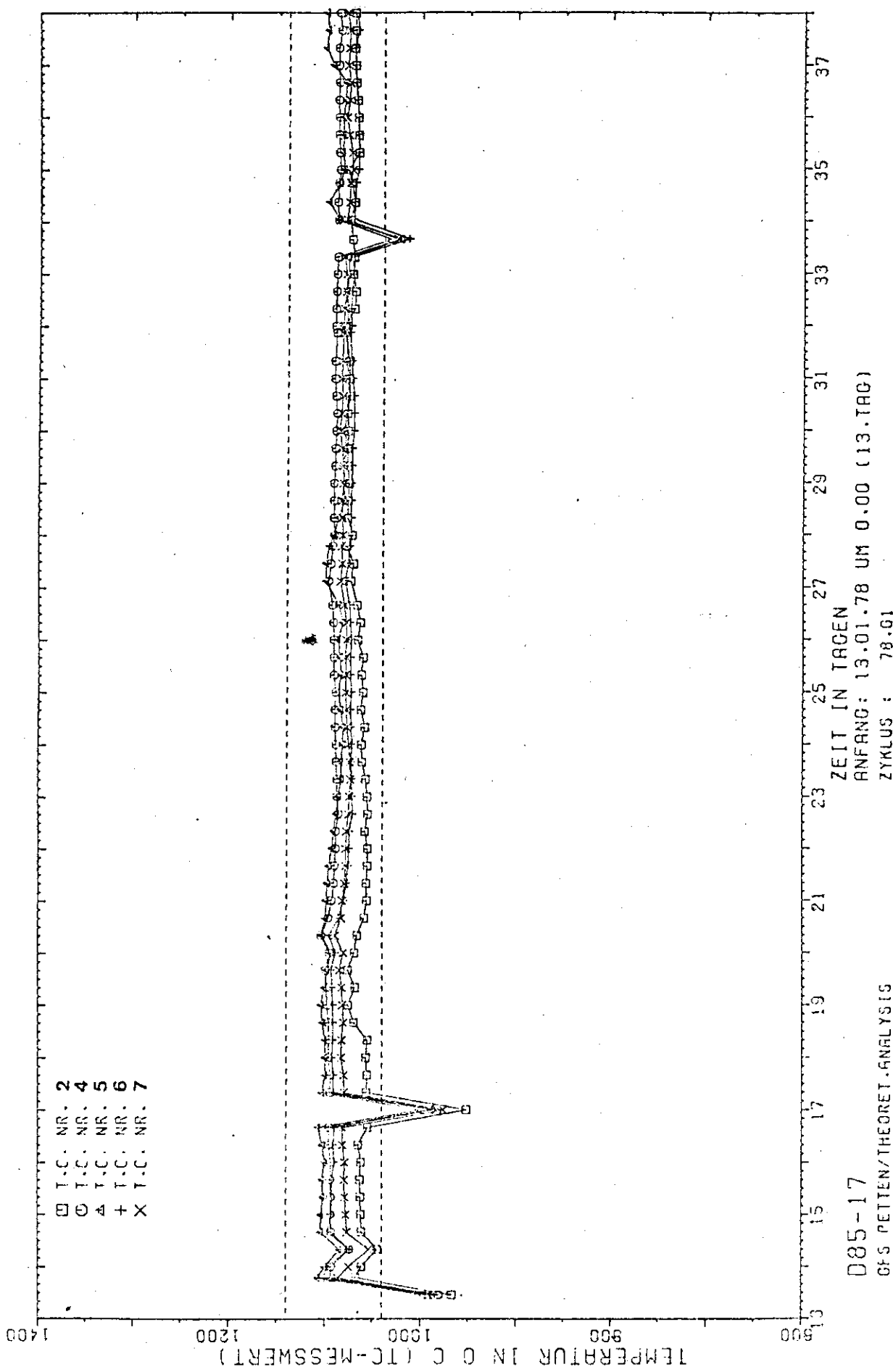


Fig. A 4



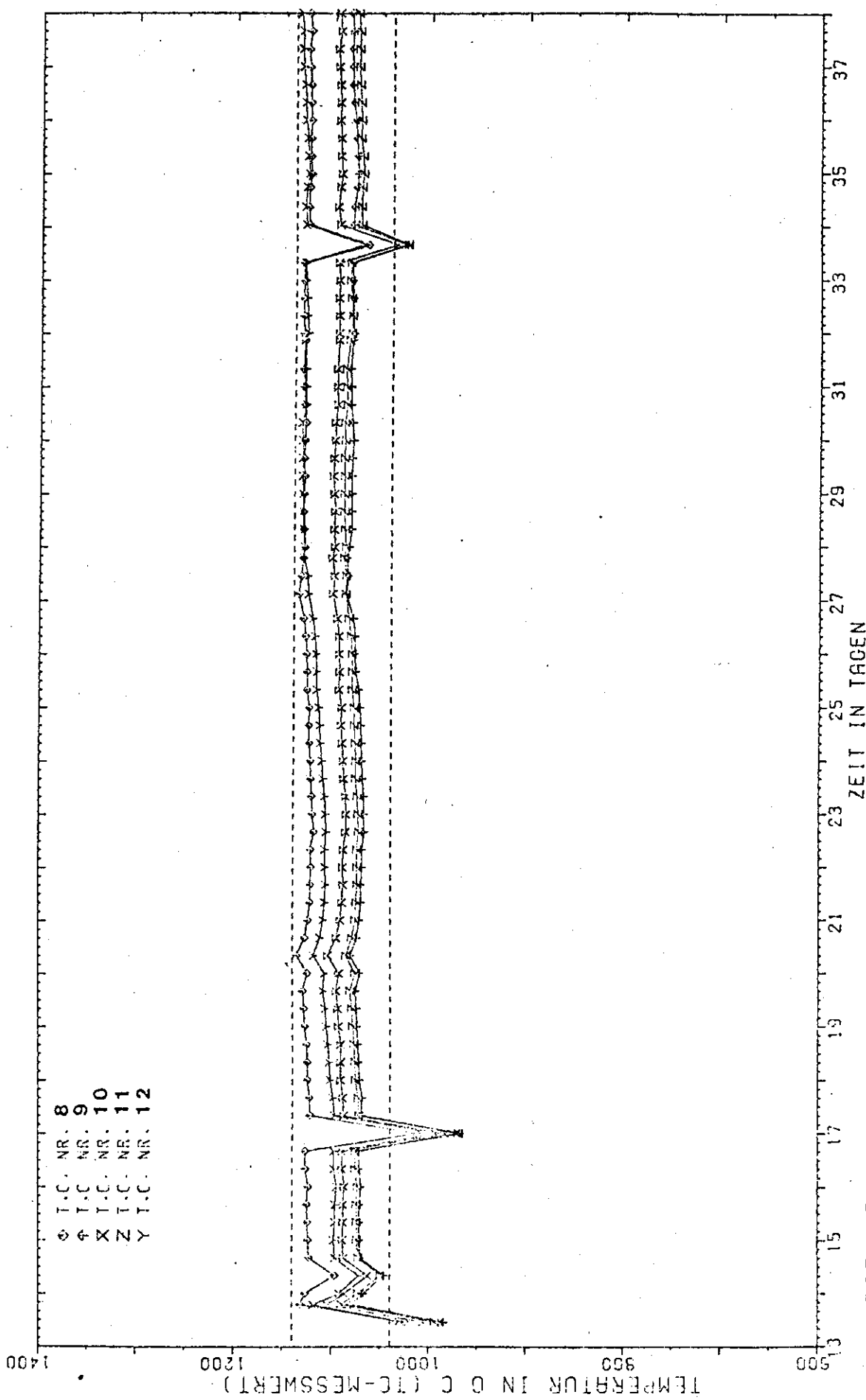


FIG. A 6

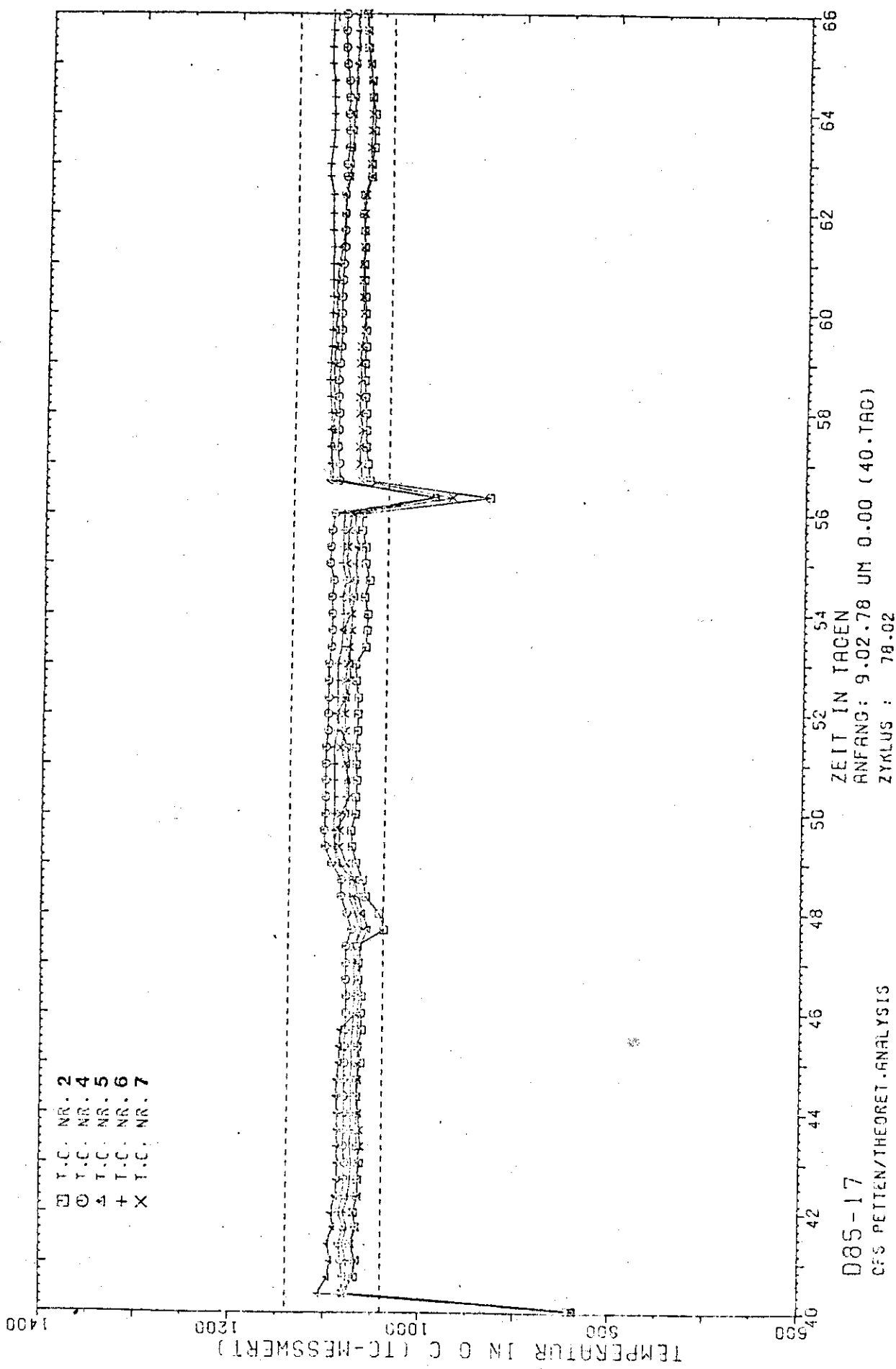


Fig. A 7

